THE INTERNATIONAL SCIENTIFIC JOURNAL

PROBLEMS
OF
TRIBOLOGY

МІЖНАРОДНИЙ НАУКОВИЙ ЖУРНАЛ

ПРОБЛЕМИ ТРИБОЛОГІЇ

CONTENTS

ЗМІСТ

Determination of Limiting Deformations at Testing Cylindrical Samples for Tension

I. Iu. Kyrytsya, O. V. Petrov, I. V. Vishtak*, S. I. Sukhorukov

Vinnytsia National Technical University, Ukraine
*E-mail: innavish322@gmail.com

Abstract

This paper proposes a method for calculating limiting deformations under conditions of localized deformation during tensile testing. The method for calculating limiting deformations was used to construct plasticity diagrams under conditions of strain localization under uniaxial tension.

The plasticity diagram is one of the material functions that forms the technological map of the material. The plasticity diagram displays the properties of a material depending on the degree of deformation and the stress state scheme.

According to the studies carried out in this work, it was established that the critical increase in plasticity with increasing stress state indicator is explained by the influence of three factors: the strain gradient, the history of deformation and the third invariant of the stress tensor.

The obtained dependencies make it possible to construct plasticity diagrams for materials whose destruction is preceded by localized deformation in the form of a "neck".

This work establishes the quantitative influence of these three factors on the magnitude of the limiting deformations of a sample stretched to the point of failure.

Application plasticity diagrams constructed using the proposed methods for cold plastic deformation processes, depending on the type of deformation path and the features of metal rheology, clarifies the value of the used plasticity resource of the metal, which allows to reduce the number of defective products for processes whose modes are calculated according to limit deformations.

Keywords: limiting deformations, stress state indicators, deformations gradient, deformation history, stress tensor, deformation tensor, plasticity diagram, tension testing.

Introduction

In the theory of pressure processing of metals, where large plastic deformations are considered (limiting deformations) of such standard mechanical characteristics as yield stress – $\sigma_{0,2}$, elastic stress – σ_{el}, proportionality stress – σ_{pr}, strength stress – σ_{st}, as well as plasticity characteristics – relative residual elongation – $\delta = \dfrac{l_i - l_0}{l_0} \cdot 100\%$, relative residual narrowing – $\psi_n = \dfrac{A_0 - A_n}{A_0} \cdot 100\%$, is far from sufficient for describing the mechanics of metal pressure processing processes.

In the modern phenomenological theory of deformability, the properties of materials are considered in the form of various functions, such as the flow curve of the material; plasticity diagram; calibration schedule: hardness – intensity of stresses – intensity of deformations. These functions form the "technological passport of the material".

When constructing diagrams of plasticity of materials, the method of their construction during stretching of the samples forming the neck remains insufficiently researched.

The development of a technique for constructing plasticity diagrams, which takes into account the peculiarities of deformation localization during the study of tensile materials, remains relevant to this day.

During the stretching of cylindrical samples, the deformation is determined by the diameter of the neck at the time of its initiation, which is significantly lower than that determined by the same diameter after the sample breaks. Therefore, tensile studies allow obtaining sufficiently reliable data only in those cases when a developed neck does not form before failure. In this regard, for a more strict definition of the limiting deformations during stretching of samples, the destruction of which is preceded by a loss of resistance to plastic deformation, it is necessary to have experimental data on the development and accumulation of damage and detected moments preceding the spontaneous development of a macrocrack.

When stretching cylindrical samples from materials, the destruction of which is preceded by the loss of resistance to plastic deformation (formation of the neck), a number of problems arise related to a strict definition:
– accumulated deformation intensity up to the moment of failure (limit deformation) – e_p;
– the stress state indicator – η – the ratio of the average stress to the stress intensity.

Strict calculation of η and e_p during stretching of the samples forming the neck will allow to establish the path of deformation of the material particles from the beginning of the loss of stability to the complete destruction of the sample. As is known, the path of deformation (the rate of change of η and e_p) affects the maximum strain intensity accumulated before failure.

With the help of the approaches proposed in this work, material models are formed, which are the basis for calculating the stress-strain state and energy parameters of deformation processes in pressure treatment processes.

Analysis of recent research and publications

In modern fracture criteria, which have been applied in the problems of metal forming by pressure [1-5], experimental data are used in the form of functions – material characteristics, called plasticity diagrams. The plasticity diagram is one of the functions, which allows in the future to form a technological map of the material.

Plasticity diagrams are obtained by testing materials in tension, compression, torsion, or a combination of these types of tests [6-10].

The calculation of the stress state index η and limit deformation e_p is carried out according to the method obtained on the basis of the solution of the problem of the stress state in the neck, proposed by N.N. Davidenkov and N.I. Spiridonova [11]. This technique was based on the Haar-Karman assumption about the equality of the circular stress to one of the main stresses in the meridional plane. As shown in [12-14], this hypothesis is valid only when determining deforming forces. When estimating the stress-strain state, this hypothesis leads to errors of unknown magnitude.

As follows from the results of the calculations (Fig. 1.), the limiting deformation determined by the diameter of the neck at the point of rupture is overestimated, and for some materials it reaches a value that exceeds even the value e_p at shear, $e_p(\eta = 1) \geq e_p(\eta = 0)$, while according to the second experiments plasticity decreases with increasing η. This is not related to a change in the stress state pattern in the neck. Since triaxial tension occurs in this region, the η index increases, which should lead to a decrease in plasticity.
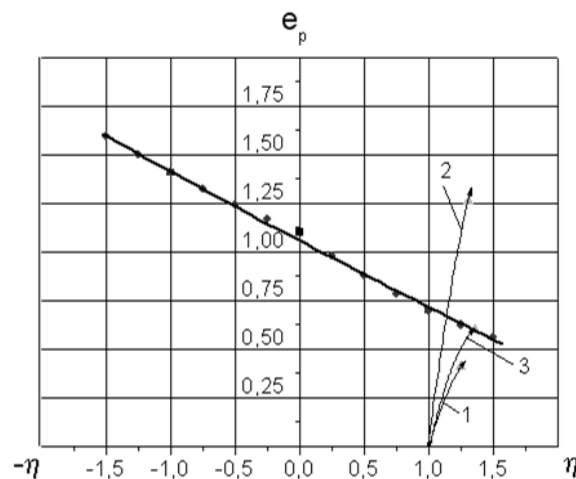
Fig. 1. Diagram of plasticity of steel 3 and pathes of deformation 1,2,3 of material particles: path 1 corresponds to the stretching of the sample before the appearance of critical stable deformation; path 2 – stretching the sample until its complete destruction; path 3 – the appearance of macrocracks before the destruction of the sample.

In our opinion, this abnormal increase in plasticity can be related to three factors. One of them is the influence of the deformation gradient on plasticity.

In work [10] it is shown that, other things being equal (while the stress state indicator remains unchanged, plasticity increases). It is also shown that if $grad\, e_u$ varies from 0 to 0,06, then plasticity increases by $\Delta e_u = 0,15$.

There are reasons to assume that the deformation gradient in the neck area can influence the growth of plasticity.

The second factor that can influence the increase in plasticity in the neck region is the rate of change of the stress state indicator, in other words, the history of deformation.

Thus, work [11] shows that when $\dfrac{d\eta}{de_u} > 0$, plasticity increases, and when $\dfrac{d\eta}{de_u} < 0$, plasticity decreases.

The reason for this abnormal increase in plasticity should also be sought in the very nature of the destruction. The highest η is obtained in the center of the neck on the axis of the sample. According to this, the macrocrack originates in this place.

Thus, in the work [12] shows an X-ray picture of the neck of an aluminum round sample immediately before destruction, while a macrocrack is observed in the center of the cross-section, which did not reach the edges of the cross-section contour. Therefore, the calculation of the limit deformation according to the formula

$e_p = 2\ln\dfrac{d_0}{d_n}$ is incorrect.

According to the observations made [13], the deformation is determined by the diameter of the neck at the time of its initiation, which is significantly lower than that determined by the same diameter after the sample rupture. Therefore, tensile studies allow obtaining sufficiently reliable data only in those cases when a developed neck does not form before failure. In this regard, for a more strict definition of the limiting deformations during stretching of samples, the destruction of which is preceded by a loss of resistance to plastic deformation, it is necessary to have experimental data on the development and accumulation of damage and detected moments preceding the spontaneous development of a macrocrack.

For further experiments, we chose steel 3, because this metal is ductile due to its low carbon content, and the formation of a neck is clearly visible on the samples during tension.

When testing for tension, compression, torsion or tension together with torsion, it is necessary that the constancy the dimensionless stress state indicators is maintained. Such indicators, which are widely used in the theory of deformability, are:

$$\eta = \frac{I_1(T_\sigma)}{\sqrt{3I_2(D\sigma)}} = \frac{3\sigma}{\sigma_i} , \tag{1}$$

$$\chi = \frac{\sqrt[3]{I_3(T_\sigma)}}{\sqrt{3I_2(D_\sigma)}} = \frac{\sqrt[3]{\sigma_1\sigma_2\sigma_3}}{\sigma_i} , \tag{2}$$

where $I_1(T_\sigma)$, $I_3(T_\sigma)$ are the respectively the first and third invariants of the stress tensor;

$I_2(T_\sigma)$ is the second invariant of the stress deviator;

σ_1, σ_2, σ_3 are the principal stresses;

σ is the average stress;

σ_i is the stress intensity.

Experimentally plotted curves $e_p(\eta, \chi)$

$$e_p = \int de_{ij} \tag{3}$$

approximate and the resulting functions are called the plasticity diagram [12, 13].

When carrying out experiments, it is necessary to observe the conditions $\eta = const, \chi = const$.

However, the specified condition of the constancy of the stress state index during the test is often not performed. The deformation path of the material particles $\eta(e_i)$, for example, under tension can vary from $\eta = 1$ (uniaxial tension) to $\eta > 2$ (biaxial tension). As shown in work [14], the limiting deformation turns out to be dependent on the history of deformation and in some cases exceeds the value of $e_p(\eta=0)$ (torsion), which contradicts the physical concepts.

Besides, as shown in work [14], when tensile samples made of materials, the destruction of which is preceded by localization and deformation in the form of a "neck", the value of $e_p(\eta=1)$ is influenced by the volumetric stress state schema. As an indicator of the stress state in work [14], the indicator (2) is proposed, which takes into account the influence of the third invariant of the stress tensor. In the same work, it was shown that $I_3(T_\sigma)$ affects the plasticity $e_p(\eta=1)$. In the range of the index $1 \geq \eta \geq -2$, the diagram is influenced by the third

invariant of the stress tensor. In the region $1 > \eta > 0$, the third invariant increases plasticity (in comparison with the plasticity diagram plotted under the conditions $I_3 (T_\sigma) = 0$) (Fig. 2).
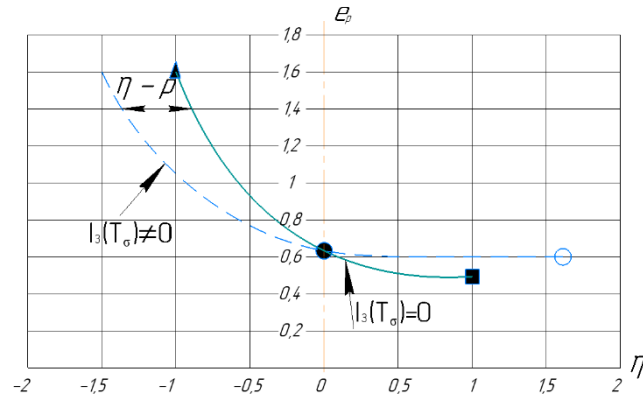
Fig. 2. Diagram of plasticity for steel 20

■ – stretching; ▲ – compression; ● – torsion; ○ – η=1,55; ---- – $I_3 (T_\sigma) \neq 0$; — – $I_3 (T_\sigma) = 0$

In work [14] is stated that at a constant stress state index, the deformations gradient increases plasticity. This work presents the results of experiments carried out on samples of high-speed steels P12 and P18 of square and rectangular cross-section. Different deformation gradients are achieved by different cross-sectional sizes. The samples were deformed under conditions of pure bending up to fracture. Deformations were determined experimentally by the method of dividing grids applied with a Vickers hardness tester with a base of 1 mm on the side surface.

Deformation degree at pure bending

$$e_i = \frac{\sqrt{2}}{3} \sqrt{\left(e_r - e_\theta\right)^2 + \left(e_\theta - e_z\right)^2 + \left(e_z - e_r\right)^2} \; . \tag{4}$$

Deformation tensor characterizing the deformations gradient

$$T_e = \sqrt{\left(\frac{\partial e_r}{\partial r}\right)^2 + \left(\frac{\partial e_\theta}{\partial r}\right)^2 + \left(\frac{\partial e_z}{\partial r}\right)^2 + 2\left(\frac{e_r}{r_0} - \frac{e_\theta}{r_0}\right)^2} \; . \tag{5}$$

The derivatives were determined as the tangent of the angle of inclination of the tangents to the corresponding dependences at the points adjacent to the fracture site. The radii of curvature were determined for the stretched surface in the area adjacent to the rupture line.

The stress state index (1) equal to the ratio of the first invariant of the stress tensor to the stress intensity was calculated by the formula

$$\eta = 2 \frac{e_r}{e_i} \; . \tag{6}$$

The value of η practically did not differ from unity.

Aim of the article is to develop the method of calculating limiting deformations at constructing plasticity diagrams at conditions of localization deformation under uniaxial tension. To investigate what factors influence the abnormal increasing in plasticity with increasing stress index under uniaxial tension.

Methods

In the process of the research the following methods have been used: analysis of the literature sources, mathematical modelling of the processes, using basic laws of solid-state mechanics, theory of modelling and system analysis, numerical methods of studying mathematical models, described by the systems of differential and algebraic equations, computer processing of information.

Methods of mathematics and applied theory of plasticity, phenomenological theory of deformability were also used to solve the problems posed in the work. The hardness method, the experimental-calculation method of

grids and the approximate engineering method for calculating the stress-strain state were also used. The results of the research were processed using the methods of mathematical statistics.

Experimental studies performed using physical modeling methods. The physical and mechanical properties of the studied materials were determined using standard equipment. Specially made devices were also used. Experiments were conducted in laboratory and production conditions.

The problems were solved, using the package of the applied programs MathCAD.

Results

Based on the processing of the experimental data obtained in work [15], proceeding from the theory of diffusion of dislocations and the assumption that at $\eta =$ const the intensity of deformations is proportional to the density of dislocations, the following equation is proposed

$$e_p = b\exp(\beta t) + \frac{4}{3}\frac{\frac{\partial e_i}{\partial x}\underset{x=l}{\int}\sqrt{Dt}}{\sqrt{\pi}}.$$
(7)

Dependence (7) is verified by experiments: $\beta t = 2{,}079$, $Dt = 16{,}78$ mm^2, $b = 0{,}00895$.

$$e_p = \frac{1}{2}\left(grad\ e_i\right)^{0,3}$$
(8)

or

$$grad\ e_i = \exp\left(\frac{\ln\frac{e_p}{0,5}}{0,3}\right).$$
(9)

The results obtained make it possible to take into account the effect of the deformations gradient at constructing the plasticity diagram.

The work [14] investigated the limiting deformation on the contour of the central circular hole in stretched plates 50 mm wide and 2 mm thick made of steel 3. The plates were stretched by a stepwise increasing load. A dividing grid with a base of 0,1 mm is applied on the plates. The specific deformations e_i were measured.

The obtained results of the dependence of the limiting deformation intensity on the deformations gradient were approximated by the relation

$$e_p = B\left(grad\ e_i\frac{1}{MM}\right)^n$$
(10)

or

$$grad\ e_i\frac{1}{MM} = \exp\left(\frac{\ln\frac{e_p}{B}}{n}\right),$$
(11)

where $B = 0{,}849$, $n = 0{,}258$.

The greatest inhomogeneity of the stress-deformation state is also found in this type of test as torsion ($\eta = 0$).

With a constant stress state index ($\eta = 0$), it is possible to carry out experiments on torsion of samples with a diameter $d = 20, 15, 10, 7,5, 5$ mm.

Along the generatrix of the cylindrical samples with the help of a vernier caliper, a longitudinal risk was drawn. After fracture, the angles of inclination of the helical lines near the fracture site were measured using an instrumental microscope. The degree of deformation was determined by the formula

$$e_p = \frac{tg\,\alpha}{\sqrt{3}}.$$
(12)

The diameter of the sample and the length of the working part were also measured before and after destruction. In the case under consideration, these parameters practically did not change. Consequently, the torsion was constrained, i.e. axial compressive stresses appeared, however, as shown in [13], they are two orders of magnitude less than tangential ones, and the elongation of the samples was practically absent.

Therefore, the hypothesis of flat sections is performed $e_z(z) = const \cong 0, \sigma_z \cong 0$.

The quadratic invariant of the deformation tensor *Te* at torsion is

$$T_e = \left[\left(\frac{e_{z\theta}}{r} \right)^2 + \left(\frac{\partial e_{z\theta}}{\partial r} \right)^2 \right]^{\frac{1}{2}}. \tag{13}$$

At torsion $grad\ e_i = \dfrac{de_i}{dr} \cdot \dfrac{1}{e_{i\,max}} = \dfrac{d\gamma}{dr} \cdot \dfrac{1}{\gamma_{max}}$, that is, with a radius $r = 4$ mm,

$grad\ e_i = \dfrac{1}{r} = 0,25 \cdot \dfrac{1}{mm}$.

Among the many approximations [13, 15] and plasticity diagrams [10, 11], let us dwell on those for which the approximation coefficients have a physical meaning. So in work [11] an approximation of the form is given:

$$e_p(\eta) = e_p(\eta = 0)\exp(-\lambda_i\eta). \tag{14}$$

where $e_p(\eta = 0)$ – limiting deformation at shear (torsion); λ_i – respectively:

$$\lambda_1 = \ln\frac{e_p(\eta = 0)}{e_p(\eta = 1)} \tag{15}$$

is the coefficient of sensitivity of plasticity to a change in the stress state diagram in the region of the index $1 \geq \eta \geq 0$;

$$\lambda_2 = \ln\frac{e_p(\eta = -1)}{e_p(\eta = 0)} \tag{16}$$

is the coefficient of sensitivity of plasticity to a change in the stress state diagram in the region of the index $0 \geq \eta \geq -1$.

In fig. 3 shows a diagram of plasticity of high-speed steel R18 approximated using formula (14), where $\lambda_1 = 1,31$, $\lambda_2 = 1,26$. The specified material was chosen due to the fact that when the samples of this material are stretched, a "neck" is not formed.
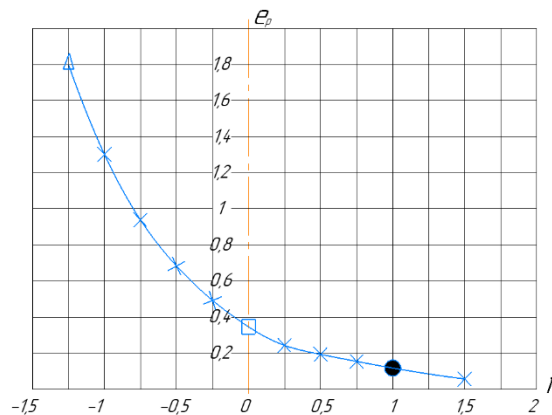
Fig. 3. Diagram of plasticity of high-speed steel R18 ▲ $- e_p(\eta=-1)$; ■ $- e_p(\eta=0)$; ● $- e_p(\eta=1)$; × **– calculation by the formula (14)**

In semilogarithmic coordinates λ_i are the tangents of the slope of the straight lines plotted in the coordinates $e_p(\eta)$. The coefficient λ_i (i = 1, 2) is essentially the coefficient of plasticity "sensitivity" to changes in the stress state diagram. The greater the value of these coefficients, the more intensive the growth of plasticity occurs with increasing hydrostatic pressure.

A similar idea of the physical essence of the coefficients λ was later published in the work [13], in which, from the point of view of the physics of metals, the expediency of introducing coefficients of "sensitivity" of plasticity to a change in the index η is shown. Thus, in this work, the inflections in the plasticity diagrams plotted in semilogarithmic coordinates are associated with the index of the relaxation capacity (plasticity) of polycrystals n:

$$n = \frac{d \ \ln\sigma}{d \ \ln e} ,\tag{17}$$

and the quantities e_p, δ, ψ are a consequence of the quantity n (but not only of it alone).

Thus, in this work, we have considered the features that arise when constructing plasticity diagrams under conditions of such tests as uniaxial tension and torsion.

Using the example of steel 3, tested under tensile conditions, let us consider our proposed algorithm for constructing plasticity diagrams in the range of variation of the index η from zero to two [14, 15].

Three standard cylindrical samples made of steel 3 (this steel was chosen due to the fact that the destruction of this steel is preceded by localization in the form of a neck) were stretched to various degrees of deformation (
$\delta = \frac{l_i - l_0}{l_0} \cdot 100\%$, $\delta_1 = 2{,}56\%$, $\delta_2 = 15{,}92\%$, $\delta_3 = 20{,}92\%$). After deformation (the third sample was destroyed),

the geometric parameters were measured (see Table 1).

Table 1

Geometric parameters and some characteristics of steel samples steel 3

Sample number	I	II	III
l, mm	12	14	16
h, mm	1,59	1,09	0,99
d_n, mm	5,09	6,08	7,68
d_0, mm	9,5	9,5	9,5
d_{st}, mm	8,01	8,06	8,47
l_0, mm	9,89	9,89	9,89
δ, %	20,89		
R, mm	11,6	22,79	34,1
r, mm	1,289	1,189	1,164
e_p	1,29	0,901	0,442
$d_{cr} = \frac{d_n + d_{st}}{2{,}22}$, mm	5,89	6,349	7,268
e_p^*	0,915	0,83	0,557

According to work [14], the neck radius was determined by the formula

$$R = \frac{l^2 + 4h^2}{8h} .\tag{18}$$

The stress state index is calculated according to Bridgman, taking into account the approach proposed in works [14, 15]

$$\eta = 1 + 3\ln\left(1 + \frac{d_{cr}}{4} \cdot \frac{1}{R}\right).\tag{19}$$

The work [10] shows a snapshot of the neck of an aluminum sample immediately before destruction. In this case, a macrocrack is observed in the center of the section, which did not reach the edges of the section contour. Therefore, the calculation of the limiting deformation using formula

$$e_p = 2\ln \frac{d_0}{d_n} \tag{20}$$

significantly overestimates the plasticity.

In works [14, 15], it is proposed to calculate the limiting deformation e_p by the formula

$$e_p^* = 2\ln \frac{d_0 \cdot 2{,}22}{d_n + d_{st}}, \tag{21}$$

where d_{st} is the cross-sectional diameter of a cylindrical sample at a distance from the minimum neck radius.

Calculation by formula (21) underestimates the plasticity, which corresponds to the physical concepts of the decrease in plasticity with an increase in the index η.
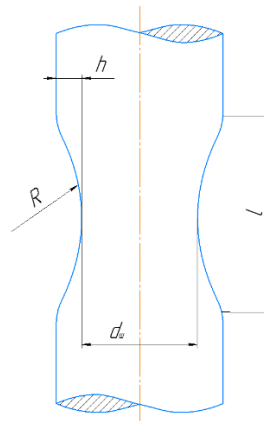
Fig. 4. Scheme of the meridional section of the sample at the site of necking

We will substantiate the possibility of such a calculation based on the above approach on the influence of three factors on plasticity – the deformation gradient, the history of deformation, and the third invariant of the stress tensor.

In the considered example of tension of cylindrical samples of steel 3 in the area of localization of deformation (in the neck), the gradient of deformations overestimates the plasticity by $\Delta ei \approx 0{,}12$, the history of deformation by an amount $\theta = \ln \dfrac{e_p(\eta)}{e_p(\eta = const)} = 0{,}12...0{,}14$, the third invariant $I_3 (T_\sigma)$ overestimates the plasticity by 10 – 12%. The calculation of the actual limiting deformation gives the result

$$e_p^a = e_p\left[1 - (0{,}12 + 0{,}13 + 0{,}12)\right] = 1{,}29\left[1 - 0{,}37\right] = 0{,}81. \tag{22}$$

Calculation by formula (21) gives satisfactory convergence with calculation by (22) $e_p^* = 0{,}915$.

Using of the plasticity diagram in the form of the dependence of the limiting deformation on the stress state parameter in the known deformation criteria for cold plastic deformation processes can significantly clarify the calculation of the used plasticity resource. In turn, this makes it possible to reduce the probability of fracture (from 30 to 40 %) in the processes of cold plastic deformation, the parameters of which are calculated with minimal margins for fracture deformations, and to expand the technological capabilities of metal pressure processing processes.

Conclusions

The method of calculating limiting deformations at constructing plasticity diagrams at conditions of localization deformation under uniaxial tension is developed in this work.

The abnormal increase of plasticity with an increase in the stress state index is explained by the influence of three factors: the gradient of deformations, the history of deformation and the third invariant of the stress tensor.

A method of constructing plasticity diagrams has been developed, which takes into account the peculiarities of deformation localization during tensile testing of materials. The method is based on the analysis of the stress-strain state in the neck of the stretched sample in the area of localization of deformation without the inclusion of the Haar-Karman hypothesis and allows determining the limit deformations during stretching of plastic materials.

Using the example of plotting the plasticity diagram of steel 3, the quantitative influence of these three factors on the value of the limiting deformation in the neck of a sample stretched to failure is shown. The total value of the overestimation of the limiting deformation is from 34 to 38 percent.

With the help of the proposed approaches, material models (technological map of the material or passport of the material) are formed, which are the basis for calculating the stress-strain state during the manufacture of blanks (parts), as well as calculating energy parameters of deformation processes.

In this work, modern phenomenological approaches are considered, which will allow structural engineers and technological engineers to create safe structures, structural elements, details, etc., even at the design stage.

The obtained dependencies will allow in the future to provide recommendations for the construction of technological processes for the manufacture of parts or structural elements, etc.

References

1. Park N., Stoughton T.B., Yoon J.W. (2019). A new approach for advanced plasticity and fracture modelling. IOP Conf. Series: Materials Science and Engineering 651. doi:10.1088/1757-99X/651/1/012097.

2. Gharehbaghi S. Gandomi M., Plevris V., Gandomi A.H., Abdulameer Kadhim A., Mohammed Kadhim H., Ham S.W., Cho J.U., Cheon S.S., Paresi P.R. (2020). Fracture Prediction in Plastic Deformation Processes. Ductile Fract. Met. Form, 7, 1–17.

3. Versaillot P.D., Wu Y.F., Zhao Z.L. (2021). An Investigation into the Phenomenon of Macroscopic Plastic Deformation Localization in Metals. Phys. Conf. Ser., 1777, 012067.

4. Paul S.K., Roy S., Sivaprasad S., Bar H.N., Tarafder S. J. (2018). Identification of Post-Necking Tensile Stress–Strain Behavior of Steel Sheet: An Experimental Investigation Using Digital Image Correlation Technique. Mater. Eng. Perform., 27, 5736–5743.

5. Jain A., Mishra A., Tiwari V., Singh G., Singh R.P., Singh S. (2022). Deformation Measurement of a SS304 Stainless Steel Sheet Using Digital Image Correlation Method. Photonics, 9, 912. https://doi.org/10.3390/photonics9120912.

6. Schwab R., Harter A. (2021). Extracting True Stresses and Strains from Nominal Stresses and Strains in Tensile Testing, 2021, 57, e12396.

7. Achineethongkham K., Uthaisangsuk V. (2020). Analysis of forming limit behaviour of high strength steels under non-linear strain paths using a micromechanics damage modelling. Int. J. Mech. Sci., 183, MS105828.

8. Matsuno T., Hojo T., Watanabe I., Shiro A., Shobu T., Kajiwara K. (2021). Tensile deformation behavior of TRIP-aided bainitic ferrite steel in the post-necking strain region. Technol. Adv. Mater. Methods, 1, 56–74.

9. Tu S., Ren X., He J., Zhang Z. (2020). Stress–strain curves of metallic materialsand post-necking strain hardening characterization. Fatigue Fract. Eng. Mater. Struct., 3–19. https://doi.org/10.1111/ffe.13134.

10. Matsuno T., Shoji H., Ohata M. (2018). Fracture-strain measurement of steel sheets under high hydrostatic pressure. Procedia Manuf., 15, 869–876.

11. Ogorodnikov V. A., Dereven'ko I. A., Poberezhnyj M.I. (2011). Karty materialov v processah obrabotki metallov davleniem. [Material Maps for Metal Forming Processes]. Visnik Nacional'nogo tekhnichnogo universitetu Ukraïni "KPI". Seriya: «Mashinostroenie»,52, 62-67.

12. Del' G.D. (1978). Tekhnologicheskaya mekhanika. [Technological mechanics]. Mashinostroenie, 174.

13. Brünig M., Gerke S., Schmidt M. (2016). Biaxial experiments and phenomenological modeling of stress-state-dependent ductile damage and fracture. International Journal of Fracture. Vol. 200, Issue 1-2, 63-76. doi: 10.1007/s10704-016-0080-3

14. Kyrytsya I.Iu. (2014). Osoblyvosti rozrakhunku parametriv napruzheno-deformovanoho stanu ta pobudovy diahram plastychnosti v zoni lokalizatsii deformatsii pid chas roztiahu tsylindrychnykh zrazkiv. [Peculiarities of calculating the parameters of the stress-strain state and constructing plasticity diagrams in the deformation zone during stretching of cylindrical samples]. Visnyk Vinnytskoho politekhnichnoho instytutu, № 2,101 – 107.

15. Ohorodnykov V. A., Kyrytsya I.Iu., Perlov V.Ie. (2015). Mekhanika protsesiv kholodnoho plastychnoho deformuvannia visesymetrychnykh zahotovok z hlukhym otvorom [Mechanics of processes of cold plastic deformation of hexagonal blanks with a blind hole]. Monograph, Vinnytsia: VNTU, 164.

Кириця І. Ю., Петров О. В., Віштак І. В., Сухоруков С. І. Визначення граничних деформацій при випробуванні циліндричних зразків на розтяг

Стаття присвячена розрахунку граничних деформацій в умовах локалізованої деформації при випробуванні на розтяг. За допомогою методу розрахунку граничних деформацій побудовано діаграми пластичності в умовах локалізації деформацій при одновісному розтягу.

Діаграма пластичності є однією з функцій матеріалу, яка формує технологічну карту матеріалу та відображає властивості матеріалу в залежності від ступеня деформації і схеми напруженого стану.

Встановлено, що критичне підвищення пластичності зі збільшенням показника напруженого стану пояснюється впливом трьох факторів: градієнта деформації, історії деформації та третього інваріанта тензора напружень. Отримані залежності дають змогу побудувати діаграми пластичності матеріалів, руйнуванню яких передує локалізована деформація у вигляді «шийки».

У роботі встановлено кількісний вплив цих трьох факторів на величину граничних деформацій розтягнутого до руйнування зразка. Прикладні діаграми пластичності, побудовані за запропонованими методами, для процесів холодної пластичної деформації залежно від виду шляху деформації та особливостей реології металу уточнюють величину використаного ресурсу пластичності металу, що дозволяє зменшити кількість бракованих виробів на процеси, режими яких розраховуються за граничними деформаціями.

Ключові слова: граничні деформації, показники напруженого стану, градієнт деформацій, історія деформації, тензор напружень, тензор деформації, діаграма пластичності, випробування на розтяг.

Modeling surface structure of tribotechnical materials

I. Drach*, M. Dykha, O. Babak, O. Kovtun

Khmelnytskyi national University, Ukraine
*E-mail: cogitare410@gmail.com

Abstract

Modern tribology makes it possible to correctly calculate, diagnose, predict and select appropriate materials for friction pairs, to determine the optimal mode of operation of the tribo-joint. The main parameter for solving friction problems and other problems of tribology is the topography of the surface. The main purpose of the models in these tasks is to display the tribological properties of engineering surfaces. In the framework of the classical approach, the topography of the surface is studied on the basis of its images from the point of view of functional and statistical characteristics: the evaluation of the functional characteristics is based on the maximum roughness along the height and the average roughness along the center line, and the statistical characteristics are estimated using the power spectrum or the autocorrelation function. However, these characteristics are not only surface properties. They depend on the resolution of the device for measuring the surface geometry and the length of the scan. However, the degree of complexity of a surface shape can be represented by a parameter called the fractal dimension: a higher degree of complexity has a larger value of this parameter. Fractal dimensionality is a characteristic of surface relief and makes it possible to explain tribological phenomena without the influence of resolution. This article provides an overview of mathematical approaches to the description of the relief of engineering surfaces, in particular statistical, stochastic and topological modeling, their limitations, advantages and disadvantages. The implementation of the principles of the theory of fractal structures is discussed, which makes it possible to introduce the degree of imbalance of the tribological system into the analysis of structure formation in the surface and near-surface layers of materials and to describe the development of friction and wear processes. This is the basis for controlling the structure of the surface layers of materials with given properties. The concept of fractals, used for the quantitative description of the dissipative structure of the tribojunction zone, makes it possible to establish a connection between its fractal dimension and mechanical properties, as well as critical states of deformation of metals and alloys. The course of research and stages of fractal modeling, the classification of methods of fractal analysis of the structure of engineering contact surfaces are considered. A critical analysis of modern models based on the energy-spectral density function, which are quite similar to fractal models, is presented. Readers are expected to gain an overview of research developments in existing modeling methods and directions for future research in the field of tribology.

Keywords: surface relief; statistical models; stochastic models; fractal models; energy spectral density function.

Introduction

Tribotechnical indicators of materials (compatibility, wear resistance, antifriction, etc.) characterize the behavior of the entire tribological system as a whole [1]. Therefore, it is not possible to establish a connection between the above indicators and the geometric and/or physical-mechanical-chemical properties of the elements of the friction pair.

The article deals mainly with engineering surfaces, that is, those used in engineering practice. It is known that all technical surfaces are rough [1, 2, 3], so contact between technical surfaces is carried out using several contact points [4]. If the surface profile z(x) is determined using the Fourier distribution, and the term "roughness" is defined as a short-wave form, then the technical surface is defined as a long-wave form and is called a "wave-like" surface [5]. If the waviness is removed from the surface profile, the rough surface can be considered

nominally flat [6]. The roughness of technical surfaces is a decisive factor for the performance of tribological components. The surface profile has a huge influence on energy dissipation during sliding of dry engineering surfaces and, accordingly, on friction [7].

Increasing the reliability of many technical systems is impossible without an in-depth study of the processes occurring on friction surfaces; development of physical ideas about friction and wear; application of modern research methods based on the results and methods used in classical fundamental and applied physical and mathematical sciences; use of computer technologies.

This article presents a critical review of some popular functional, statistical, fractal, and related methods for modeling and analyzing surface roughness. Prospective trends in the development of mathematical modeling in tribology are proposed, determined on the basis of the obtained data and statistics of the published literature in this field. After all, the choice of appropriate surface characterization methods and calculation methods for the study of various surfaces is the main problem of current studies of engineering surface topography.

Modern mathematical modeling in the study of the mechanism of contact and destruction of engineering friction surfaces develops in the following main directions: statistical modeling, stochastic modeling, topological modeling, fractal modeling.

Probabilistic and statistical characteristics of surface roughness

Modern research involves a systematic approach to the study of tribotechnical problems. The importance of such an approach increases in the case of applying probabilistic statistical methods in solving problems in the field of friction, since this process is quite complex and has a stochastic nature of functioning. The method of creating mathematical models of the friction and wear process using the apparatus of the theory of similarity, dimensions and mathematical planning of the experiment is quite progressive, since the transition to generalized coordinates sharply reduces the number of factors that must be taken into account and gives sufficiently justified values of the initial parameters. Most tribological systems work in accordance with the Pareto principle, which states that only some of the many factors are significant from the point of view of the system's characteristics. The methods of group consideration of arguments, a priori ranking of factors, rank correlation, random balance and others are used to determine essential factors. The rational choice of the appropriate method is determined by the availability of a priori information about the researched object. Regression analysis is widely used to establish the relationship between input and output parameters and to obtain a mathematical model adequate for the object under study.

One of the first attempts to apply statistical methods to describe surface roughness was presented by Abbott and Firestone, who calculated the cumulative distribution function of surface heights:

$$\Phi(z) = \int_z^\infty \varphi(t)\mathrm{dt},$$

where $\phi(z)$ is the probability density function.

In tribology, this parameter is called the Abbott-Firestone curve or the bearing area curve. Subsequently, a huge number of statistical roughness parameters were introduced [8]. These characteristics were related to both the vertical distribution of heights and the horizontal distribution of rough profiles [9].

The next step in surface roughness research was the idea of modeling based on the theory of random processes. This idea was first implemented by Linnik and Khusu [10], who suggested using the details of the stationary Gaussian random process graph and the correlation function for the Gaussian random process N(x) to describe the surface roughness:

$$N(x) = N(0) \cdot e^{(-\alpha|x|)}, \tag{1}$$

where N(0) and α are some roughness parameters. A similar idea was presented later by Whitehouse and Archard [11]. They proposed to describe the Gaussian profile z(x) of a random rough surface by the distribution of the heights of its protrusions and the correlation (autocorrelation) function of the process R(δ):

$$R(\delta) = \lim_{T \to \infty} \frac{1}{2T} \int_{-T}^{T} [z(x + \delta) - \bar{z}] [z(x) - \bar{z}]\mathrm{dx}, \tag{2}$$

where $\bar{z}$ is the middle line of the profile.

Statistical modeling results are effective if the roughness is Gaussian (normal). If the roughness is not normal, then the properties of the sample trajectory are not fully determined by the mean and covariance functions. Therefore, the statistical modeling technique includes a stage of assessing the reliability of the model, which is based on proving the assumption of a Gaussian (normal) distribution of the heights of the projections of the rough surface.

There are many criteria for testing this assumption. Each of these criteria provides a quantitative assessment of the closeness between a theoretical Gaussian distribution and an observed sample of measurements by

calculating a p-value. Estimates are based on certain statistics of the relevant criterion. According to the literature review, the most popular criteria for checking the normality of roughness of different surfaces are: Pearson, Kolmogorov-Smirnov (KS), Anderson-Darling (AD), Cramer-von Mises (CVM), Shapiro-Wilk (SW), Shapiro-Francia (SF) criteria), Lilliefors (LF) [12]. The p-value is a number that characterizes, for the observed measurements, the significance on a scale of [0, 1] that the hypothesis of a normal distribution law is true. As a rule, an acceptable level of significance is nominated (5%). The trend of using statistical tests on both nano and micro scales is relevant.

Non-Gaussian processes can be generated by a stochastic differential equation:

$$dX(\mathrm{x}) = -\,\theta(X(\mathrm{x}) - \mu)dx + \sigma(X(\mathrm{x}))dWB(\mathrm{x}),$$

where $\mathrm{x} \geq 0$ and WB(x) is a standard Brownian motion (Wiener process). Choosing the appropriate value of the parameter μ and the function $\sigma(\cdot)$, we obtain a certain distribution of the process X(x) by height with the autocorrelation function $\rho(\mathrm{x}) = \mathrm{e}{-}\theta|\mathrm{x}|$, by the power spectrum G(ω)=2$\pi\theta$/(θ2+ω2) for any choice of μ and $\sigma(\cdot)$.

Research has proven that the surface relief is a non-stationary random process, that is, this statistical parameter depends on the scale. In other words, the accuracy of this characteristic parameter of the contact problem is affected by the length of the sample and the resolution of the measuring device [13].

Statistical models of contact with multiple protrusions between two nominally flat surfaces are the most popular for predicting the contact behavior of rough surfaces, their assumptions and simplifications greatly limit their reliability, and the criteria for identifying protrusions and their characteristics lead to significant deviations in the calculated topographic input parameters, which are also strongly dependent from the resolution of the topography measurement technique. Typical engineering surfaces are also not isotropic, and the distribution of ledge heights is not Gaussian [14].

Methods of topological modeling of the structure of the surface layer

Traditional methods of topological modeling (geometric assessment) of the formation of various objects, including in tribology, are based on the approximate approximation of the structure of the object under study (in tribology of surface and near-surface layers) by geometric shapes, for example, lines, segments, planes, polygons, polyhedra, spheres. These techniques are based on classical Euclidean geometry, the topological dimension of which is an integer. At the same time, the internal structure of the object under study is usually ignored, and the processes of structure formation and their interaction with each other and with the environment are characterized by integral thermodynamic parameters. This, naturally, leads to the loss of a significant part of information about the properties and behavior of the studied systems, which, in fact, are replaced by more or less adequate models. In some cases, such a replacement is quite justified. However, there are problems when the use of topologically non-equivalent models is fundamentally unacceptable. In particular, for the modeling of structurally complex objects, where a generalized concept of a specific physical representation of the structure and description of the properties of the object is necessary.

An example of topological modeling of elastic contact between two nominally flat metal surfaces is the Greenwood-Williamson model [6]. The surface relief model is a set of spherical segments having the same radius of rounding of the upper part of the protrusions and located on the middle plane of the rough surface. The model is based on fairly clear physical provisions about the contact interaction of rough surfaces in the elastic state of frictional contact spots (the number of contacting spheres of a certain height increases when the surfaces approach each other) [6]. Adopting a constant radius of the upper part of the protrusions simplifies the modeling of the contact interaction process, while the accuracy of the calculations decreases. And at low loads, when we have to take into account sub-roughness when determining the contact parameters (when the contact between two rough surfaces consists of a large number of contact spots of different sizes), the Greenwood-Williamson model is inapplicable. Majumdar [14] managed to eliminate the shortcomings inherent in the Greenwood-Williamson model using fractal modeling.

Fractals Approaches to Surface Topography

In fact, the fractal terminology for describing surface roughness was pioneered by Berry and Hannay [16], who argued that the geometric properties of rough surfaces can be characterized by a new concept of "fractal", which was described in detail by Mandelbrot [17]. He introduced the concepts of fractal, fractal geometry and fractal dimension (FD).

Fractal geometry became widespread in tribology thanks to the works of A.-K. Janahmadov, V. Ivanova [18, 19], which are devoted to the analysis and control of structure formation in alloys, surface and near-surface layers of materials as open nonlinear systems that are far from a state of thermodynamic equilibrium. Such systems are unbalanced due to the dissipation of energy received from the outside. As a result of self-organization, stable structures can arise in such systems, which exist under the condition of constant dissipation, that is, loss of energy by the system. With the appearance of a complex ordered structure in the system, entropy increases, which is compensated by a negative flow of entropy from the outside.

To date, it has been established that the resistance to destruction of metals and alloys is determined by the dynamic structure that is formed in the process of deformation and has dissipative properties. In tribology, surface layers and all internal boundaries should be considered as an independent planar nonlinear subsystem with broken translational invariance, which is the leading functional subsystem in a deformed solid. The main part of the stresses arising during friction is concentrated in the near-surface layers of the friction elements. The reconstruction of the surface layer under the action of external thermal loads occurs precisely in the process of establishing the temperature field and is a process of dissipative structure formation associated with deformation defects [19].

Self-organized dissipative structures in open systems are fractal [17]. This makes it possible to apply fractal modeling when studying the physical and mechanical nature of the destruction of materials by introducing new quantitative indicators of structures in the form of fractal dimensions.

The basis of fractal modeling is the concept of a fractal - a self-similar structure with a fractional dimension, which has the property of scale invariance. In general, fractals are a powerful tool for understanding and designing materials with complex structures and properties [17]. It is based on the works of Russ JC [20], Mandelbrot [17], Feder [21], and others.

The fractal dimension FD characterizes any self-similar system: when the linear dimensions change by u times, the fractal value changes by uFD times. The fractal dimension is not related to the topology, but to the method of construction of the considered object [21].

For a fractal structure, the dimensionality or, usually, the fractional parameter FD, describes the preservation of statistical characteristics when scaling. Fractal dimensionality allows you to quantitatively describe microstructures and their constituent elements, to establish the actual area of collision of phases, the actual lengths of "rough" lines and surfaces, and to determine other structural parameters related to the properties of materials. The fractional metric dimension of such objects not only characterizes their geometric image, but also reflects the processes of their formation and evolution, as well as determines their dynamic properties. Fractals provide a compact way of describing objects and processes in strictly quantitative terms.

The fractal model assumes that the engineering surface is self-similar (a part of the surface reflects the entire object) and scaling (a part repeats its structural features at a different measurement scale). Thus, the fractal approach has the potential to predict the behavior of a surface phenomenon at a particular length scale based on observations at other length scales.

The self-similarity of structures is established on the basis of the analysis of certain geometric patterns and their measurements at different magnification scales. In order to establish the fractality of the structure, it is necessary [22]: 1) to check self-similarity; 2) determine the limits of self-similarity; 3) calculate the fractal dimension.

The fractal tribomodeling methodology is explained in Figure 1, where the main stages of the research and their results are defined.
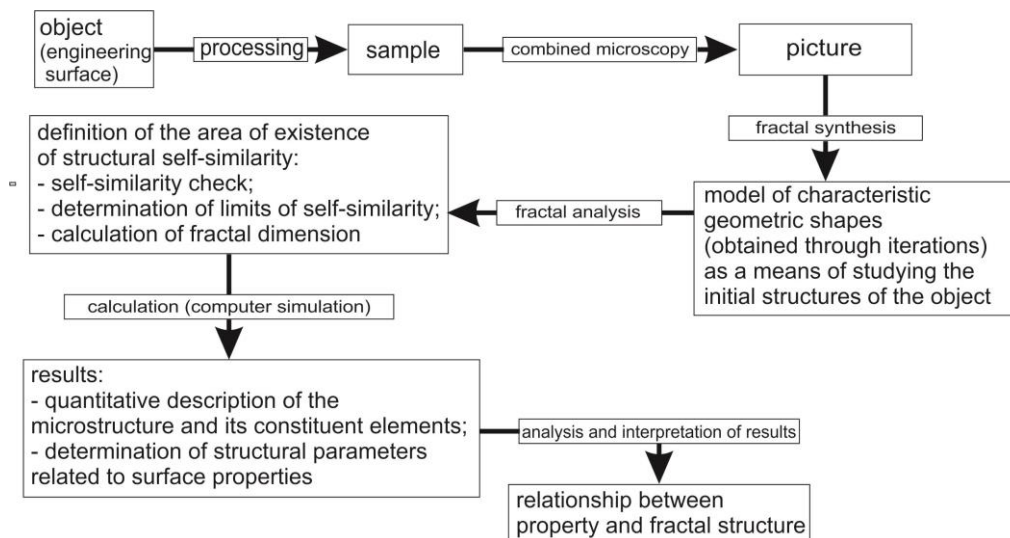
Fig. 1. Information model of the study of structural characteristics of the engineering surface based on fractal analysis

It should be noted that determining the relationship between a property and a fractal structure is a difficult task, since the existing models establishing these relationships for periodic structures are not applicable to fractal ones [23]. The solution of this problem requires the development of fractal analysis of microstructures, the determination of the area of existence of structural self-similarity, as well as the development of fractal synthesis, which includes the modeling of characteristic geometric shapes (through iterations) as a way to study initial structures in real materials.

Below (Figure 2) is a classification of the main experimental methods of studying statistically self-similar tribo-structures.

experimental methods for determining fractal dimension

| porous surfaces | - porometry method;
- according to secondary electronic emission data;
- small-angle scattering method |

| rough surfaces | - according to the physical properties of the object;
- adsorption methods |

| failure surfaces | - by the mechanical properties of the object
- fractographic (metallographic) methods:
    - the method of cut islands
    - Fourier analysis of profiles
    - method of vertical sections
    - similarity transformation method |

| to identify dendritic structures | visual identification |

Fig. 2. Classification of experimental methods for determining the fractal dimension of statistically similar structures

It should be noted that fractographic (metallographic) studies are the most direct methods of determining the fractal dimension of statistically self-similar profiles and surfaces of natural objects.

Fractal theory is used as a mathematical model for random surface topography, which can be used as input in modeling contact mechanics. In many tribological applications, some geometric parameters defined in Euclidean space, such as the unfolded area, bearing surface, cavity, and material volume, are very difficult to measure independently of the unit of measurement. The values of these parameters increase when the measurement scale is reduced. Fractal geometry can be used as an adaptive space for rough morphology, in which the roughness can be considered as a continuous but non-differentiable function, and the FD dimension of this space is an intrinsic parameter to characterize the surface topography [15]. Fractal dimensionality is used as an indicator of the real values of various scale-dependent parameters, such as length, surface, and roughness volume, and as an invariant parameter for analyzing the distribution law of the area of contact points.

Real physical objects, which have signs of self-similarity, can rarely be described using only one value of the fractal dimension. That is why the analysis based on the theory of multifractals - non-homogeneous fractal objects - has become very popular recently. A characteristic of a multifractal is an infinite spectrum of such dimensions, which is called the generalized fractal dimension or Renyi dimension [21].

With the help of multifractal characteristics, phenomena in contact mechanics, wettability, and lubrication of rough material are described, where knowledge of the area of the supporting surface, the developed area, or the volume of voids is directly related to the scale of observation [22].

Another important step in advancing the fractal approach to the description of surface roughness was the study of the Weierstrass-Mandelbrot fractal function by Berry and Lewis [24]. Mandelbrot [17] generalized the Weierstrass function, the graph of which is continuous everywhere and nowhere differentiable, and introduced the complex-valued Weierstrass-Mandelbrot (WM) function W(x) and its special real case C(x; p):

$$W(x; p) = \sum_{n=-\infty}^{\infty} p^{-\beta n}\left(1 - e^{ip^n x}\right)e^{i\varphi_n},$$

$$C(x; p) = \sum_{n=-\infty}^{\infty} p^{-\beta n}\left(1 - \cos(p^n x)\right), \text{ p > 1, 0<}\beta\text{<1.}$$

(3)

where ϕn are arbitrary phases. Box-counting dimension (the Minkowski dimension) of graphs C(x; p) is equal to D = 2 − β. There is no rigorous mathematical proof that its Hausdorff dimension is the same. The plot of the function C(x; p) has often been used to model rough profiles.

Later, Weierstrass-type functions were used by many researchers as a model of rough surfaces [22].

For a while, fractal models were all too popular. There are reviews of the application of fractal concepts in contact problems, in fracture mechanics, and several articles on the use of fractal concepts in tribology [25, 26].

Thus, let's define some main features of the fractal approach.

1. The authors in [25] divided fractals into mathematical and physical (natural) fractals. Both mathematical and physical fractals use the concept of coverage. This means that the object (set) is covered by cubes of size greater than or equal to δ. Fractal geometry is based on mathematical fractals. Mathematical methods of fractal geometry are described in many books and articles where various FDs are studied as applied to mathematical objects. Various FDs are used in research, mainly Hausdorff dimension (dimH) and box-counting dimension (the Minkowski dimension) (dimB) (and the Hausdorff dimension of the set S may not be equal to the box-counting dimension of dimBS, but it is known that dimHS ≤ dimBS.) These FDs can be calculated by taking the limit at δ → 0 [17].

A mathematical fractal curve has an infinite length. Even if a mathematical fractal curve is continuous everywhere, it is non-differentiable. Therefore, it is often very difficult to formulate a boundary value problem for solids that have a fractal boundary.

If real-world objects or numerically modeled objects have a power-law number-radius relationship, then those objects are physical fractals. The power law of the number-radius ratio has the form:

$$N(\delta) \sim \delta - D, \; \delta* \le \delta \le \delta*, \; N(R) \sim (R/\delta)D, \; r* \le R \le R*, \tag{4}$$

where $N(\delta)$ is the number of elements covering the object of size δ, D is the dimension of the object FD, $\delta*$ and $\delta*$ are the upper and lower limits of the physical fractal law, respectively. The first relation (4) is used when the coverage size δ varies and the object size R is fixed, while the latter relation is used when the coverage size δ is fixed and the object size R varies. In the latter case, R* and r* are the upper and lower cutoff limits. The ratio $\ln(N(\delta*)) / \ln(R)$ is used to estimate the D value.

The main difference between these types of fractals is as follows: the physical behavior of the fractal (4) is observed only in a limited range of scales, while for the study of mathematical fractals it is necessary to take into account the scales of consideration up to the zero limit.

If FD is specified, it is convenient to use the fractional part FD – D*. Then FD of fractal profiles and surfaces are equal to 1 + D* and 2 + D*, respectively.

2. Self-similar sets are a very specific kind of fractals. In general, self-similarity is not related to mathematical fractals. Their scaling properties are based on the scaling of the fractal measure or quasi-measure [25], while for physical fractals their scaling properties are reflected by relations (4).

3. On average, the estimate of the FD value is 1.5. However, if the FD value is less than two or three orders of magnitude, the fractal concept is not useful [26].

4. In addition, the term fractal geometry is also quite often loosely applied to a set of semi-empirical or empirical methods for estimating the FD of objects. In general, the FD values obtained by different practical methods are not reliable [25].

5. As noted by Whitehouse [27], there is very little scatter in the FD values obtained for surfaces produced by different manufacturing processes. In addition, there is no well-established algorithm for estimating the intercepts of the fractal law (3).

6. The roughness of real bodies is not a mathematical fractal. In [25] using fractal parametrically homogeneous surfaces, it is shown that the tribological properties of a rough surface cannot be characterized only by the fractal dimension of the surface.

Fractals are only mathematical idealizations of complex forms of natural objects. Of course, it is possible to use a mathematical fractal as a possible model that reflects the power dependence of the number-radius of a natural object within a limited range of scales. However, the resulting task can be very difficult.

Thus, the physical value of the fractal approach is very limited. Furthermore, if the fractal scaling has a small range that spans only 1.5 or 2 orders of magnitude, then fractals do not provide a scale-independent description of surface roughness.

Power Spectral Density Function (PSDF) Approaches to Rough Surfaces

Currently, another trend is quite popular, namely the description of rough surfaces using exclusively the PSDF (power spectral density function) of the surface relief [28]. By Fourier transformation of expression (2) for $R(\delta)$, we obtain the power spectrum $G(\omega)$ or the power spectral density function (PSDF). If the frequency of the signal is denoted by ω, then the PSDF is defined as:

$$G(\omega) = \frac{2}{\pi} \int_0^\infty R(\delta)\cos\omega\delta \, d\delta. \tag{5}$$

Developing the random signal approach, Sayles and Thomas [29] presented experimental relationships between wavelength and scaled power spectral density for many different surfaces. They argued that the scaled spectral density functions of many surface profiles can be approximated as $G(\omega) = 2\pi\Lambda/\omega2$. Sayles and Thomas [29] called Λ the surface topothesis.

Borodich et. al. in [25] showed that models based solely on the power spectral density function (PSDF) are quite similar to fractal models, and these models do not reflect the tribological properties of surfaces. In particular, it is shown that different profiles can have the same PSDF.

Conclusions

An overview of mathematical approaches to the description of the topography of engineering surfaces is given. It is noted that, despite a fairly large number of parameters used to characterize the surface relief, only some parameters are quite useful. However, their use is quite limited, for example these parameters may be useful at the meso- or even micro-scale, but they may be useless at the nano-scale.

There are many models of random processes, but only the case of Gaussian processes is well developed. An analysis of the publications showed that undamaged surfaces are quite often Gaussian at both the micro- and nanoscales, while polished surfaces are not normal.

Based on the analysis of literary sources, an information model for the study of the structural characteristics of the engineering surface based on fractal analysis and the classification of experimental methods for determining the fractal dimension of statistically similar structures have been developed. Some shortcomings of fractal approaches and typical incorrect statements about fractals are identified. It is argued that the practical utility of fractal approaches is quite questionable. It should not be expected that the use of a mathematical fractal model of a rough surface will give significant advantages. Usually, such models are mathematically complex. Thus, a strict approach to fractal modeling can only replace a complex problem with another, more complex than the original one. In addition, the dimensions of physical (natural) fractals cannot be used as scale-independent parameters. Adequate explanations of the fractal concepts used must also be provided, otherwise results may be misinterpreted.

Surface roughness models based solely on the properties of the autocorrelation function or its Fourier transform (PDSF) are also discussed. It was pointed out that the PDSF approach to non-Gaussian surfaces does not reflect the tribological properties of the surfaces.

References

1. Ramezani, M., Zaidi Mohd Ripin, T.-P., Cho-Pei J. (2023). Surface Engineering of Metals: Techniques, Characterizations and Applications. Metals 13, no. 7: 1299.

2. Kapłonek, W., Ungureanu, M., Nadolny, K., Sutowski1, P. (2017). Stylus Profilometry in Surface Roughness Measurements of the Vertical Conical Mixing Unit used in a Food Industry. Journal of Mechanical Engineering, Vol. ME 47.

3. Zhou, G. Statistical, random and fractal characterizations of surface topography with engineering applications. 1993. Dissertations. 1166.

4. Aulin, V., Zamota, T., Hrynkiv, A., Lysenko, S., Bondarets, O., & Yatsun, V. (2019). Increase of formation efficiency of gears contact spot at electrochemical-mechanical running-in. Problems of Tribology, 24(4/94), 33–39.

5. Borodich, FM, Bianchi, D. (2013). Surface synthesis based on surface statistics. In Encyclopedia of Tribology, eds QJ Wang and YW Chung (New York, NY: Springer), 3472–3478.

6. Greenwood, JA, Williamson JBP (1966). Contact of nominally flat surfaces. Proc. Roy. Soc. London. Ser. AV 295. P. 300-319.

7. Borodich, FM, Savencu, O. (2017) Hierarchical models of engineering rough surfaces and bioinspired adhesives. In Bio-Inspired Structured Adhesives, eds L. Heepe, S. Gorb, and L. Xue (Springer). 179–219.

8. Whitehouse, DJ (1982) The parameter rash–is there a cure? Wear. 83, 75–78.

9. Pawlus, P., Reizer, R., Wieczorowski, M., Królczyk, G. (2022) Parametric description of one-process surface texture.
Measurement. Volume 204. 112066.

10. Linnik, Yu. V., and Khusu, AP (1954) Mathematical and statistical description of unevenness of surface profile at grinding. Bul. Acad. Sci. Div. Techn. Sci. 20, 154–159.

11. Whitehouse, DJ, Archard, JF (1970). The properties of random surfaces of significance in their contact. Proc. R. Soc. Lond. A 316, 97–121.

12. Pawlus, P., Reizer, R., Wieczorowski, M. (2020). A review of methods of random surface topography modeling. Tribology International. Vol. 152. 106530.

13. Peng, L., Pan, B., Liu, Zhijiang, Liu, Ziyu, Tan, S. (2020). Investigation on abrasion-corrosion properties of Wc-based composite with fractal theory. International Journal of Refractory Metals and Hard Materials, Volume 87, 105142.

14. Zugelj, B., Kalin, M. (2017). Submicron-scale experimental and theoretical analyzes of multi-asperity contacts with different roughnesses. Tribology International. 119.

15. Majumdar, A., Bhushan, B. (1990). Role of Fractal Geometry in Roughness Characterization and Contact Mechanics of Surfaces. ASME. J. Tribol. April 1990; 112(2): 205–216.

16. Berry, MV, Hannay, JH (1978). Topography of random surfaces. Nature. 273:573.

17. Mandelbrot, BB (1998). Is nature fractal? Science 229:783.

18. Jabbarov, J., Mukhtorov, D., Mustaffaqulov, M., Baxromov, A. (2023). Geometric Modeling of Self-Similar Fractal Structures. International Journal of Advance Scientific Research, 3(12), 185-197.

19. Janahmadov, A.-K., Javadov, M. (2016) Synergetics and Fractals in Tribology. Springer Cham. Springer International Publishing Switzerland. 381 p.

20. Feder, J. (2013) Fractals. Springer Science & Business Media. Springer New York, NY. 284 p.

21. Russ, JC (1944) Fractal Surfaces. Plenum Press, New York.

22. Zhang, B., Zhou L. (2021). Feature Analysis of Fractal Surface Roughness Based on Three-dimensional WM Function. J. Phys.: Conf. Ser. Vol. 1906. 012020.

23. Al-Quraan, TMA, Ilina, O., Kulyk, M. et. al. (2023) Dynamic processes of self-organization in non-stationary conditions of friction. Advances in Tribology, Vol. 2023.

24. Berry, MV, Lewis, ZV (1980). On the Weierstrass-Mandelbrot fractal function. Proc. R. Soc. A 370, 459–484.

25. Borodich, FM, Jin, X., Pepelyshev, A. (2020) Probabilistic, Fractal, and Related Techniques for Analysis of Engineering Surfaces. Front. Mech. Eng. 6:64.

26. Babiä, M., Fragassa, C., Lesiuk, G., Marinkoviä, D. (2020). A New Method for Complexity Determination by Using Fractals and its Applications in Material Surface Characteristics. International Journal for Qualitative Research. 14. 705-716.

27. Whitehouse, DJ (2001) Fractal or fiction. Wear. 249, 345–353.

28. Cutler, C., Thackeray, J., Trefonas, P., Millward, D., Lee, C.-B., Mack, C. (2021). Pattern roughness analysis using power spectral density: application and impact in photoresist formulation. Journal of Micro/Nanopatterning, Materials, and Metrology. 20.

29. Sayles, RS, Thomas, TR (1978) Surface topography as a nonstationary random process. Nature. 271, 431–434.

Драч І.В., Диха М.О., Бабак О.П., Ковтун О.С. Моделювання поверхневої будови матеріалів триботехнічного призначення

Сучасна трибологія дає можливість правильно розраховувати, діагностувати, прогнозувати й підбирати відповідні матеріали пар тертя, призначати оптимальний режим роботи трибоз'єднання. Основним параметром для вирішення проблем тертя та інших проблем трибології є топографія поверхні. Основне призначення моделей в цих задачах – відображення трибологічних властивостей інженерних поверхонь. В рамках класичного підходу топографія поверхні досліджується на основі її зображень з точки зору функціональних і статистичних характеристик: оцінки функціональних характеристик мають за основу максимальну шорсткість за висотою і середню шорсткість по центральній лінії, а статистичні характеристики оцінюються за допомогою спектра потужності або функції автокореляції. Однак, ці характеристики не є лише властивостями поверхні. Вони залежать від роздільної здатності приладу для вимірювання геометрії поверхні та довжини сканування. Однак, ступінь складності форми поверхні можна подати через параметр, який називається фрактальною розмірністю: вищий ступінь складності має більше значення цього параметра. Фрактальна розмірність є характеристикою рельєфу поверхні та дає можливість пояснити трибологічні явища без впливу роздільної здатності. У цій статті подано огляд математичних підходів до опису рельєфу інженерних поверхонь, зокрема статистичне, стохастичне і топологічне моделювання, їх обмеження, переваги і недоліки. Обговорюється впровадження принципів теорії фрактальних структур, що дає можливість увести в аналіз структуроутворення в поверхневих і приповерхневих шарах матеріалів ступінь нерівноважності трибологічної системи й описати розвиток процесів тертя й зношування. Саме це є основою керування структурою поверхневих шарів матеріалів із заданими властивостями. Концепція фракталів, використовувана для кількісного опису дисипативної структури зони трибоз'єднання, дозволяє встановити зв'язок її фрактальної розмірності з механічними властивостями, а також критичними станами деформації металів і сплавів. Розглянуто хід дослідження і етапи фрактального моделювання, класифікацію методів фрактального аналізу структури інженерних поверхонь контакту. Подано критичний аналіз сучасних моделей, які мають за основу енергоспектральну функцію щільності, і є досить схожими на фрактальні моделі. Очікується, що читачі отримають огляд розвитку досліджень існуючих методів моделювання та напрямки майбутніх досліджень у галузі трибології.

Ключові слова: рельєф поверхні; статистичні моделі; стохастичні моделі; фрактальні моделі; енергоспектральна функція щільності

Study of Wear Resistance of Cylindrical Parts by Electromechanical Surface Hardening

D.D. Marchenko*, K.S. Matvyeyeva

Mykolayiv National Agrarian University, Mykolayiv, Ukraine
*E-mail: marchenkodd@mnau.edu.ua

Abstract

The work scientifically substantiates the use of an effective technology for increasing the wear resistance of cylindrical parts, using the example of protective sleeves of cantilever pumps, due to electromechanical surface hardening. A review of research was carried out and it was established that the achievement of the highest values of microhardness of the surface layer at a depth of up to 1.2 mm is possible during electromechanical processing of protective sleeves of cantilever pumps. The application of various modes and schemes of electromechanical surface hardening (EMSH) is accompanied by a change in structure and, as a result, an increase in the hardness of the surface layer of the bushings. The actual contact area of the tool roller with the processed surface and the depth of the temperature-deformation effect depend on the physical and mechanical properties of the materials and the pressing force. The formation of a temperature gradient in the hardened zone at a depth of up to 1.2 mm from the surface has been proven. Metallographic analysis of the surfaces of the sleeves treated by EMSH shows the formation of a white layer with reduced etchability and increased hardness in the hardening zones. The results of the X-ray structural analysis confirmed the formation of the martensite phase in the hardening zone. The microhardness of the hardened steel zone increased by 2.6...3.6 times compared to the initial values at a depth of up to 1 mm from the surface, depending on the materials. In the case of their overlap, the alternation of a fully hardened zone, a partially hardened zone, and a self-relief zone is observed. At the same time, the microhardness of steels along the surface depends on the hardening scheme.

Wear tests under friction conditions of parts of cantilever pumps paired with stuffing boxes showed that the wear resistance of protective sleeves after EMSH increased by 3.1 times for 45 steel, 1.9 times for U8 steel, 2.5 times for SHKH15 steel, for cast iron by 1.9 times compared to the initial values. The use of U8 steel samples after EMSH, instead of serial bushings made of steel 45, allows to increase the wear resistance of parts by 6.1 times, which allows us to recommend U8 steel for use in the manufacture of protective bushings for console pumps. On the basis of the research, recommendations are given for the application of EMSH for the formation of a surface layer with increased wear resistance of protective sleeves during their production and during repair of console pumps in workshops or service centers of agribusiness companies.

Key words: wear resistance, electromechanical hardening, durability, surface hardening, cylindrical parts

Introduction

In most cases, the structural characteristics and properties of the surface layer of parts have a decisive influence on the ability of materials to break. The failure of metals and alloys usually originates from the surface. The reasons for the violation of integrity can be: low quality of production of protective bushings of cantilever pumps, unreasonable choice of materials for their manufacture, ineffective technologies for their strengthening (34...40 HRC), not taking into account operating conditions and types of friction with packing stuffing. Increasing the hardness of the surface is one of the main measures to increase the durability by increasing the wear resistance of the surface layers of materials. Existing methods of strengthening and increasing surface hardness are associated with the use of methods of surface plastic deformation, thermal, chemical-thermal, laser, magnetic-pulse, thermomechanical and combined methods of increasing durability [1]. Today, the technology of processing surfaces with concentrated flows of electric energy is one of the most popular methods of reducing the manufacturing cost, strengthening and improving the quality of parts.

Electromechanical processing (EMP) provides: increase in hardness of steel surfaces up to 70 HRC (steels KhVG, U10...13A); hardening of low-carbon steels (steel 20) up to 42 HRC, cast iron up to 75 HRC; replacement of chemical and thermal treatment (cementation, nitrocementation...); increasing the limit of endurance by 30...80%; increase in wear resistance by 3...12 times; lack of oxidation and decarburization of the surface layer; lack of grooving of the product; reduction of production cost by 2.. 4 times; hardening in air and without the use of coolants, environmental cleanliness and safety; technological simplicity of processing methods.

The specifics of the work of experimental and repair organizations that produce artificial products or parts in small batches do not allow them to maintain workshops and sites with equipment and qualified specialists capable of ensuring the quality of manufacturing machine parts only at the level of industrial enterprises. However, even machine-building enterprises do not guarantee the necessary quality of performance of executive surfaces for a wide range of parts, primarily in terms of hardness, roughness, structure and texture of metal fibers on one part, in various combinations, there may be seats for rolling and sliding bearings, slots and keyways, toothed profiles, holes, threads and grooves. Since the operating conditions and load schemes of the listed surfaces are not the same, their optimal performance cannot be ensured only by means of thermal or chemical thermal treatment [2]. Electromechanical surface hardening is one of the methods of processing products with concentrated energy flows, forming high quality indicators of the surface layer of steel and cast iron parts.

A feature of electromechanical surface hardening (EMSH) is the combination of surface plastic deformation and thermomechanical hardening in a single technological scheme for processing workpieces and the possibility of forming gradient hardened layers of metal with a finely dispersed structure on the surface. This makes it possible to significantly increase the wear resistance of cylindrical parts, including protective sleeves of console pumps.

Literature review

EMP refers to modern science-intensive technologies of impact by concentrated flows of energy on the surface of machine parts. EMP processes successfully compete with such classic technologies as: surface plastic deformation (SPD), heat treatment (HT) and thermomechanical treatment (TMT). By changing the technological modes of EMP (current density J, processing speed and pressure of the processing tool on the surface of the part) on the machine tool, it is possible to perform operations with hot SPD, surface TMT and surface maintenance.

The technology of EMP was developed at the Ulyanovsk Agricultural Institute. The founder of the EMP method is B.M. Askinazi. He investigated heat generation in the surface layer, the method of calculating the depth of the hardened layer, the peculiarities of thermomechanical processes in the surface layer; the nature and structure of the surface layer, the roughness and accuracy of the finished surface; internal stresses of the surface layer during EMP; the effect of EMP strengthening on the fatigue strength, wear resistance and corrosion resistance of parts; conducted research on the technology of restoration of parts with additional metal and without additional metal by electromechanical method; studied the processes of turning parts with a thread [3].

The activities of V.P. Bagmutova, I.N. Zakharova and their colleagues outlined the technological and physical foundations of EMP. The classification of EMP processes according to technological and energy criteria is given. Technological equipment and schemes of contact interactions of the electrode-tool with the surface of the part during EMP, calculation of optimal structural and technological processing parameters have been developed. The conditions of formation of surface layers of structural steels are described, their physical and mechanical properties and stress-strain state are determined [4]. Thermal processes and properties of the surface layer of steels are presented: strength, fatigue strength, wear resistance, corrosion and heat resistance after electromechanical processing. The influence of the structure and properties of the surface layer on the fatigue strength of hardened steels strengthened by combined electromechanical processing was studied [5]. In works [6, 7], the processes of strengthening of the surface layer of titanium alloys during EMP and strengthening by combined electromechanical processing are investigated.

Activities of V.V. Safronov developed, theoretically indicated and experimentally implemented an effective technological method of increasing the durability of cylinder-type steel parts by electromechanical processing. The nature of the influence of technological factors of EMP cylinders on the accuracy of processing, surface quality and heat distribution in the surface layer has been established. The dependence of the thickness of the hardened layer on the initial structure of the processed metal is theoretically justified and experimentally confirmed. An explanation of the increase in corrosion resistance of the surface layer after EMP is given on the basis of the electrode potential studies.

S.K. Fedorov investigated the peculiarities of work and the main defects of threaded joint parts under different operating conditions, substantiated and investigated the principles of electromechanical restoration of parts with external metric threads, developed a design and technological method of increasing the durability of remanufactured threaded parts connections Proposed a method of restoring the profile of the thread at the time of the initiation of defects due to the plastic redistribution of the material of the parts. Introduced EMP to improve the operational properties of parts [8].

In the work of N.G. Dudkina, the main regularities of the formation of the surface structure during electromechanical processing and the influence of the given structure of the white layer on the change in mechanical properties, kinetics of deformation and destruction of steel 45 under load were revealed; the nature of

pressures during EMP is revealed, as a complex parameter of contact stresses from mechanical pressure on the tool and thermoelastic stresses arising during heating of the local microvolume. The regularities of changes in the physicomechanical properties and kinetics of microplastic deformations of steel 45 due to the structural inhomogeneity of the strengthened surface during EMP were established, and the regularities of changes in the cyclic strength of steel 45 due to different surface topography after EMP were determined. The properties of the surface layer were studied when EMP was combined with other methods [9].

In work [10], an improved EMP method is given in relation to the strengthening of the previously obtained profile of the metric thread and fundamentally new methods of restoring the defective screw surface are developed due to the plastic thermodynamic redistribution of the metal of the distorted areas, squeezing the material from the base and moving it in the desired direction with the simultaneous formation of a cavity and side surfaces. The conditions for the formation of the profile of thread turns with a hardened surface and a viscous core have been determined. The sophisticated possibility of electromechanical restoration of the worn thread profile. The dependence of the pressure in the contact zone on the geometrical parameters of the tool and on the physical and mechanical properties of the metal was established [11].

In the work of G.D. Fedotov, approximate analytical equations for the distribution of temperature fields in the tool from a constantly operating normal-circular heat source in the part, when the heat source moves along a helical line, were obtained. The possibility of using tungsten-free tool materials with low thermal activity during EMP is shown in order to increase the efficiency of EMP operations due to a greater strengthening effect on the surface layers of the processed parts with equal heat release in the contact zone of the tool with the part; the use of hard alloys with high electrical resistance makes it possible to achieve an even strengthening effect with lower energy costs and obtaining compressive residual stresses in the surface layers of the processed parts. A.V. Morozov investigated the improvement of the operational properties of thin-walled steel bushings by electromechanical mandrel (EMM). He proposed mathematical models of the EMM process, which allows studying the influence of EMM modes on the depth and structure of the strengthened layer, roughness, wear resistance of the inner surfaces of the bushings [12]. Selected EMM modes that allow obtaining a high-quality connection with tension along the outer diameter of a thin-walled steel sleeve with simultaneous surface hardening and a reduction in the roughness of the treated hole. Edigarov V.R. improved the processing method with preliminary application of antifriction material on the surface of the part followed by electromechanical processing (AFEMP). AFEMP of the surfaces of steel parts of tribosystems with preliminary application of a thin anti-friction layer made of various solid lubricants to the surface of the processed parts, which allows to change the structure of the surface layer, increase its wear resistance and operational characteristics, especially anti-friction due to the reduction of the friction moment of the tribopair samples. In A.V. Pavlov developed a method and technological equipment for electromechanical strengthening of shafts using three-phase current. He studied the influence of processing parameters when using three-phase current on the depth and hardness of the hardened layer, the wear resistance of the surface after EMP. Based on the analysis of the methods of manufacturing and restoration of threaded joint parts, in [13] a method of finishing and strengthening electromechanical processing of parts with an external metric thread to increase the fatigue life of threaded joints is proposed. The optimal values of current density, force in the contact zone and processing speed and their influence on the depth of hardening were determined. V. A. Petrushenko developed a method for calculating EMP modes for the production of various standard sizes of metric threads; calculated the contact temperature to ensure the specified depth of hardening; established the relationship between the temperature in the contact zone of the tool and the workpiece with technological modes of EMP and geometric parameters of the tool. S.M. Parshev studied the technological hardening by pulse electromechanical processing (PEP). The effect of PEP on the wear resistance of medium-carbon structural steels under conditions of abrasive wear and limit friction, the issue of accuracy during electromechanical processing, the stability of the cutting edges of blade tools when strengthened by the PEP method was studied.

In [14], he developed a method of improving the operational properties of threading parts of lifting mechanisms based on electromechanical processing. At the same time, mathematical models were obtained that establish the relationship between the technological modes of electromechanical processing and the depth of the hardened layer for screws made of 35, 45, 18KHT steels. It was established that the maximum hardness is achieved at a depth of 0.05...0.15 mm from the surface, and an increase in the carbon content in steel leads to an increase in the depth of the hardened layer.

Purpose

The purpose of the research is to increase the durability of console pumps by increasing the wear resistance of the executive surfaces of protective sleeves by electromechanical surface hardening.

Research methodology

Samples for bench tests were made of steel 40G, 40X, 45, U8, SHKH15 and cast iron SCH35 of the following sizes: outer diameter 25 mm; hole diameter 15 mm; height 20 mm. The roughness of the surfaces of the studied samples before EMSH corresponded to Ra3.2 μm according to DSTU 2789.

EMSH of the samples was performed on a lathe and screw-cutting machine with the modes: hardening speed 1.2 m/min; the current in the secondary circuit is 1600 A; secondary circuit voltage 3; force of adjustment of the tool 400 N; tool feed 2.5 mm/rev.

For carrying out wear tests, a stand was developed and manufactured, which allows simulating the operating conditions, the load pattern and the nature of the wear of the protective bushings.

The wear of the samples was determined by weighing on analytical balances AND GH-252 before and after the tests with a maximum weighing mass of 250 g with an accuracy of 0.00001 m. Before weighing, the samples were wiped with acetone, blown with air and dried in a muffle furnace at a temperature of 60 °C.

Research results

The formation of the structure of the strengthened zone of the surface layer during EMSH is a set of processes associated with the simultaneous influence of heating, plastic deformation and high cooling rate. This effect is accompanied by plastic deformation by grinding the grain and increasing the density of dislocations, and by hardening by changing the structure of the material.

The study of the microstructure of the samples after EMSH was performed on an metallographic microscope. The results of studies of the microstructure of steel and cast iron samples indicate the formation of a white layer with increased hardness and reduced corrosion in the hardening zones, even with large increases [15]. Depending on the original structure and modes of strengthening, the thickness of this zone can be different.

Studies of the structure of the surface layer after EMSH have shown that the structure of the white layer, observed in an optical microscope, looks like a continuous, uniform light field. This is due to the fact that with EMSH the process occurs instantly, phase transformations are combined with plastic deformations.

The specific properties of the white layer are explained by the occurrence in it of a special structureless martensite [16], which is characterized by a large dispersion of the structure, significant concentration heterogeneity and significant distortions of the crystal structure. In addition, the reason for reduced etchability and high hardness is changes in the electronic structure and chemical bonds of individual elements as a result of action in the processing zone of extreme temperatures and pressures. The white layer formed on the surface of the metal under the action of concentrated energy flows inherits both the heterogeneity of the composition and properties of austenite, which originates, generally speaking, under abnormal conditions, and the close to critical fineness of its structure.

The kinetics of austenite formation in pre-eutectoid steel during heating is characterized by certain features associated with the presence of structurally free ferrite in it. With high-speed heating of pre-eutectoid steel under EMSH conditions, independent transformation of structurally free ferrite into carbon-free iron becomes possible, i.e. e. without interaction between it and carburized austenite. With an increase in the heating rate, the dissolution of excess ferrite into austenite is gradually "suppressed", as a result of which most of the ferrite is overheated to higher temperatures, at which thermodynamic prerequisites are created for its diffusion-free transformation into austenite, typical for pure iron (at temperatures above 905°C), the subsequent (upon cooling) formation of low-carbon martensite in such areas. In addition, in the transition zone there is an area of incomplete hardening, as a result, when such an area is heated, the process of austenite formation does not proceed completely, and when it cools, an inhomogeneous structure is formed in it (Fig. 1). As the white layer is removed from the fragment, the temperature in the zone of thermal influence decreases, which leads to the formation of transitional structures. Their presence in the surface layer improves the surface quality of the protective sleeve.

After EMSH, the microhardness of the surface layer of steels increased by 2.6...3.6 times compared to the initial values. This hardness is much higher than the initial one and is 700...940 HV depending on the brand of material. The microhardness of cast iron SCH35 after EMSH is high (943 HV), but the depth of hardening is not great (0.2...0.3 mm).

For example, for U8 steel, the increase in microhardness at a depth of 0.05 mm from the surface was 3.6 times. Gradient layers with increased values of microhardness are observed at a depth of up to 1 mm under these regimes.
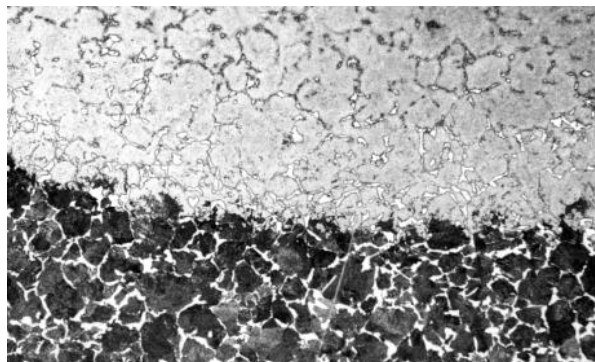
Fig. 1. The structure of the transition zone of 40G steel at EMSH

With removal from the surface, the microhardness decreases to the initial values. The transition zone has a microhardness lower than that of the white layer zone. This is explained by the presence of very high local heating temperatures at a high cooling rate, but insufficient for hardening these volumes.

The undulating change in microhardness values is associated with the specifics of electromechanical processing. If necessary, by choosing the appropriate processing parameters, you can possibly minimize this effect.

Reheating the previous track when the next one is applied leads to the release of previously formed martensite. An area of repeated hardening with heating close to the maximum temperature of heating for hardening, upon cooling, martensite, which has high microhardness, forms again in this area [17].

Analysis of the phase composition of steel was performed on a DRON-4-07 X-ray phase diffractometer in the following modes: Shooting step, gr. 0.050; tube mode BSV-27(Co) 20 mA, 35 kV; beta - filter - Fe; shooting method: according to Bragg - Brentano - w/2t; combined t=3000 s, V=4.0 g/min.

In the Table 1 and Fig. 2 presents the results of wear of the surfaces of the studied samples before and after EMSH.

Table 1

The results of wear measurements of samples before and after strengthening

Sample type	Wear, g			
	45	U8	SHKH15	SCH35
Initial	0,04199	0,01308	0,01696	0,02295
EMSH	0,01371	0,0068	0,0081	0,01222
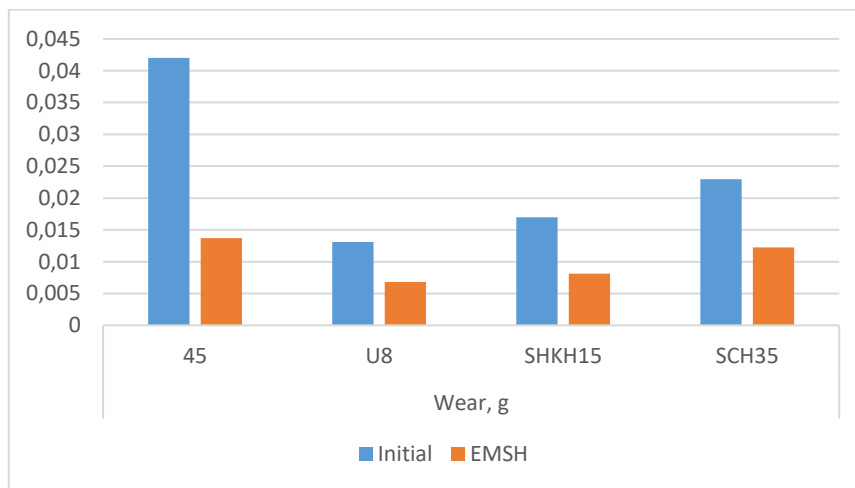
Fig. 2. Results of wear tests

The results of the research showed that in the conditions of contact between the protective sleeve and the oil seal in the friction zone of the abrasive during 30 min of tests, the wear resistance of the surface layer of steel 45, U8, SHKH15 and cast iron SCH35 after EMSH increased for steel 45 by 3.1 times, for steel U8 - by 1.9 times, SHKH15 steel - 2.5 times, cast iron - 1.9 times compared to the initial values. At the same time, the use of U8 steel samples after EMSH, instead of serial bushings made of 45 steel, allows to increase the wear resistance. details by 6.1 times.

Conclusions

1. An overview of modern methods of strengthening, their advantages and disadvantages allows recommending the technology of electromechanical processing and, in particular, electromechanical surface hardening, as one of the effective ways to increase the wear resistance of protective sleeves of cantilever pumps. The development of a mathematical model allows you to determine the temperature field in the contact zone, to get a visual picture of the change in the depth of hardening depending on the processing modes, with the possibility of its application to other materials.

It was established that the achievement of the highest values of microhardness of the surface layer at a depth of up to 1.2 mm is possible during electromechanical processing of the protective sleeves of cantilever pumps. The use of different modes and schemes of EMSH is accompanied by a change in the structure and, as a result, an increase in the hardness of the surface layer of the bushings.

2. The actual contact area of the tool roller with the treated surface and the depth of the temperature-deformation effect depend on the physical and mechanical properties of the materials and the pressing force. The calculation of the temperature field at the EMSH was carried out. The formation of a temperature gradient in the hardened zone at a depth of up to 1.2 mm from the surface has been proven.

3. Metallographic analysis of the surfaces of the sleeves treated by EMSH indicates the formation of a white layer with reduced corrosion and increased hardness in the hardening zones. The results of the X-ray structural analysis confirmed the formation of the martensite phase in the hardening zone. The microhardness of the hardened steel zone increased by 2.6...3.6 times compared to the initial values at a depth of up to 1 mm from the surface, depending on the materials. In the case of their overlap, the alternation of a fully hardened zone, a partially hardened zone, and a self-relief zone is observed. At the same time, the microhardness of steels along the surface depends on the hardening scheme.

4. Wear tests under friction conditions of parts of cantilever steam pumps with gland packing showed that the wear resistance of the protective bushings after EMSH increased by 3.1 times for steel 45, for steel U8 by 1.9 times, for steel SHKH15 by 2.5 times, for cast iron by 1.9 times compared to the initial values.

5. The use of U8 steel samples after EMSH, instead of serial bushings made of steel 45, allows to increase the wear resistance of parts by 6.1 times, which makes it possible to recommend U8 steel for use in the manufacture of protective bushings for console pumps.

References

1. Edenhofer, B. An overview of advances in atmosphere and vacuum heat treatment / B. Edenhofer // Heat treatment of metals. – 1999. – № 26. – P. 1–7.

2. Kula, P. New vacuum carburizing technology / P. Kula, J. Olejnik, J. Kowalewski // Heat treatment progress. – 2001. – № 1. – P. 57–65.

3. Felice Rubino. Thermo-mechanical finite element modeling of the laser treatment of titanium cold-sprayed coatings / Felice Rubino, Antonello Astarita, Pierpaolo Carlone // Coatings. – 2018. – P. 1–17.

4. W. Cheng, F. Dai, S. Huang, and X. Chen. Plastic deformation behavior of 316 stainless steel subjected to multiple laser shock imprinting impacts. Opt. Laser Technol. – 2022. – 153. doi: 10.1016/j.optlastec.2022.108201.

5. H. Liu. Effect of laser surface texturing depth and pattern on the bond strength and corrosion performance of phosphate conversion coating on magnesium alloy. Opt. Laser Technol. – 2022. – 153. doi: 10.1016/j.optlastec.2022.108164.

6. J. Jones, P. McNutt, R. Tosi, C. Perry, and D. Wimpenny. Remanufacture of turbine blades by laser cladding, machining and in-process scanning in a single machine. – 2012.

7. Rahito D. A. Wahab and A. H. Azman. Additive manufacturing for repair and restoration in remanufacturing: An overview from object design and systems perspectives" – 2019. – Processes, 7(11). MDPI AG. doi: 10.3390/pr7110802.

8. M. S. Alam and A. K. Das, Advancement in cermet based coating on steel substrate: A review," Mater. Today Proc. – 2022 – 56, pp. 805–810. doi:10.1016/j.matpr.2022.02.260

9. O. Lymar, D. Marchenko, "Prospects for the Application of Restoring Electric Arc Coatings in the Repair of Machines and Mechanisms", Proceedings of the 2022 IEEE 4th International Conference on Modern Electrical and Energy System, MEES 2022. https://doi.org/10.1109/MEES58014.2022.10005709.

10. R. Ranjan and A. K. Das. A review on surface protective coating using cold spray cladding technique. Mater. Today Proc., 56, pp. 768–773, (2022). doi: 10.1016/j.matpr.2022.02.254.

11. Marchenko, D., & Matvyeyeva, K. (2022). Increasing warning resistance of engine valves by gas nitrogenization method. Problems of Tribology, 27(2/104), 20–27. https://doi.org/10.31891/2079-1372-2022-104-2-20-27.

12. R. Ranjan and A. K. Das. A review on surface protective coating using cold spray cladding technique. Mater. Today Proc., 56, pp. 768–773, (2022), doi: 10.1016/j.matpr.2022.02.254

13. Marchenko, D., & Matvyeyeva, K. (2022). Study of the Stress-Strain State of the Surface Layer During the Strengthening Treatment of Parts. Problems of Tribology, 27(3/105), 82–88. https://doi.org/10.31891/2079-1372-2022-105-3-82-88.

14. X. Hu. Rolling contact fatigue behaviors of 25CrNi2MoV steel combined treated by discrete laser surface hardening and ultrasonic surface rolling" Opt. Laser Technol., 155, (2022) doi: 10.1016/j.optlastec.2022.108370.

15. Dykha A.V., Marchenko D.D. Prediction the wear of sliding bearings. International Journal of Engineering and Technology (UAE). India: "Sciencepubco–logo" Science Publishing Corporation. Publisher of International Academic Journals. 2018. Vol. 7, No 2.23 (2018). pp. 4–8. DOI: https://doi.org/10.14419/ijet.v7i2.23.11872.

16. Marchenko, D., & Matvyeyeva, K. (2023). Increasing the Wear Resistance of Restored Car Parts by Using Electrospark Coatings. Problems of Tribology, 28(1/107), 65–72. https://doi.org/10.31891/2079-1372-2023-107-1-65-72.

17. Marchenko, D., & Matvyeyeva, K. (2023). Research of Increase of the Wear Resistance of Machine Parts and Tools by Surface Alloying. Problems of Tribology, 28(3/109), 32–40. https://doi.org/10.31891/2079-1372-2023-109-3-32-40.

Марченко Д.Д., Матвєєва К.С. Дослідження зносостійкості циліндричних деталей електромеханічним поверхневим загартуванням

У роботі науково обґрунтовано застосування ефективної технології підвищення зносостійкості циліндричних деталей, на прикладі захисних втулок консольних насосів, за рахунок електромеханічного поверхневого загартування. Проведено огляд досліджень і встановлено, що досягнення найбільш високих значень мікротвердості поверхневого шару на глибині до 1,2 мм можливо при електромеханічній обробці захисних втулок консольних насосів. Застосування різних режимів та схем електромеханічного поверхневого загартування (ЕМПЗ) супроводжується зміною структури і, в результаті, підвищенням твердості поверхневого шару втулок. Фактична площа контакту інструментального ролика з оброблюваною поверхнею і глибина температурно-деформаційної дії залежать від фізико-механічних властивостей матеріалів та зусилля притискання. Доведено утворення температурного градієнта у зміцненій зоні на глибині до 1,2 мм від поверхні. Металографічний аналіз поверхонь втулок, оброблених ЕМПЗ свідчить про формування в зонах загартування білого шару зі зниженою травимістю і підвищеною твердістю. Результати рентгеноструктурного аналізу підтвердили утворення фази мартенситу в зоні зміцнення. Мікротвердість зміцненої зони сталей збільшилася в 2,6...3,6 рази порівняно з вихідними значеннями при глибині до 1 мм від поверхні в залежності від матеріалів. У випадку їх перекриття спостерігаються чергування повної загартованої зони, часткової загартованої зони і зони самовідпустки. При цьому мікротвердість сталей вздовж поверхні залежить від схеми зміцнення.

Випробування на зношування в умовах тертя деталей консольних насосів у парі з сальниковою набивкою показали, що зносостійкість захисних втулок після ЕМПЗ збільшилася для сталі 45 в 3,1 рази, для сталі У8 в 1,9 рази, для сталі ШХ15 у 2,5 рази, для чавуну в 1,9 рази порівняно з вихідними значеннями. Використання зразків зі сталі У8 після ЕМПЗ, замість серійних втулок із сталі 45, дозволяє підвищити зносостійкість деталей у 6,1 разів, що дозволяє рекомендувати до впровадження сталь У8 при виготовленні захисних втулок консольних насосів. На основі проведення досліджень дані рекомендації по застосуванню ЕМПЗ для утворення поверхневого шару з підвищеною зносостійкістю захисних втулок при виготовленні їх на виробництві та при ремонті консольних насосів в майстернях або сервісних центрах компаній АПК.

Ключові слова: зносостійкість, електромеханічне закалювання, довговічність, поверхневе зміцнення, циліндричні деталі

Experimental installation for wear tests of materials and coatings

M. Stechyshyn[1], O. Dykha[1*], V. Oleksandrenko[1], M. Tsepenyuk[2],V. Kurskoi[1], Ye. Oleksandrenko[1]

[1]Khmelnytskyi national University, Ukraine
[2]Ternopil National University, Ukraine
*E-mail: tribosenator@gmail.com

Abstract

On the basis of the analysis of existing tribological testing methodologies, which includes the selection of controlled wear parameters, the influence of the type of friction, contact geometry, surface roughness, the scheme of tribological research, the choice of a machine 2168UMT for friction testing of materials is substantiated. The friction machine allows you to install three samples at the same time, change the pressure in the contact zone in a wide range, control the moment of friction, the rotation frequency of the counterbody, the number of revolutions (friction path), change the rotation frequency, respectively, the sliding speed, automatically limit the distance traveled and other functions. The method of wear is adopted according to the finger-ring scheme, linear wear is monitored using an indicator rack with a value of divisions of the measuring device of 0.001 mm. To fix the samples on the machine caliper, holders were designed and manufactured, which ensure the self-fixation of the sample on the counterbody - a spherical joint made of the rolling body of the bearing. due to the fact that the samples were pressed against the counterbody with a force corresponding to the nominal contact pressure, they were self-aligned. After the sample was self-assembled, the whole structure was fixed by tightening the nuts. The counterbody is made of a rolling bearing ring, the material is steel SHX15, the hardness of the base is HRC 61. Three devices are mounted on the caliper for permanent lubrication of the running track immediately before the approaching sample. Thus, at certain values of pressure and speed, the mode of marginal friction can be reached, which was marked by a low coefficient of friction.

Key words: friction, installation, sample, wear, contact pressure, lubrication.

Introduction

It is desirable to evaluate the effectiveness of the surface modification of metal parts, tools, and equipment taking into account the conditions of further operation of the processing objects. Naturally, the rationale and choice of test methodology are of fundamental importance in forming conclusions regarding the effectiveness of the processing technology. At the same time, it is important, first of all, to ensure, to the extent that it is realistic, the adequacy of the test conditions to the modes of practical application of the processed parts. It is obvious that in this case, deviations not only in the type or method of testing, but also in the choice of limits for changing the main parameters of research can significantly affect the objectivity of the conclusions regarding the final results of the modification [1].

The main purpose of surface modification is, among other things (strengthening, increased corrosion resistance, fatigue resistance, etc.), increasing the wear resistance of friction pairs. Indeed, almost all processes of loss of performance of processing objects begin from the surface, among them wear is perhaps the most significant [2]. Therefore, it is important to choose a method of testing for wear resistance in such a way as to ensure adequacy to the conditions of future operation to the maximum extent possible, while the duration of the tests would be minimal, but this condition should not significantly affect the objectivity of the conclusions [3].

In general, most of the real operating schemes of general-purpose friction pairs refer to the model of frictional interaction, which is characterized by a system of parameters. These parameters precisely reflect the main processes of wear and strengthening of the surface as a result of frictional interaction, the mechanism of

movement of fracture fragments, elastic and plastic phenomena on the surface that take place as a result of frictional interaction, up to adhesion (caking) of surfaces.

Literature review

Let's consider the existing designs of friction machines that implement tests according to the "pin-disk" scheme. In [4], pin-on-disc sliding wear tests for each experimental condition were performed with a commercial tungsten carbide (WC) pin on silicon carbide (SiC) discs to determine the variance of the wear and friction data. In [5], each case study included an explanation of the individual modifications required to set up the test, including hardware and software settings. These case studies represented several application areas generated annually by the CSM Instrumentation Test Laboratory. Paper [6] describes a new universal tribometer design that allows simulation of various contacts and test types, such as pin-on-disc, ball-on-disc, and linear reciprocating tests. The new equipment allows tribological testing of samples of piston rings and cylinder liners at low and high temperatures and extreme lubrication conditions of any typical gasoline or diesel engine. Some friction results were shown under boundary conditions of lubrication between piston ring and cylinder liner sliding pairs, describing how the Tribotest machine is driven by an AC servo motor, which is more accurate than a DC motor. In [7], a study of the rate of wear and friction for various materials under the influence of load according to the pin-on-disk scheme was carried out. The tests were carried out using a pin disc tribometer using SKD II and aluminum alloy A 5083 as the workpiece material. The test was tested using different types of grease with different loads. The article [8] presents the design of a "pin-on-disc" type tribometer designed for experimental characterization of static and dynamic friction behavior for various pairs of sliding samples. The normal force, sliding speed and temperature, as the main influencing parameters, are precisely controlled during the experiments by using vertical and rotational servo axes and an electric heater embedded in the rotating disk. A compact triaxial piezoelectric force sensor placed between the vertical-axis screw driver and the friction specimen provides direct measurement of normal and tangential forces used to calculate the coefficient of friction of the specimen. The document [9] exposes a machine built for testing the friction, lubrication and spoilage. Its test conditions have a large file of options to execute tribology tests checking the working conditions, like movement way (reciprocating or linear), parts in contact, movement speed, self-lubrication, part geometry, temperature range, humidity, materials. To perform this test, the tribometer uses the principle of the disc revolution, the load is applied directly over the arm and do the measure according to the standard obtaining the results with accuracy. In [10] pin on disc tribometer is a device to determine coefficient of friction and wear rate of the different materials. There is a need to design a tribometer as per standards for different applications. This study was about designing and developing a low-cost tribometer to study the wear of automotive engine materials under lubricants with nano additives. Pin on disc arrangement was designed as per ASTM standard G 99–17. The parameters that can be controlled in the test rig are load, sliding distance, sliding speed, wear track diameter, lubricant temperature, mixing time of nano additives in lubricants, mixing speed to the stirrer. A pin-on-disk tribometer for micro-scale applications is presented in paper [11]. The tribometer consists of a stationary mm-scale pin and a rotating disk. Friction and lubrication film thickness are measured by a laser position detector and a laser displacement sensor. Using this tribometer, hydrodynamic tests have been carried out with the specimens fully submerged in a lubricant. Results suggest that the sliding motion in the mm-scale operates with a direct contact at low speed, and in the hydrodynamic regime at a higher speed. When the sliding reaches the critical speed, the lubricant film is established, and the thickness of the film stabilizes and the friction increases with the sliding speed. The tribometer shows good repeatability in these tests. In [12] the design and fabrication of the apparatus are presented with initial test results conducted to investigate the power efficiency and wear performances of several polymer and metal samples. Our results show that for a fixed power transmission torque, there exists a critical pre-load between the drive components at which the wear and slip are maximum and the value of critical pre-load is independent of the material. Both wear and slip can be minimized to near-zero if an optimum pre-load, which is higher than the critical pre-load, is applied between the two components. Therefore, expanding the technological parameters of machines for friction and wear tests is an urgent task. hydrodynamic tests have been carried out with the specimens fully submerged in a lubricant. Results suggest that the sliding motion in the mm-scale operates with a direct contact at low speed, and in the hydrodynamic regime at a higher speed. When the sliding reaches the critical speed, the lubricant film is established, and the thickness of the film stabilizes and the friction increases with the sliding speed. The tribometer shows good repeatability in these tests. In [12] the design and fabrication of the apparatus are presented with initial test results conducted to investigate the power efficiency and wear performances of several polymer and metal samples. Our results show that for a fixed power transmission torque, there exists a critical pre-load between the drive components at which the wear and slip are maximum and the value of critical pre-load is independent of the material. Both wear and slip can be minimized to near-zero if an optimum pre-load, which is higher than the critical pre-load, is applied between the two components. Therefore, expanding the technological parameters of machines for friction and wear tests is an urgent task. hydrodynamic tests have been carried out with the specimens fully submerged in a lubricant. Results suggest that the sliding motion in the mm-scale operates with a direct contact at low speed, and in the hydrodynamic regime at a higher speed. When the sliding reaches the critical speed, the lubricant film is established, and the thickness of the film stabilizes and the friction increases with the sliding speed. The tribometer shows good repeatability in these tests. In [12] the design

and fabrication of the apparatus are presented with initial test results conducted to investigate the power efficiency and wear performances of several polymer and metal samples. Our results show that for a fixed power transmission torque, there exists a critical pre-load between the drive components at which the wear and slip are maximum and the value of critical pre-load is independent of the material. Both wear and slip can be minimized to near-zero if an optimum pre-load, which is higher than the critical pre-load, is applied between the two components. Therefore, expanding the technological parameters of machines for friction and wear tests is an urgent task.

Selection and assessment of wear parameters

In setting up the test methodology, a special role belongs to the selection of wear parameters that need to be controlled. The nature of the friction process from the point of view of the lubrication regime is easiest to control by determining the friction coefficient [13]. In most experimental friction machines, this parameter is calculated by comparing the force of normal pressure in the contact zone with the circular force, to determine which it is necessary to control the moment of friction. In principle, linear and volumetric wear are interrelated, however, accurate determination of the volumetric parameter requires no less accurate knowledge of the actual contact area, and this parameter even in the theoretical aspect is somewhat complicated (taking into account the configuration of the microprofile).

The mass parameter of wear is determined in principle easily, but the main methodological problem when using it is that it is necessary to remove the samples from the stand every time, and re-installing them in the same position is practically impossible. For this reason, after each measurement, the reproduction of previous friction conditions in the sense of mutual abutment of surfaces, uniform pressure across the contact plane, etc. is unrealistic, and hence inevitable problems with the reliability of each subsequent measurement. True, in this sense, the method when the samples are installed in the head, modified together with it and tested in this form deserves attention. However, such a technique significantly increases the duration of tests.

Type of friction

The choice of the type of friction, as a rule, mainly depends on the design features of the real operating conditions of the friction pairs. It is obvious that most often in the conditions of most typical designs, sliding friction is observed, which, among other things, is the most productive in terms of wear rate. A special role is played by the choice of lubrication mode [13]. Dry friction, which would obviously ensure the maximum rate of wear and, accordingly, the minimum duration of the tests, nevertheless could slightly distort the wear process, since in this case the temperature in the contact zone and the parts of the friction pair as a whole would increase significantly [14]. In addition, it is problematic to find pure dry friction in real friction pairs. The liquid mode of friction requires special devices or test conditions that would guarantee this mode. In most real pairs of friction, there is a limit mode of friction, the provision of which is relatively easy to control through the coefficient of friction [15].

Contact geometry

The geometry of the contact is to some extent related to the type of mutual movement of the sample and the counterbody. In principle, the contact surface can be in the form of a plane, cone, cylinder or sphere. In addition to the plane, all other types theoretically provide contact geometry in the form of a line - straight or curved, including - spatial. It is obvious that depending on what the force characteristics of the contact will be, and, accordingly, its type - elastic or plastic, including intermediate forms, the real contact area will change significantly, which makes comparison of experimental results problematic. The contact in the form of a plane is most simply implemented, since in this case there are no issues with determining the nominal contact area. As for the type of mutual movement, with flat contact, the relative velocity vector should be directed tangential to the contact plane [14]. At the same time, in order to ensure equal wear conditions at all contact points, it would be desirable for the magnitude and direction of the relative velocity vector to be the same, since in this case, for example, a friction scheme similar to rotational friction or a variant of end friction, when the speed at different contact points is excluded is significantly different (a relatively large ratio of the width of the contact pad to the radius of rotation).

Surface roughness

Finally, a very important, if not decisive, role is played by the roughness of the contacting surfaces, both in particular and the established one, which is formed as a result of running-in. At the same time, the following is essential.During the run-in process, the surface of the sample is compacted due to the action of normal pressure and the interaction of the surface and the destruction fragments (depending on the type of movement mechanism of these fragments). In this way, the problem of choosing the value of the nominal pressure in the friction pair arises, since the test process will go differently if it is gradually increased during the experiment, while the surface microhardness will increase, or if a certain value of this pressure is immediately established. In the first case, the

process is possible at certain, sometimes very large, values of the nominal pressure in the contact zone. An attempt to start the test immediately at this pressure value can usually lead to adhesion of the surfaces [14, 15].

Selection of the scheme and parameters of tribological studies

Thus, as a result of the above analysis, the following priorities emerge when choosing the scheme and parameters of experimental studies [13-15]:

1. The contact area should be as small as possible. In this case, both the distribution and magnitude of pressure stresses in the contact zone will be almost uniform over the entire area of the research object. True, then the ratio of the area of the zone near the edge to the total area increases, but this shortcoming can be compensated by more careful sample preparation. At the same time, chamfers or rounding of edges should be minimal and as stable as possible. In addition, minimization of the size of the contact surface will facilitate the installation of samples on the counterbody, in which case tight contact would immediately be ensured over the entire area.

2. The nature of the mutual movement of the sample and the counterbody, taking into account certain complexities of the design of their fixation, which must be self-installed on the counterbody, should be optimally chosen according to the scheme: the sample is stationary, the counterbody rotates. Then the sample slides over the counterbody along a track with a sufficiently large radius, which, compared to the size of the sample, ensures a minimal difference in speeds at all points of the contact area.

3. The optimal shape of the contact pad is a plane, and to minimize the impact of uneven pressure distribution around the edges, the shape of the contact pad of the sample is round. Among other things, in this case fixing and processing of samples with high accuracy is simplified. For the convenience of measurements, basing samples in, as well as minimizing the duration of tests, linear wear was chosen as a control parameter. In this case, there is no need to remove the samples from the stand and thus the problem of re-basing the samples disappears.

Presenting main material

The 2168UMT model friction testing machine was chosen as the test stand, which allows you to set three samples at the same time, change the pressure in the contact zone in a wide range, control the friction moment, the frequency of rotation of the counterbody, the number of revolutions (friction path), change the frequency in a wide range rotation, respectively - sliding speed, automatically limit the distance traveled and other functions. The method of wear is adopted according to the finger-ring scheme, linear wear is monitored using an indicator rack with a value of divisions of the measuring device of 0.001 mm. To fix the samples on the caliper of the machine, holders were designed and manufactured, the construction of which is shown in fig. 1.
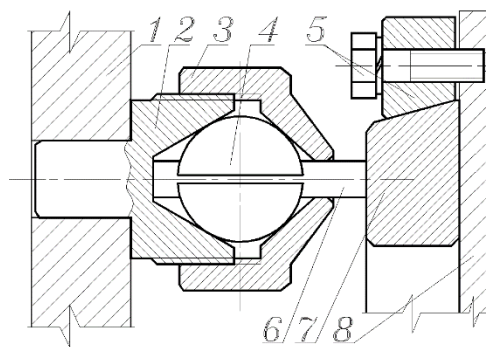
Fig. 1. Sample fastening scheme: 1 – caliper, 2 – saddle, 3 – nut, 4 – spherical joint, 5 – counterbody retainer, 6 – sample, 7 – counterbody, 8 – washer

The main element of the design, which ensures the self-fixation of the sample on the counterbody, is a spherical joint made of the rolling body of the bearing. Previously, the ball was released, a hole was drilled in a special centering device along the diameter of the sample, and then the ball was sprayed into two parts. To install the samples, the support with the holders is brought to the counter body and due to the fact that the samples were pressed against the counter body with a force corresponding to the nominal contact pressure, they were self-installed. After the sample was self-assembled, the whole structure was fixed by tightening the nuts. Visual control indicates a high quality of contact, since a stain is observed over the entire area of the sample already on the first segments of the friction path. The counterbody is made of a rolling bearing ring, the material is steel SHX15, the hardness of the base was HRC 61. The taper necessary for fixing the counterbody was formed by processing the ring using a mineral-ceramic cutter. The general appearance of the stand is shown in fig. 2 (a – a general view of the caliper in the retracted state, b – the holder in the working state). Three devices are mounted on the caliper for continuous lubrication of the running track immediately before the running sample. Thus, at certain values of pressure and speed, the mode of liquid friction can be achieved, which was marked by a low coefficient of friction. Samples of various steels were produced by fine turning (the tolerance was minus 0.05 to 0.01 mm). Within the

limits of tolerance, samples were sorted into groups through selective selection, which made it possible to use samples of only one size group for a specific mode of modification in the following [15].

a)   b)
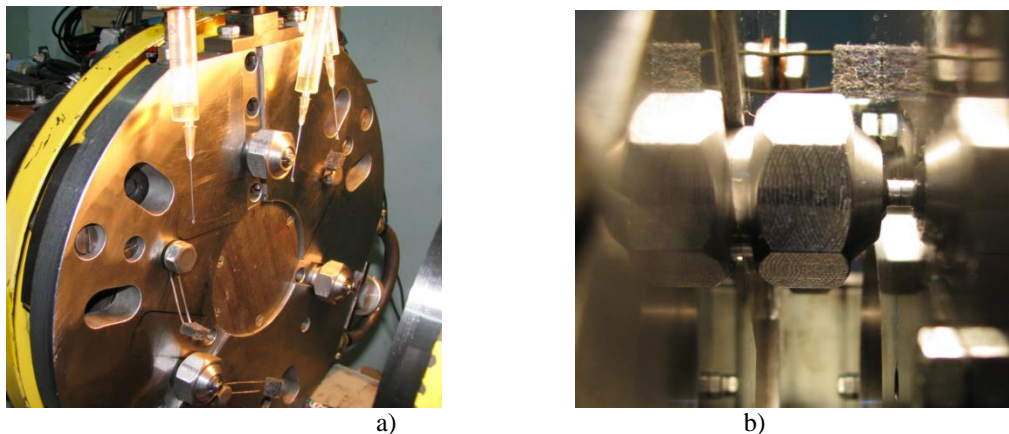
Fig. 2. General view of the caliper of the friction machine

The latter makes it possible to achieve approximate equality of the contact area, simplifies modeling of the nominal pressure in the contact zone. Next, the samples were first ground in a special multi-position mandrel from one end (base), then to size along the length from the other. The design of the mandrel made it possible to ensure the perpendicularity of the ends of the cylindrical surfaces with high accuracy, but, as the practice of using samples in the friction machine showed, this accuracy is not enough for contact over the entire surface of the end from the very beginning of the wear resistance studies. This explains the need for the design of the holder described above. In the axial direction (the direction of the normal force), the samples are based on the bottom of the saddle 2 (Fig. 1), so the distance from the bottom plane to the base surface of the caliper must be maintained with high accuracy. The caliper disc itself is polished with high precision both on the plane of contact with the saddle and in the mounting holes for the shank of the saddles.

Conclusion

Thus, on the basis of the analysis of existing tribological testing methodologies, which includes the selection of controlled wear parameters, the influence of the type of friction, contact geometry, surface roughness, the scheme of tribological research, the choice of a machine 2168UMT for friction testing of materials with a device that ensures self-installation of samples on the counterbody is justified, namely, a spherical joint made of a rolling bearing body.

References

1. Stechyshyna N.M. Corrosion-mechanical wear resistance of food production equipment parts: monograph / N.M. Stechyshina, M.S. Stechyshyn, N.S. Mashovets – Khmnelnytskyi: KhNU, 2022. 181p.

2. M. Stechyshyn, M. Macko, O. Dykha, S. Matiukh, J. Musial. Tribotechnologies of strengthening and wear modeling of structural materials. Bydgoszcz: Foundation of Mechatronics Development, 2023. 196p.

3.Kornienko A.O. Formation of tribotechnical properties of nickel-based composite electrolytic coatings by creating gradient structures: autoref. thesis Ph.D. technical of science K.: NAU, 2007. 21 p.

4. Guicciardi, S., Melandri, C., Lucchini, F., & De Portu, G. (2002). On data dispersion in pin-on-disk wear tests. Wear, 252(11-12), 1001-1006.

5. Nair, RP, Griffin, D., & Randall, NX (2009). The use of the pin-on-disk tribology test method to study three unique industrial applications. Wear, 267(5-8), 823-827.

6. Kaleli, H. (2016). New Universal Tribometer as Pin or Ball-on-Disc and Reciprocating Pin-on-Plate Types. Tribology in Industry, 38(2).

7. Syahrullail, S., & Nuraliza, N. (2016). Effects of different load with varying lubricant on the friction coefficient and wear rate using pin on disk tribometer. Applied Mechanics and Materials, 819, 495-498.

8. Hoić, M., Hrgetić, M., & Deur, J. (2016). Design of a pin-on-disc-type CNC tribometer including an automotive dry clutch application. Mechatronics, 40, 220-232.

9. Hidalgo, BDA, Erazo-Chamorro, VC, Zurita, DBP, Cedeño, EAL, Jimenez, GAM, Arciniega-Rocha, RP, ... & Pijal-Rojas, JA (2022). Design of Pin on Disk Tribometer Under International Standards. In Applications of Computational Methods in Manufacturing and Product Design: Select Proceedings of IPDIMS 2020 (pp. 49-62). Singapore: Springer Nature Singapore.

10. Singh, H., Singh, AK, Singla, YK, & Chattopadhyay, K. (2020). Design & development of a low-cost tribometer for nanoparticulate lubricants. Materials Today: Proceedings, 28, 1487-1491.

11. Wu, J., Liu, T., Yu, N., Cao, J., Wang, K., & Sørby, K. (2021). A pin-on-disk tribometer for friction

and lubricating performance in mm-scale. Tribology Letters, 69, 1-6.

12. Sinha, SK, Thia, SL, & Lim, LC (2007). A new tribometer for friction drives. Wear, 262(1-2), 55-63.

13.Stechyshyn M.S. Durability of food industry equipment parts under corrosive-mechanical wear. Diss. Ph.D. Khmelnytskyi: TUP. 1998. 329p.

14. MS Stechishyn, M.Ye. Skyba, AV Martynyuk, D.V Zdorenko. Wear resistance of structural steels nitrided in a cyclically switched discharge with dry friction. Problems of Tribology, V. 28, No. 1/107-2023, 20-24.

15. MS Stechyshyn, VV Lyukhovets, NM Stechyshyn, MI Tsepenyuk.Wear resistance of structural steels nitroded in cyclic-commuted discharge at limit modes of friction. //Problems of Tribology. – Khmelnytskyi: KHNU, 2022. – V. 27. - No. 3/105. - P.27-33.

Стечишин М.С., Диха О.В., Олександренко В.П., Цепенюк М.І., Курской В.С., Олександренко Є.Г.
Експериментальна установка для випробувань на знос матеріалів і покрить

На основі проведеного аналізу існуючих методологій трибологічних випробувань, що включає вибір контрольованих параметрів зношування, впливу виду тертя, геометрії контакту, шорсткість поверхні, схеми трибологічних досліджень обгрунтовано вибір машини для випробувань матеріалів на тертя. Машина тертя дозволяє одночасно встановлювати три зразки, в широкому діапазоні змінювати тиск в зоні контакту, контролювати момент тертя, частоту обертання контртіла, кількість обертів (шлях тертя), змінювати частоту обертання, відповідно, швидкість ковзання, автоматично обмежувати пройдений шлях та інші функції. Метод зношування прийнято по схемі палець-кільце, лінійне зношування контролюється за допомогою індикаторної стійки з ціною поділок вимірювального приладу 0,001 мм. Для закріплення взірців на супорті машини спроектовано та виготовлені державки, які забезпечують самовстановлюваність зразка на контртілі – сферичний шарнір, виготовлений з тіла кочення підшипника. за рахунок того, що зразки притискалися до контртіла з силою, котра відповідає номінальному тиску в контакті, вони самовстановлювалися. Після того, як взрець самовстановився, вся конструкція фіксувалась шляхом затягування гайок. Контртіло виготовлене з кільця підшипника кочення, матеріал – сталь ШХ15, твердість основи становила HRC 61. На супорті змонтовано три пристрої для постійного змащення бігової доріжки безпосередньо перед зразком, який набігає. Цим, при певних значеннях тиску та швидкості, може досягатись режим граничного тертя, що відмічалось низьким показником коефіцієнта тертя.

Ключові слова: тертя, самовстановлення, зразок, знос, контактний тиск, змащування

Determination of the regularity of the rate of wear of the working hydraulic cylinder of the mechanism of the sealing plate of the garbage truck from the pressing force

O.V. Bereziuk[1*] , V.I. Savulyak[1] , V.O. Kharzhevskyi[2] , A.Ye. Alekseiev[1]

[1] *Vinnytsia National Technical University, Ukraine*
[2] *Khmelnytskyi National University, Ukraine*
*E-mail: berezyukoleg@i.ua

Abstract

The article is dedicated to the study of the influence of the pressing force on the wear resistance of the working hydraulic cylinder of the mechanism of the sealing plate of the garbage truck. The usage of a mathematical dependencies and appropriate software programs for regression analysis made it possible to determine the exponential regularity of the change in the rate of wear of the working hydraulic cylinder of the mechanism of the sealing plate of the garbage truck depending on the pressing force. A graphical dependence of the change in the rate of wear of the working hydraulic cylinder of the mechanism of the compacting plate of the garbage truck on the pressing force was made up, which confirmed the sufficient convergence of the obtained regularity. Graph of the influence of pressing force on wear rate of working hydraulic cylinder of the mechanism of the compacting plate of the garbage truck demonstrates the expediency of its increase. It was established that for the garbage truck of Ukrainian production of serial model KO-436, the rate of wear of the working hydraulic cylinder of the mechanism of the sealing plate of the garbage truck according to the obtained regularity will be 0.257 μm/h. The expediency of conducting additional studies to determine further ways to increase the wear resistance of the working hydraulic cylinder of the sealing plate mechanism of the garbage truck has been established.

Key words: wear, wear resistance, wear rate, hydraulic cylinder, mechanism, sealing plate, garbage truck, pressing force, municipal solid waste, regression analysis.

Introduction

An important task of mechanical engineering is to increase the wear resistance and reliability of the executive bodies of machines [1, 2], in particular, utility machines equipped mainly with a hydraulic drive of working bodies [3]. One of the main technologies of primary processing of municipal solid waste (MSW) in order to reduce the costs of their transportation, as well as the negative impact on the natural environment, is their compaction during the process of loading into a garbage truck. Compaction of MSW in the garbage truck is performed by a compacting plate, the working hydraulic cylinder of the mechanism of which undergoes from intensive wear, which is caused by a large number of work cycles, as well as significant efforts of pressing solid waste, which have a non-linear compression characteristic. Hydraulic cylinders are usually made of alloy steel. The usage of wear-resistant coatings to increase their wear resistance is explained. Therefore, the urgent task is to determine the regularity of the change in the rate of wear of the working hydraulic cylinder of the mechanism of the sealing plate of the garbage truck due to the pressing force.

Analysis of recent research and publications

The work [1] gives the research results of the processes of destruction during friction on the example of composite electrolytic coatings. By means of the analysis methods of theoretical and experimental research results within the energy model of the formation of wear particles in the near-surface zones of the friction pair, an

assessment of the process of destruction of the surface layers was made. The dependence of the size of the wear particles on the mechanical properties of the material was established.

In the article [3], using the results of computer modeling of the hydrodynamic processes of the flow of the working fluid through the hydraulic valve, its pressure losses are determined. In order to reduce pressure losses, it is proposed to make changes to the design of the hydraulic valve without impairing its performance. It made it possible to reduce pressure losses on the working part of the hydraulic distributor, which reduces overall losses in the hydraulic drive.

In the article [4], a study of the peculiarities of the process of pressing wood shavings in screw machines, as well as the processes taking place in different sections of the screw, was carried out also, appropriate regularities were determined. It allows to calculate the loads acting on the turns of the screw, as well as determine the pressing power. The degree of heating of raw materials and specific energy consumption during the pressing process were determined.

In the article [5], a regression analysis was used to determine a power law that describes the dynamics of wear and tear of garbage trucks in the Khmelnytskyi region that allows to forecast and plan the infrastructure of communal enterprises, in particular, the renewal of garbage trucks, the base for maintenance and repair, which is necessary to solve the problem of solid waste management. It has been predicted that by 2030, the wear and tear of garbage trucks in the Khmelnytskyi region will decrease to 51.9% at the current rate of decline.

The logarithmic regularities of screw wear depending on the hardness of its surface for different values of the friction path are defined in the paper [6]. Conducting an additional regression analysis made it possible to obtain the dependence of wear of the auger depending on the hardness of its surface and the friction path. The obtained dependence permitted to establish that during two-week operation and wear of the auger during the dehydration of MSW in the garbage truck, an increase in the surface hardness of the auger from 2.31 GPa to 10.05 GPa leads to a decrease in the rate of growth of the energy intensity of solid waste dehydration from 16.7% to 1.5%, and, therefore, to the cheaper process of their dehydration in the garbage truck.

Among the main components of garbage trucks with a side-loading method of MSW, the hydraulic system, according to the research [7], has the shortest mileage before failure, which makes the most significant contribution to increasing the wear and tear of garbage trucks. Based on the results of research [8], the structure and most frequent causes of failures of the hydraulic equipment of garbage trucks were determined: hydraulic cylinders – 34.92% (wear of cuffs, seals, rod; rupture of the nut attaching the piston to the rod; bending of the rod; mechanical damage), hydraulic pump – 16.40% (casing failure, wear of gears, extrusion of oil seals, cracks in the casing), pipelines, hoses – 15.34% (breakage of hoses, wear of pipelines), hydraulic distributor – 13.23%, (wear of seals, spools; cracks in the casing).

An analysis of the causes of typical technical failures of garbage truck units [9] also showed that the majority of malfunctions (about 45%) are associated with failures of the hydraulic drive, which mainly are due to manufacturing defects caused by the installation of low-quality components on the hydraulic drive, as well as large fluctuations of loads on working bodies. The study of the causes of failures of working bodies showed that breakdowns occur due to defects in heat treatment and deviations from structural dimensions during mechanical processing (35%), defects in assembly, adjustment, tightening of threaded connections (30%), poor-quality welding (30%), etc. It was established that most failures (80-90%) occur due to wear and corrosion phenomena on the working surfaces of machine parts. At the same time, the failure does not occur immediately, but after the wear or corrosion reaches a certain, critical value, that is, when the limit state of the machine or its units comes. It was also established that failures of hydraulic cylinders due to wear of the working surfaces of couplings, deformation of the rod and cylinder during operation account for up to 28% of all failures of hydraulic drive elements. The analysis of durability results shows that the average working time before failure of the hydraulic drive elements, in particular the hydraulic cylinder, is about 1/3 of the maximum, that is, the resource planned by the manufacturer is not produced by 45-55%. The main share of failures of hydraulic cylinder parts since the start of operation or after previous repair is accounted for by rods - 31% and sealing sleeves - 42%. Analysis of failures of hydraulic system elements showed that the main manifestations of malfunctions are the loss of external and internal tightness due to contamination of the working fluid, which causes a malfunction of the units.

The given data are also correlated with the data published in the article [10], which also states the main reasons for the failure of the hydraulic system of garbage trucks caused by wear: for the hydraulic pump – gear wear; for hydraulic cylinders – wear of cuffs, seals, rod; for the hydraulic distributor – wear of seals, spools; for hoses – wear and tear of pipelines. Adequate dependencies, according to the Fisher criterion, of wear of garbage truck tires on the front and rear axles due to the mass of MSW transported and mileage of the garbage truck are determined. It was established that, according to the Student's criterion, among the investigated factors of influence, the weight of the transported MSW has the greatest influence on the wear of the tires of the garbage truck on both the front and rear axles, and the mileage of the garbage truck has the least influence. The regularities of the number of trips of the garbage truck to the maximum allowable tire wear on the front and rear axles were obtained.

In work [11], the distribution of the reasons for failure of garbage trucks is given, from which it follows that the main causes of malfunctions are external and internal leakage of hydraulic systems. It was established that the external leakage is 48% of all failures in the hydraulic system and occurs as a result of the destruction of hoses and pipelines, as well as depressurization of the seals of hydraulic cylinders and other units. Another common cause of failure is internal leakage, which was observed in 36% of cases. Most of the malfunctions caused by internal leakage have such units as spool distributors, safety and non-return valves, hydraulic cylinders and hydraulic pumps.

In the work [12] it was established that "conical" wear of the hydraulic cylinder rod from 0.2 to 0.4 mm in length during the operation of the hydraulic cylinder before the first overhaul causes a drop in pressure by 7.2%, an increase in specific fuel consumption by 11, 4% and the content of carbon monoxide in exhaust gases – by 26%; an increase in the wear of the rods in their working area by 0.6-0.7 mm causes a drop in pressure in the hydraulic system by 13.4%, an increase in specific fuel consumption by 21.3% and an increase in the toxicity of exhaust gases from 25% to 59%, which exceeds the permissible norms. It was proposed to consider the value of 0.4 mm as the maximum allowable wear value of the geometric parameters of the rod of the hydraulic cylinder of the hydraulic drive of construction and road machines. It was also established that wear of the rod deteriorates the physical and chemical properties of the working fluid, doubles the content of iron and impurities in the working fluid, which leads to the need for its frequent replacement and overspending, which significantly reduces efficiency and durability, shortens the service life of the hydraulic drive of construction and road machines.

In the work [13] it is stated that the wear of sealing elements in hydraulic systems leads to the gradual ingress of hydraulic fluid into non-working cavities of hydraulic machines. Although this process is not visually apparent, it causes unproductive losses of power of the hydraulic drive, which, in turn, leads to excessive consumption of fuel, lubricants and power losses of working bodies. Loss of power in the elements of the hydraulic system due to the wear of the sealing elements can lead to suboptimal operating modes of the hydraulic motor, which leads to a decrease in the efficiency of the hydraulic drive in a whole. The mechanical system "hydraulic cylinder – compacted piston – compressed hydraulic fluid" is considered. The dependence of the efficiency of the hydraulic cylinder on the size of the leak was established. The piston subsidence results for the working fluid were determined. The mechanism of liquid flow through the hydraulic cylinder seal is also determined.

The authors of the work [14], during the evaluation of the observation results of garbage trucks, found that the largest number of failures occurs due to wear and corrosion of the working surfaces of the working equipment parts. Failures of hydraulic cylinders caused by wear of the working surfaces of couplings, deformations of the rod and cylinder during operation are 32% of all failures of hydraulic drive parts. It happened due to the uneven loading of the body, as well as the abrasive wear of the working surfaces in the hard conditions of the work of garbage truck. The research of the reasons for failures that was carried out, allowed to establish that the main cause is wear of the working surfaces of the main parts in the design of the hydraulic drive, namely spools and housings of hydraulic distributors, hydraulic cylinder rods, etc. The main cause of wear was hydroabrasive damage due to untimely replacement of the working hydraulic fluid and the use of poor-quality or worn sealing parts such as oil seals of hydraulic cylinders, which causes dust particles and wear products to enter the sliding zone, which lead to the acceleration of the process of wear of the working surfaces of the parts. One of the most promising ways to restore worn parts is chrome plating in a cold self-regulating electrolyte in order to obtain chrome coatings with high deposit quality and high productivity.

The paper [15] provides data on the effect of pressing force on the rate of wear of hydraulic press mechanism parts, in particular, the working hydraulic cylinder. It was established that with an increase in the force of the hydraulic press, the acceleration coefficient of the tests of the working cylinder decreases. It is also noticed that the development of measures for permanent automatic control and prevention of the approach of the hydraulic press to the emergency limit is a main factor for ensuring the trouble-free operation of its basic components, at conditions if they are optimally designed and that the performance indicators correspond to the specified operational characteristics.

However, as a result of the analysis of known publications, the authors did not find specific mathematical dependencies of the change in the rate of wear of the working hydraulic cylinder of the mechanism of the sealing plate of the garbage truck due to the pressing force.

Aims of the article

Determination of the dependence of the change in the rate of wear of the working hydraulic cylinder of the mechanism of the sealing plate of the garbage truck as a result of the acting of the pressing force.

Methods

The determination of the paired regularity of the change in the rate of wear of the working hydraulic cylinder of the mechanism of the compacting plate of the garbage truck from the pressing force was carried out by the method of regression analysis. Regression was determined on the basis of linearization transformations that allow to reduce the non-linear dependence to a linear one. The coefficients of the regression equation were determined by the method of least squares using the developed computer software "RegAnaliz", which is protected by a certificate of copyright law.

The results

The values of the rate of wear of the working hydraulic cylinder of the hydraulic press mechanism at different values of the pressing force are given in the Table 1 [15]. The rate of wear decreases with increasing

pressing force. This is explained by the fact that with a constant power of the drive, an increase in the pressing force leads to a decrease in the pressing speed and the amount of work performed.

Table 1

The influence of pressing force on the rate of wear of the working hydraulic cylinder of the hydraulic press mechanism [15]

№	Pressing force F_{PR}, MN	Wear rate v_w, μm/h
1	30	0.191
2	40	0.169
3	50	0.151
4	60	0.138
5	70	0.124
6	80	0.111
7	90	0.102
8	100	0.089
9	110	0.080
10	120	0.071
11	130	0.067
12	140	0.062
13	150	0.053

As a result of the regression analysis of the data in the Table 1, the dependence of the change in the rate of wear of the working hydraulic cylinder of the mechanism of the sealing plate of the garbage truck is determined depending on the pressing force

$$v_w = 0{,}2575\mathrm{e}^{-0{,}01047 F_{PR}} \text{ [μm/h]},\qquad(1)$$

where v_w is the rate of wear, μm/h; F_{PR} – pressing force, MN.

The results of the regression analysis are shown in Table 2, where cells with the maximum values of the correlation coefficient R for paired regression are marked in gray color.

Table 2

The results of the regression analysis of the dependence of the change in the rate of wear of the working hydraulic cylinder of the mechanism of the sealing plate of the garbage truck on the pressing force

№	Type of regression	Correlation coefficient R	№	Type of regression	Correlation coefficient R
1	$y = a + bx$	0.98253	9	$y = ax^b$	0.97824
2	$y = 1 / (a +)\_$	0.98588	10	$y = a + b \cdot \lg x$	0.99858
3	$y = a + b / x$	0.96354	11	$y = a + b \cdot \ln x$	0.99858
4	$y = x / (a + bx)$	0.96953	12	$y = a / (b + x)$	0.98588
5	$y = ab^x$	0.99892	13	$y = ax / (b + x)$	0.83269
6	$y = ae^{bx}$	0.99893	14	$y = ae^{b/x}$	0.90835
7	$y = a \cdot 10^{bx}$	0.99892	15	$y = a \cdot 10^{b/x}$	0.90835
8	$y = 1 / (a + be^{-x})$	0.38561	16	$y = a + bx^n$	0.93336

It was established that the rate of wear of the working hydraulic cylinder of the mechanism of the compacting plate of the garbage truck decreases exponentially with increasing pressing force.

In the Fig. 1 is shown the graphical dependence of the change in the rate of wear of the working hydraulic cylinder of the mechanism of the compacting plate of the garbage truck on the pressing force, which is made up using dependence (1), which confirms the sufficient convergence of the obtained dependence compared to the data given in Table 1.

For a garbage truck of serial model KO-436, manufactured in Ukraine, which is equipped with a hydraulic cylinder of a sealing plate with an effective area of $9.5 \cdot 10^{-3}$ m^2 at a maximum pressure of the working fluid in the hydraulic system of 10 MPa, the pressing force will be 0.095 MN, and the rate of wear of the working hydraulic cylinder of the sealing mechanism plates of the garbage truck according to the obtained dependence (1) will be

$$v_w = 0.2575\mathrm{e}^{-0.01047 \cdot 0.095} = 0.257 \text{ [μm/h]}.$$
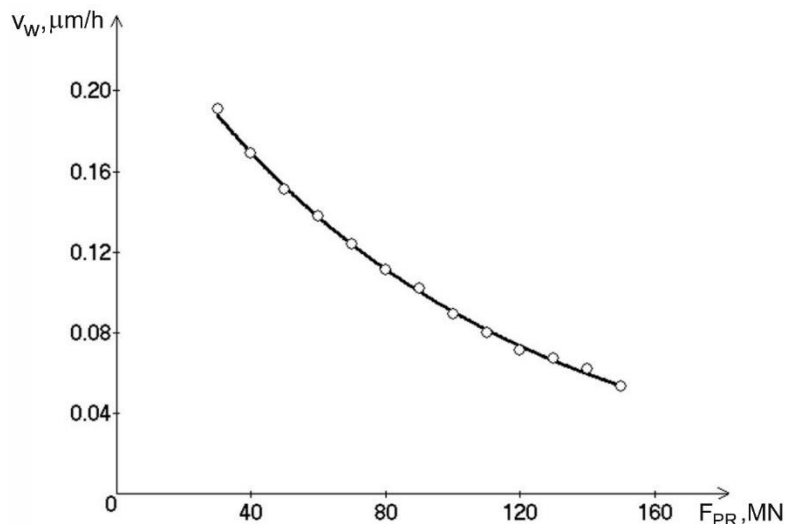
Fig. 1. Dependence of the change in the rate of wear of the working hydraulic cylinder of the garbage truck sealing plate mechanism, depending on the pressing force: actual ○ , theoretical —

It can be seen from the Fig. 1 that the increase in pressing force from 30 MN to 150 MN leads to a decrease in the rate of wear of the working hydraulic cylinder of the hydraulic press mechanism by 3.6 times, which indicates the importance of determining further ways to increase its wear resistance.

Conclusions

The exponential dependence of the change in the rate of wear of the working hydraulic cylinder of the mechanism of the sealing plate of the garbage truck, depending on the pressing force, was determined. It was established that for the garbage truck of Ukrainian production of serial model KO-436, the rate of wear of the working hydraulic cylinder of the mechanism of the sealing plate of the garbage truck, according to the obtained dependence, will be 0.257 μm/h. Therefore, the establishment of further ways to increase the wear resistance of the working hydraulic cylinder of the mechanism of the sealing plate of the garbage truck requires additional research.

References

1. Kramar V.M., Kindrachuk M.V., Loburak V.Ya. (2013). Znosostiikist yak enerhetychna kharakterystyka mitsnosti materialu v zoni tertia [Wear resistance as an energy characteristic of material strength in the friction zone]. East European Journal of Advanced Technologies, 4(7(64)), 8-11, https://doi.org/10.15587/1729-4061.2013.16678

2. Dykha O.V.(2018) Rozrahunkovo-eksperymental'ni metody keruvannja procesamy granychnogo zmashhuvannja tehnichnyh trybosystem [Computational and experimental methods of controlling processes of boundary lubrication of technical tribosystems]: monograph. Khmelnytskyi: KhNU

3. Petrov O., Kozlov L., Lozinskiy D., Piontkevych O. (2019) Improvement of the hydraulic units design based on CFD modeling. In: Lecture Notes in Mechanical Engineering XXII, 653-660, https://doi.org/10.1007/978-3-030-22365-6_65

4. Tataryants MS, Zavinsky SI, Troshin AG (2015) Development of a methodology for calculating loads on the screw and energy consumption of screw presses. ScienceRise, 6 (2), 80-84.

5. Bereziuk OV, Savulyak VI, Kharzhevskyi VO (2022) Dynamics of wear and tear of garbage trucks in Khmelnytskyi region. Problems of Tribology, 27(3/105), 70-75 , https://doi.org/10.31891/2079-1372-2022-105-3-70-75

6. Bereziuk OV, Savulyak VI, Kharzhevskyi VO (2021) Regression analysis of the influence of auger surface hardness on its wear during dehydration of solid waste in a garbage truck. Problems of Tribology, 26(3/101), 48-55, https://doi.org/10.31891/2079-1372-2021-101-3-48-55

7. Nosenko AS, Domnickij AA, Altunina MS, Zubov VV (2019) Theoretical and experimental research findings on batch-operation bin loader with hydraulically driven conveying element. MIAB. Mining Informational and Analytical Bulletin, 11, 119-130, http://dx.doi.org/10.25018/0236-1493-2019-11-0-119-130

8. Lobov NV, Maltsev DV, Genson EM (2019) Improving the process of transportation of solid municipal waste by automobile transport. Proceedings of IOP Conference Series: Materials Science and Engineering. IOP Publishing, 1(632), 012033, https://doi.org/10.1088/1757-899X/632/1/012033

9. Kotomchin AN, Lyakhov Yu.G. (2019) Analysis of failures of knots and units of construction, road, lifting and transport machines and specialized motor transport on the example of MUE "Communalderservice". Engineering & Computer science, 3, 174-178.

10. Bereziuk OV, Savulyak VI, Kharzhevskyi VO (2023) Establishing the peculiarities of tire wear of garbage trucks during the transportation of municipal solid waste. Problems of Tribology, 28(1/107), 59-64, https://doi.org/10.31891/2079-1372-2023-107-1-59-64

11. Kabashev RA (1997) Road and construction machines: abrasive wear of the working parts of earthmoving machines. Almaty: Gylym.

12. Nurakov SN, Savinkin VV (2008) About development methods for calculating the wear of the rod cylinder interface of hydraulic machines. Proceedings of the Karaganda State Technical University, 3 (32), 96.

13. Shalapai V.V., Machuga O.S. (2023) Vtraty potuzhnosti u hidrotsylindri vnaslidok protikannia hidravlichnoi ridyny cherez neshchilnist [Power losses in a hydraulic cylinder due to leakage of hydraulic fluid through a leak] : materials of the XIII International Scientific and Practical Conference "Comprehensive quality assurance of technological processes and systems", - May 25-26, 2023, Chernihiv. Chernihiv Polytechnic National University, 287-289.

14. Kargin RV, Yakovlev IA, Shemshura EA (2017) Modeling of workflow in the grip-container-grip system of body garbage trucks. Procedia Engineering, 206, 1535-1539, https://doi.org/10.1016/j.proeng.2017.10.727

15. Korchak O.S., Bilenets K.E. (2019) Doslidzhennia trybotekhnichnykh vlastyvostei sylovykh tsylindriv hidravlichnykh presiv na bazi inzhenernoi metodyky otsinky yikh resursu bezvidmovnoi roboty [Study of the tribotechnical properties of power cylinders of hydraulic presses based on the engineering methodology of assessing their resource of trouble-free operation]. Materials Processing by Pressure, 1, 186-192, http://dx.doi.org/10.37142/2076-2151/2019-186(48)

Березюк О.В., Савуляк В.І., Харжевський В.О., Алексеєв А.Є. Визначення закономірності швидкості зношення робочого гідроциліндра механізму ущільнюючої плити сміттєвоза від зусилля пресування

Стаття присвячена дослідженню впливу зусилля пресування на зносостійкість робочого гідроциліндра механізму ущільнюючої плити сміттєвоза. Використання математичного апарату та відповідних програм регресійного аналізу дозволило визначити експоненціальну закономірність зміни швидкості зношування робочого гідроциліндра механізму ущільнюючої плити сміттєвоза залежно від зусилля пресування. Побудована графічна залежність зміни швидкості зношування робочого гідроциліндра механізму ущільнюючої плити сміттєвоза від зусилля пресування, яка підтвердила достатню збіжність отриманої закономірності. Графік впливу зусилля пресування на швидкість зношування робочого гідроциліндра механізму ущільнюючої плити сміттєвоза демонструє доцільність його підвищення. Встановлено, що для сміттєвоза українського виробництва серійної моделі КО-436 швидкість зношування робочого гідроциліндра механізму ущільнюючої плити сміттєвоза за отриманою закономірністю складатиме 0,257 мкм/год. Встановлена доцільність проведення додаткових досліджень з визначення подальших шляхів підвищення зносостійкості робочого гідроциліндра механізму ущільнюючої плити сміттєвоза.

Ключові слова: знос, зносостійкість, швидкість зношування, гідроциліндр, механізм, ущільнююча плита, сміттєвоз, зусилля пресування, тверді побутові відходи, регресійний аналіз

Optimization of technological parameters at discrete strengthening of steel cylindrical surfaces

O. Dykha*, V. Dytyniuk, N. Grypynska, A. Vychavka

Khmelnytskyi national University, Ukraine
*E-mail: tribosenator@gmail.com

Abstract

The technologies of continuous strengthening of technological surfaces have practically exhausted their capabilities, which calls for the creation of fundamentally new approaches. The application of the principles of discrete-oriented strengthening of tribosystems has wide prospects for improving existing methods of strengthening due to the selection of modes and control of the geometric structure of the surface layer. The essence of the discrete-oriented strengthening method is the application of combined electromechanical processing and electrocontact cementation of cylindrical surfaces. The purpose of the work is to determine the parameters of discrete processing of cylindrical steel parts that are optimal according to the surface hardness criterion. Using the Statistica program, a factorial experiment was implemented according to the Box-Behnken plan, and the results of dispersion and regression analysis of the influence of processing parameters on microhardness were obtained. It was established that the following optimal parameters of DOZ processing are necessary to achieve the maximum values of microhardness (5950 MPa): current strength-500A, force-350 N, contact time-0.3 s.

Key words: strengthening, surface, hardness, technological parameters, optimization, Statistica

Introduction

Widely used technologies of continuous strengthening of technological surfaces have practically exhausted their capabilities, which calls for the creation of fundamentally new approaches. The application of the principles of discrete-oriented strengthening of tribosystems has broad prospects for improving existing approaches due to the choice of strengthening technology and the principles of the geometric arrangement of strengthening islands. Bearing tribosystems are one of the most common types of friction nodes, which are an integral and responsible component of modern machines: bearings, axles, shafts, bushings of technological and transport machines. When analyzing the performance of bearing tribosystems, an algorithm for assessing the impact of technological and design factors on their wear resistance and durability is necessary.

Literature review

Much attention is paid to the problem of creating discretely reinforced surfaces in modern scientific literature. In [1], a study of the properties and characteristics of the surfaces of a discrete structure with mechanically formed depressions was carried out. In work [2] a mathematical model of discrete frictional contact of bodies with periodic surface textures is proposed. The contact problem is reduced to a system of singular integral equations for the functions of the heights of the contact gaps and the relative displacement of the surfaces in the sliding zones. Characteristics of contact deformation and wear of materials with a smooth and discrete track were investigated using nanoindexing and nanoscratching [3]. Wear tests have shown that wear is less for discrete discs than for smooth discs.

Research [4] determined the effect of discrete point laser hardening on abrasion and contact fatigue resistance during rolling. Samples hardened with adjacent and separated laser spots showed higher abrasion resistance than surfaces treated with overlapping laser spots.

In order to improve the surface tribological properties of titanium alloy, laser processing technology was used in [5] to obtain a cellular texture on the surface of the material. Surface textures of grooves with different orientation and distance between them were obtained on the Ti–6Al–4V alloy using a laser in the study [6].

In contrast to traditional research and development of new materials and coatings, three types of surface microstructure, including V-shaped, U-shaped and ring-shaped groove microstructures, were performed in [7] to increase the erosion resistance of sludge. In [8], a groove of a certain size was made, then it was filled with pure phenolic resin and molybdenum sulfide additives to obtain a surface with time-varying contact characteristics. Operational characteristics of friction pairs of a cylinder liner - piston ring of a diesel engine with different surface textures were studied in [9].

Therefore, the problem of creating discrete structures on the surfaces of materials and researching the technological parameters of their formation is an urgent task.

The essence of the process of discrete strengthening of cylindrical parts.

The essence of the discrete-oriented strengthening method is the application of combined electromechanical processing and electrocontact cementation of cylindrical surfaces using a carbide roller as a tool. The schematic diagram of DOZ is shown in fig. 1.

The working tool-roller 4 is pressed against the processed workpiece with a given spring force in the range of 100...500 N. One current pole from the power transformer is supplied to the workpiece through the contact roller. The second pole is brought to the processed workpiece. At the same time, an electric discharge occurs between the roller and the tool, which leads to local heating of the contact point. Due to heating, structural transformations similar to the hardening process occur in the surface layers of the metal with the formation of a so-called white layer. Additionally, during processing, the outer surface of the shaft is covered with a layer of graphite by rubbing it with a graphite rod. Graphite, falling into the place of contact between the tool and the workpiece, is also heated and can diffuse into the surface under the action of contact pressure from the roller. That is, there is a local high-temperature diffusion of carbon into the surface of the workpiece, that is, the process of cementation.

The roller and cylinder are set by the shaping movements inherent in the usual processing on a lathe. By setting the movement-feed step, it is possible to form specified processing tracks on the surface of the workpiece.When a large amount of Joule heat is released, the surface of the microvolume is rapidly heated (1000C/s) with its plastic deformation.
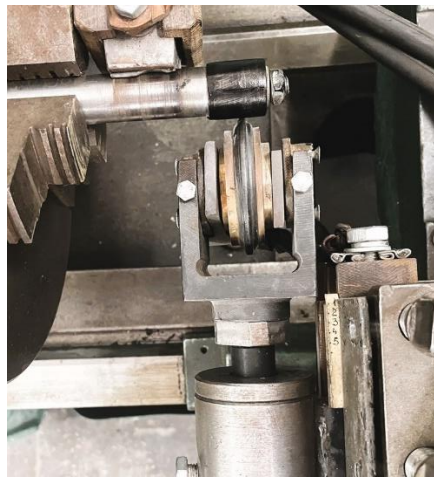
Fig. 1. Schematic diagram of the discrete-oriented method of strengthening cylindrical surfaces

Then intense cooling takes place due to heat dissipation inside the material. As a result, a finely dispersed and hard martensitic "white layer" structure with high strength and wear resistance is formed in the surface layer.

The installation allows strengthening of various cylindrical parts, including the bearing necks of the camshaft of the internal combustion engine. To apply the graphite layer on the surface of the workpiece, cylindrical graphite rods with a diameter of 10 mm were used. Samples made of 20X steel were mounted on a cylindrical mandrel, which rested on the conical center of the installation. In the process of rolling with a roller on the surface of the samples, strengthened strips were formed with a step in accordance with the given feed of the movement of the roller (1.5...2 mm).

Optimization of technological parameters of the discrete-oriented method of strengthening bearing tribosystems

The software package for statistical analysis STATISTICA was used to plan the experiment to determine the optimal values of the technological factors of the electrical contact strengthening process. The STATISTICA DOE package module is intended for experiment planning.

The 3-level Box-Behnken plan was used for planning. In statistics, Box–Behnken plots are experimental plots for response surface methodology developed by George E.P. Boxing. Each factor or independent variable is assigned one of three equidistant values, usually coded as -1, 0, +1. (At least three levels are required to achieve the next goal.) The plan should be sufficient to fit a quadratic model, that is, a model containing elements in a square, product of two factors, linear. The ratio of the number of experimental points to the number of coefficients in the quadratic model must be justified (in fact, their plans are kept in the range from 1.5 to 2.6). The variance of the estimate should depend only on the distance from the center of the plan.

The STATISTICA DOE module contains a complete implementation of standard (block) 3**(kp) plans. The module also includes standard Box-Behnken plans. As with other plans, it is possible to display and save these plans in standard or random order, request replicas or individual experiments, view the plan and block generators, and more. The program performs a complete analysis of 3**(kp) plans. It is possible to include any effects in the analysis. Main effects are broken down into linear and quadratic effects, and interactions are broken down into linear-linear, linear-quadratic, quadratic-linear, and quadratic-quadratic effects. You can view correlation matrices of factors and effects. The program calculates standard estimates of variance analysis parameters (standard errors, confidence intervals, statistical significance, etc.), coefficients for recoded (-1, 0, +1) factors and coefficients for untransformed factors. The analysis of variance table will contain tests for the linear and quadratic components of each effect and combined tests for effects with many degrees of freedom. If the design contains replicates, the net error estimate can be used for analysis of variance and significance testing; in this case, a general loss of consent test will also be conducted. To interpret the results, the program calculates a table of means (and confidence intervals), as well as marginal means (and confidence intervals) for the interactions. Graphical options include plots of means and marginal means (with confidence intervals), Pareto effects plots, normal and semi-normal probability effect plots, response surface plots, and contour plots.

On the Pareto diagram of the effects, the estimates of the effects of the analysis of variance are arranged by the absolute magnitude of the values: from the largest to the smallest. The magnitude of each effect is represented by a bar, and the bars are crossed by a line indicating how large the effect must be (ie, how long the bar must be) to be statistically significant. It has been established that the main technological parameters affecting the parameters of hardening at DOZ are: the amount of operating current of the power source, the force of pressing the working roller against the surface of the shaft, and the duration of contact between the tool and the processed part. The duration of contact depends on the speed of rotation of the cylindrical part and the size of the contact area, which was estimated when setting the contact parameters. In order to evaluate the influence of the specified factors and determine their optimal values according to the criterion of ensuring maximum hardness, it is advisable to use the methodology of planning the experiment, with the accepted ranges:

Factor	Current strength, A	Effort, N	Contact time, p
min	200	200	0.1
max	800	500	0.3
average	500	350	0.5

In this case, taking into account the planning of the experiment to determine the optimal values of the technological factors of the electrical contact strengthening process, the software package for statistical analysis STATISTICA was used. Taking into account the number of factors and their independent influence on the response function, the 3-level Box-Behnken plan was used for planning:

No. of the experiment	Current strength, A	Effort, N	Contact time, p
1	-1	0	-1
2	-1	-1	0
3	+1	-1	0
4	+1	0	+1
5	0	+1	-1
6	0	0	0
7	0	0	0
8	-1	0	+1
9	+1	0	-1
10	+1	+1	0
11	+1	-1	+1
12	-1	+1	0
13	+1	+1	+1
14	+1	-1	-1
15	+1	0	0

Using the program menu, an experiment plan was formed, which consists of 15 experiments, presented in table 3.1.

Factorial experiment plan for the DOZ method

No. of the experiment	Current strength, A	Effort, N	Contact time, p	Microhardness, MPa
1	200	350	0.1	4500
2	200	200	0.3	4400
3	800	200	0.3	4900
4	800	350	0.5	5300
5	500	500	0.1	6050
6	500	350	0.3	5800
7	500	350	0.3	6150
8	200	350	0.5	4750
9	800	350	0.1	5000
10	800	500	0.3	5750
11	500	200	0.5	6300
12	200	500	0.3	5250
13	500	500	0.5	6400
14	500	200	0.1	5750
15	500	350	0.3	5900

Microhardness was taken as the response function. Next, the Statistica program allows you to perform a variance analysis to determine the effect of processing parameters on the response function. To assess the significance of the factors, a Pareto map was constructed, shown in Fig. 2.

Pareto map of standardized effects; Change:Microhardness, MPa
3 3-level f, 1 Blocks; Residual SS=326614,6
3П Microhardness, MPa

Load, N(K) — 2,276529
Amperage, A(K) — 1,898275
(1)Amperage, A(L) — -,835163
Duration of contact, s(K) — -,791532
(2)Load, N(L) — ,6186389
(3)Duration of contact, s(L) — -,092796

p=,05

Effect Score (Absolute Value)
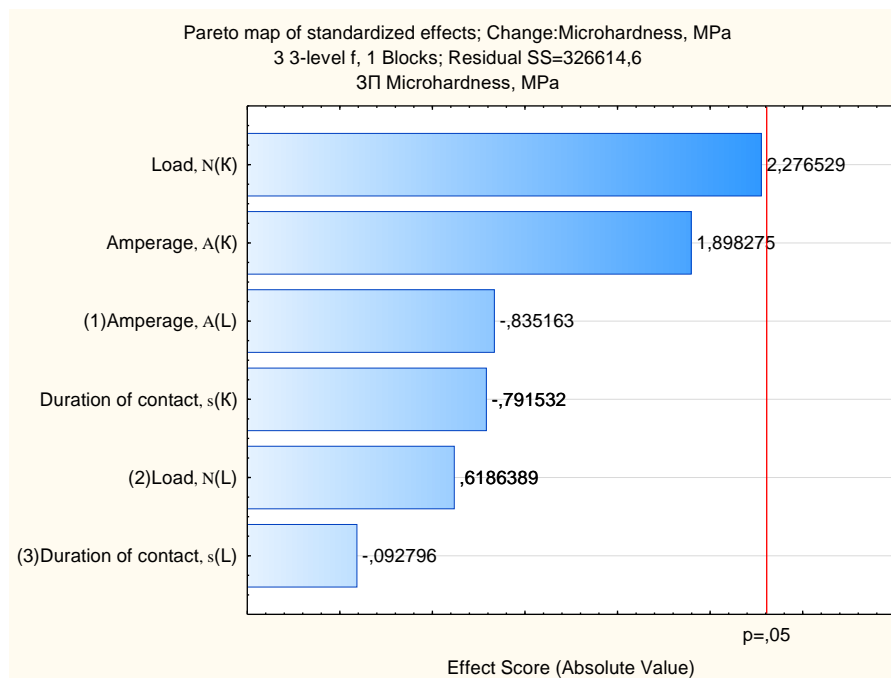
Fig. 2. Pareto map of the importance of operating factors

On the diagram, the letter L indicates the linear effect of the factor, and the letter K indicates the effect of the factor value in the quadratic equivalent. From the analysis of the diagram, it can be seen that the quadratic value of the current and the linear value of the pressing force have the greatest influence on the microhardness, the contact time has a smaller influence, and the squares of the force and the contact time in the response functions can generally be neglected, since they are beyond the red limit of significance.

The results of variance analysis are presented in Table 2.

Table 2

Results of dispersion analysis

Factor	Analysis of variance; Prm.: Microhardness, MPa; R-squared=.94983; Rate.9122 (3 fact. Box-Behnken plan (Data table 1) in Plan_7n.stw) 3 3-level f, 1 Blocks; Final.SS=37812.5 ZP Microhardness, MPa				
	SS	ss	MS	F	p
(1) Current strength, A(L)	525313	1	525313	13.8926	0.005810
Current strength, A(K)	4119375	1	4119375	108.9421	0.000006
(2) Effort, H(L)	551250	1	551250	14.5785	0.005103
Effort, N(K)	121298	1	121298	3.2079	0.111060
(3) Contact time, s(L)	262812	1	262812	6.9504	0.029882
Contact time, s(K)	144	1	144	0.0038	0.952269

In the table, the value of Fisher's test is indicated by the letter F, and the Student's probability test by the letter p. The results shows the adequacy parameters of the built experiment plan, that is, in general, the obtained experiment plan can be considered adequate. Next, graphs of response functions for microhardness from a combination of determining factors were constructed with the help of a software package (Fig. 3).

Fitted surface; Change.: Microhardness, MPa
3 3-level f, 1 Blocks; Residual SS=326614,6
ЗП Microhardness, MPa

$$z=1309;4328703703+5;7106481481481*x-;0062731481481481*x^2+21;898148148148*y-;030092592592593*y^2-557;8125$$

a)

Fitted surface; Change.: Microhardness, MPa
3 3-level f, 1 Blocks; Residual.SS=326614,6
ЗП Microhardness, MPa

$$z=1309;4328703703+5;7106481481481*x-;0062731481481481*x^2-3625;*y+5885;4166666666*y^2+3978;00926$$

b)

Fitted surface; Change.: Microhardness, MPa

3 3-level f, 1 Blocks; Residual.SS=326614,6

3П Microhardness, MPa

Color	Value
■	> 6400
■	< 6300
■	< 5900
■	< 5500

z=1309;4328703703+21;898148148148*x-;030092592592593*x^2-3625;*y +5885;4166666666*y^2+1287;03704

c)

Fig. 3. Graphs of response functions and approximating correlation functions

Predicted value profiles and desirability functions

Fig. 4. The value of desirability indicators for the maximum value of the response function (microhardness)

So, it follows from the results that to achieve the maximum values of microhardness (5950 MPa), the following optimal parameters of DOZ processing are necessary: current strength - 500A, force - 350 N, contact time - 0.3 s.

Analysis of the obtained graphs shows that the current strength has a clearly defined extreme influence on the microhardness, while the influence of other factors is almost linear.

The results of the regression analysis, that is, the determination of the coefficients of the regression equations, are shown in Table 3.3.

Table 3

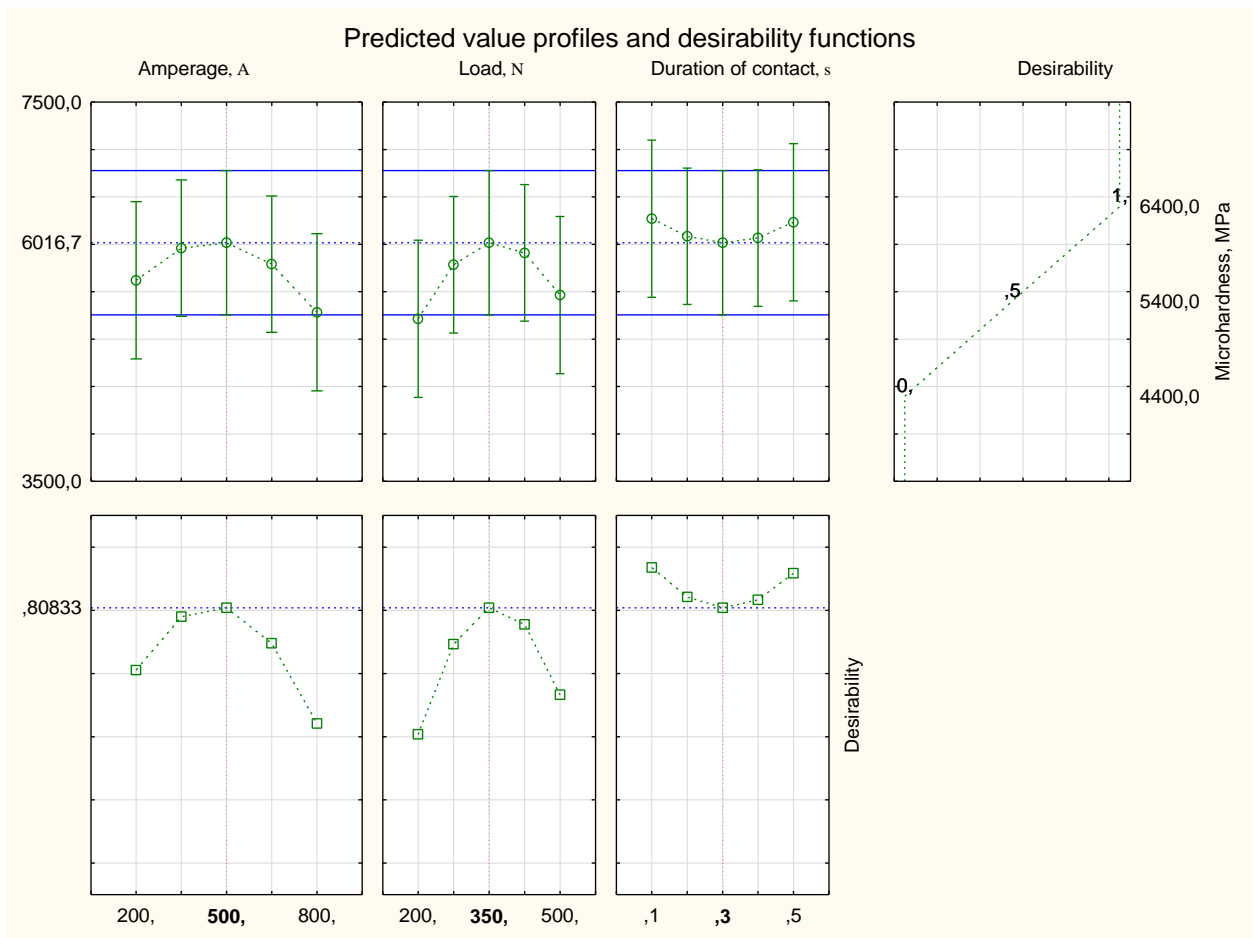**Results of regression analysis**

Factor	Regression; R-squared=.94983; Rate.9122 (3 fact. Box-Behnken plan (Data table 1) in Plan_7n.stw) 3 3-level f, 1 Blocks; Final.SS=37812.5 ZP Microhardness, MPa					
	Regression. Coef.	St. Osh.	t(8)	p	-95.% Dov. Pred	+95.% Dov. Pred
Average/St. Member	2677,257	646,147	4.1434	0.003238	1187.24	4167.275
(1) Current strength, A(L)	12,590	1,148	10.9716	0.000004	9.94	15,236
Current strength, A(K)	-0.012	0.001	-10.4375	0.000006	-0.01	-0.009
(2) Effort, H(L)	-3,889	3,182	-1.2223	0.256372	-11.23	3,448
Effort, N(K)	0.008	0.004	1.7911	0.111060	-0.00	0.018
(3) Contact time, s(L)	1000,000	1556,394	0.6425	0.538515	-2589.05	4589.052
Contact time, s(K)	-156,250	2529,931	-0.0618	0.952269	-5990.28	5677,782

To determine the optimal values of the determining factors of the processing process, a spline approximation of the plan results was carried out using the discrete method according to the criterion of maximum microhardness. In fig. 4 are given by the results of such approximation.

Conclusions

In order to determine the optimal technological parameters of the discrete-oriented method of strengthening with the help of the Statistica program, a factorial experiment according to the Box-Behnken plan was implemented, and the results of dispersion and regression analysis of the influence of processing parameters on microhardness were obtained. It was established that the following optimal parameters of DOZ processing are necessary to achieve the maximum values of microhardness (5950 MPa): current strength-500A, force-350 N, contact time-0.3 s.

References

1. Marchuk V., Kindrachuk M., Kryzhanovskyi A. System analysis of the properties of discrete and oriented structure surfaces. Aviation. 2014. No. 18 (4). R. 161-165. http://dx.doi.org/10.3846/16487788.2014.985474

2. Slobodyan BS, Lyashenko, BA, Malanchuk, NI, Marchuk VE, Martynyak RM Modeling of Contact Interaction of Periodically Textured Bodies with Regard for Frictional Slip. 2016. Volume 215, Issue 1. P 110–12. https://doi.org/10.1007/s10958-016-2826-x

3. Yoon Y. & Talke FE Microsyst Technol. 2011. 17: 733. https://doi.org/10.1007/s00542-011-1239-5

4. Ann Zammit, Stephen Abela, John Charles Betts, Remigiusz Michalczewski, Marek Kalbarczyk, Maurice Grech. Scuffing and rolling contact fatigue resistance of discrete laser spot hardened austempered ductile iron. Wear. 2019. Volumes 422-423. Pages 100-107. https://doi.org/10.1016/j.wear.2019.01.061

5. Qi Liu, Yang Liu, Xing Li, Guangneng Dong. Pulse laser-induced cell-like texture on the surface of titanium alloy for tribological properties improvement. Wear. 2021. Volume 477. https://doi.org/10.1016/j.wear.2021.203784

6. Jianfei Wang, Weihai Xue, Siyang Gao, Shu Li, Deli Duan. Effect of groove surface texture on the fretting wear of Ti–6Al–4V alloy. Wear. 2021. Volumes 486-487. https://doi.org/10.1016/j.wear.2021.204079

7. ZX Chen, HX Hu, YG Zheng, XM Guo. Effect of groove microstructure on slurry erosion in the liquid-solid two-phase flow. Wear. 2021. Volumes 466-467. https://doi.org/10.1016/j.wear.2020.203561

8. AY Wang, JL Mo, HH Qian, YK Wu, ZY Xiang, W. Chen, ZR Zhou. The effect of a time-varying contact surface on interfacial tribological behavior via a surface groove and filler. Wear. 2021. Volumes 478-479. https://doi.org/10.1016/j.wear.2021.203905

9. Liang Rao, Chenxing Sheng, Zhiwei Guo, Chengqing Yuan. Effects of thread groove width in cylinder liner surface on performances of diesel engine. Wear. 2019. Volumes 426-427. Part B. Pr. 1296-1303. https://doi.org/10.1016/j.wear.2018.12.0703.

Диха О.В., Дитинюк В.О., Грипинська Н.В., Вичавка А.А. Оптимізація технологічних параметрів дискретного зміцнення сталевих циліндричних поверхонь

Технології суцільного зміцнення технологічних поверхонь практично вичерпали свої можливості, що викликає потребу у створення принципово нових підходів. Застосування принципів дискретно-орієнтованого зміцнення трибосистем має широкі перспективи для вдосконалення існуючих способів зміцнення за рахунок вибору режимів та керування геометричною будовою поверхневого шару. Сутність дискретно-орієнтованого методу зміцнення полягає у застосуванні комбінованої електромеханічної обробки і електроконтактної цементації циліндричних поверхонь. Метою роботи є визначення оптимальних за критерієм поверхневої твердості параметрів дискретної обробки циліндричних сталевих деталей. За допомогою програми Statistica реалізований факторний експеримент за планом Бокса-Бенкена, отримані результати дисперсійного і регресійного аналізу впливу параметрів обробки на мікротвердість. Встановлено, що для досягнення максимальних значень мікротвердості (5950 МПа) необхідні наступні оптимальні параметри обробки ДОЗ: сила струму-500А, зусилля-350 Н, час контакту-0,3 с.

Ключьові слова: зміцнення, поверхня, твердість, технологічні параметри, оптимізація, Statistica

Systematic approach to the study of working surfaces wear of automotive and tractor equipment parts

M.I. Chernovol, V.M. Kropivniy, Y.V. Kuleshkov, I.V. Shepelenko*, V.I. Gutsul

Central Ukrainian National Technical University, Kropyvnytsky, Ukraine
*E-mail: kntucpfzk@gmail.com

Abstract

The paper uses the principles of the system approach to establish the relationship between wear of individual surfaces on the example of a gear drive of the GP type pump. The hierarchical structure of the part is considered, its individual functional parts are classified as subsystems, and the working surfaces are classified as system elements. A systematic approach to the study of part wear condition included, in addition to identifying the relationships between the wear of individual elements of the part, the creation of a mathematical statistical model of the worn part as a whole, as a system. The main types of wear of the gear working surfaces were determined. The laws of wear distribution of gear working surfaces and their main numerical characteristics were found. The established relationship between the wear of individual gear elements has become the basis for the system quality of the technical system "gear drive of the GP pump" in relation to the wear of its elements. A mathematical statistical wear model was obtained in the form of linear regression equations system of gear elements wear dependence on their outer diameter wear. This makes it possible, using the principles of a systematic approach based on the data of a single defect – gear wear along the outer diameter, to create a complete statistical image of the worn part, i.e., to determine the wear of other elements of the drive gear. The results obtained allow us to reasonably approach the issue of choosing a method for restoring parts and forming routes for the technological process of restoring a part.

Key words: systematic approach, restoration of parts, wear of the working surface, drive gear, automotive and tractor equipment, mathematical statistical model.

Introduction

The restoration of worn parts remains a very important reserve for increasing the efficiency of equipment use, saving material, fuel and energy, and labor resources. The technical and economic feasibility of restoring parts is due to the possibility of reusing 65-75% of the parts (often repeatedly). The cost of restoring worn parts does not exceed 50% of the cost of new ones, and material costs are 15-20 times lower than during the manufacture of parts [1].

At the same time, the problem of restoring parts is complex in nature [2]. To study and solve it, it is possible to apply a systematic approach, which is a methodological orientation of study based on the consideration of objects in the form of systems, that is, a set of elements connected by interaction, and therefore acting as a single whole in relation to the environment [3].

The choice of optimal restoration methods and their sequence is determined by many factors and in many cases is associated with increasing hardness, achieving a set of mechanical properties, wear resistance, as well as the roughness of the restored surface and the dimensional accuracy of the restored part [4].

Each restoration method has its own niche of optimal conditions of use, including even the technological traditions that have developed at a particular enterprise, so the implementation of a systematic approach to the restoration of parts, in particular, vehicles, is a decisive factor in the selection of primary processing methods in the technological restoration process and the possibility of integrating them into a single technological cycle [5].

Literature review

The technological process of restoring machine parts, including automotive and tractor equipment, has all the necessary properties that are required for systems [1, 3, 4]:

- is an integral complex of interconnected elements, such as parts, technological operations, modes, etc;
- is an element of a higher-order system, in particular, the production process of machine repair;
- technological process elements can be considered as lower-order systems (a technological operation consists of the following interconnected elements: equipment, fixtures, tools, part, transition).

It should be noted that a part as an object of design or restoration also corresponds to all the above system concepts [6]. Possessing integrity, it consists of interconnected parts, functional and structural components depend on the type and complexity of the part design, its purpose. Considering a part as a system, it can be divided into subsystems or only into elements. In a part-system, one of the subsystems (or one of the elements) is the main one, its role in determining the state of the entire system is more significant than the influence of other subsystems. The main elements of a part are the mating surfaces.

As an example, consider the hierarchical structure of the drive gear of hydraulic pumps (Figs. 1, 2), which are widely used in hydraulic systems of automotive and tractor equipment.
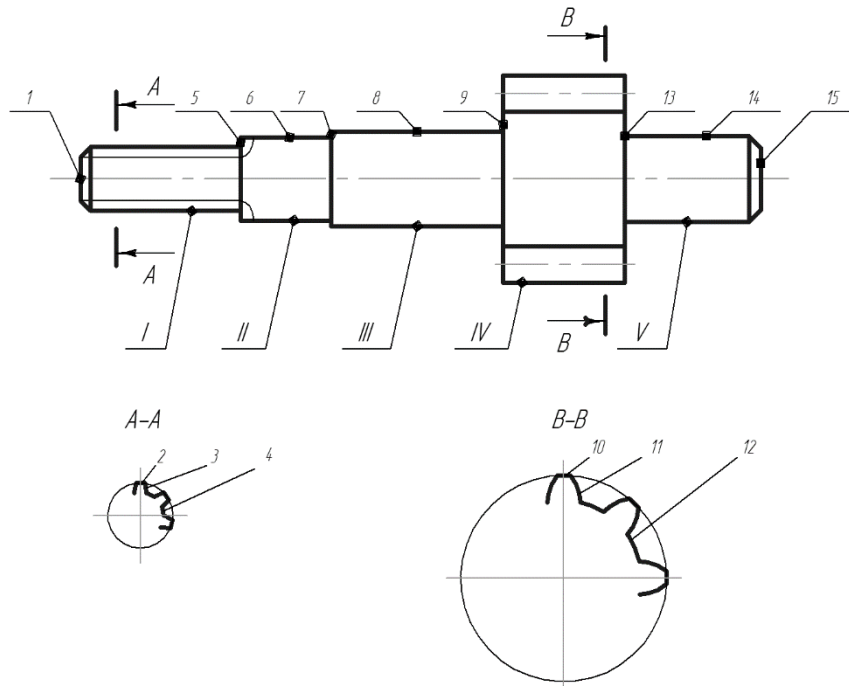
Fig. 1. Structure of the part design: I-V – functional parts of the part; 1-15 – surfaces of the part
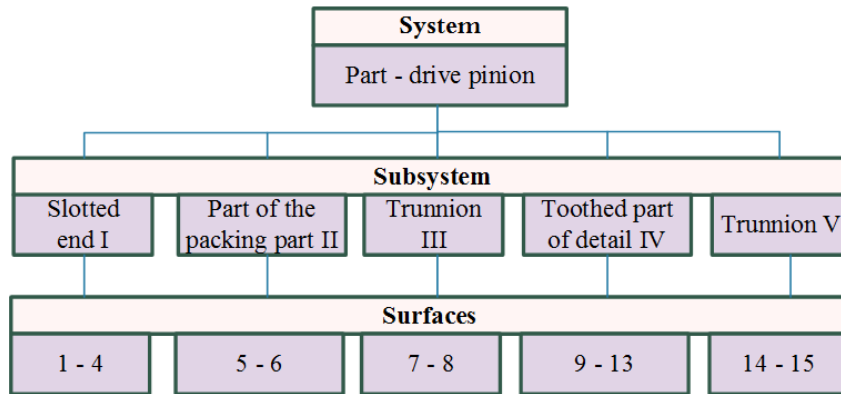
Fig. 2. Scheme of the hierarchical structure of the part

In such a system, one of the subsystems is the main one, and its role in determining the state of the entire system is more significant than the influence of other subsystems. The main elements of a part are the mating surfaces.

As a rule, there are no more than six types of defects in a part [7]. However, combinations of two, three, and sometimes four defects are most common. The probability of n defects occurrence out of m possible in worn parts can be determined using a binomial distribution:

$$P_m(n) = C_m^n P^m q^{m-n},$$ (1)

where C_m^n – the number of n defect combinations out of m possible; P – the probability of defect occurrence; q – the probability of defects occurrence.

The connection between individual surfaces can be functional and correlative.

The functional connection feature allows classifying defects and their combinations into separate classes by combining such defects into common restoration routes.

Usually, when studying the wear of a part, the wear of each element of the part is considered separately. The wear of one surface (element) of the part is not related to the wear of other surfaces. A systematic approach to studying the wear state of a part involves studying and finding relationships between the wear of individual elements of the part, i.e. creating a mathematical statistical model of the worn part as a whole, as a system.

Purpose

The aim of this paper is to use a systematic approach to construct a mathematical statistical model of a worn part that will establish the relationship between the wear of individual surfaces on the example of a gear drive of the GP type pump.

Research Methodology

A static mathematical model of a worn part will be understood as a mathematical image of a part whose characteristics that determine the type, degree, and relationship of wear are adequate to the real picture.

The construction of the mathematical model of the worn gear was as follows:
1. Collecting information about the wear of pump gears by micrometering.
2. Determining the minimum required sample size.
3. Determining the numerical characteristics of a random sample:

average wear value; absolute scattering index – dispersion and average square deviation and relative scattering index – coefficient of variation.
4. Checking the collected information for dropout points.
5. Selecting a theoretical distribution law and determining its parameters.
6. Using a systematic approach to creating a mathematical image of a worn part, the characteristics of which determine the type, degree and relationship of wear, are adequate to the real picture. This involves determining the pairwise correlation coefficients, creating regression equations for the relationship between the wear of individual elements of the part, checking the coefficients of the resulting regression equations for significance, and the entire regression equation for adequacy.

The main defects of the GP pump drive gear are shown in Fig. 3.
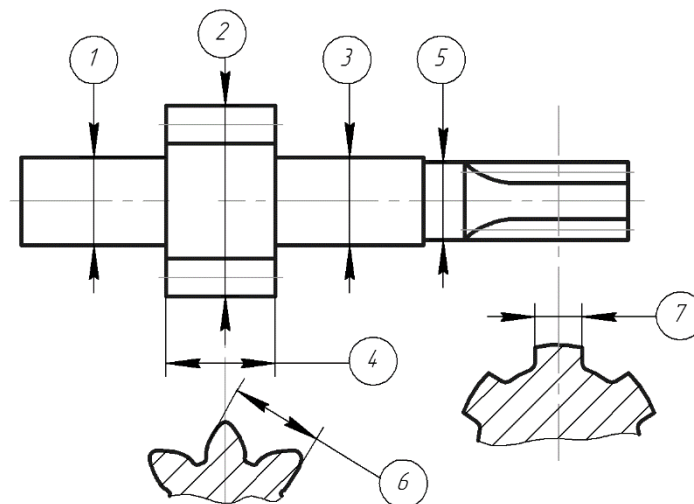
Fig. 3. Defects of the drive gear of the GP-46U pump: 1,3 – wear of the trunnion diameter; 2 – wear of the gear outer diameter; 4 – wear of the width of the gear crown; 5 – wear of the neck diameter under the oil seal; 6 – wear of the general normal of the gear teeth; 7 – wear of the drive gear splines in width

The measuring tool for determining the amount of wear was chosen based on the accuracy of the dimensions in the manufacture of gears and the amount of wear on its working surfaces.

A micrometer MK-50-1 DSTU GOST 6507:2009 Micrometers was used to determine the wear of the trunnion and neck for the oil seal by diameter, as well as the gear by tooth length. Technical specifications (GOST 6507-90) with a division price of 0.01 mm.

The spline thickness wear was determined by a vernier caliper SHTS-II-250-0.05 DSTU GOST 166:2009 Vernier calipers. Technical specifications (GOST 166-89 (ISO 3599-76), IDT) with a division price of 0.05 mm.

To determine the wear of the gear teeth along the involute profile, the length of the general normal was measured with a micrometer M3-25-I according to DSTU GOST 6507:2009 Micrometers. Technical specifications (GOST 6507-90) with a division price of 0.01 mm.

Statistical processing method of the obtained experimental data on the wear of the drive gear of the GP type pump as a system was performed according to the recommendations given in paper [8].

Statistical processing of information on the wear of gear elements was performed in accordance with the recommendations using the Statistica software [9].

The systematic approach to building a statistical mathematical image (model) of a worn part, in addition to the laws of part wear distribution, involves determining the relationship between the wear of the part's working surfaces.

The presence and closeness of the relationship between the wear of gear elements, i.e., the qualitative side of the issue, is determined by correlation analysis methods.

The stochastic relationship between the wear of gear working surfaces is determined by regression analysis methods. The method allows determining how the resultant attribute changes quantitatively when the factor attribute changes.

When obtaining regression equations for the relationship between the wear of gear elements, the wear of gears along the outer diameter was chosen as an independent factor. This is due to the fact that:

- first, it is the wear of the gears on the outer diameter that largely determines the volume flow rate of the pump;

- secondly, due to the uniform wear of the gears along the outer diameter, the determination of wear of this element is technologically advanced and accurate;

- thirdly, the wear of other gear elements also depends on the wear of the gears along the outer diameter.

The experimental information on gear wear was processed by regression and correlation analysis according to the method given in paper [10].

Results

It was found that abrasive wear is the predominant type of wear on the gear working surfaces. This is evidenced by the characteristic marks on the wearing surfaces (Fig. 4, a-c). Wear of the involute tooth profile should be attributed to mechanical abrasion (Fig. 4, d).
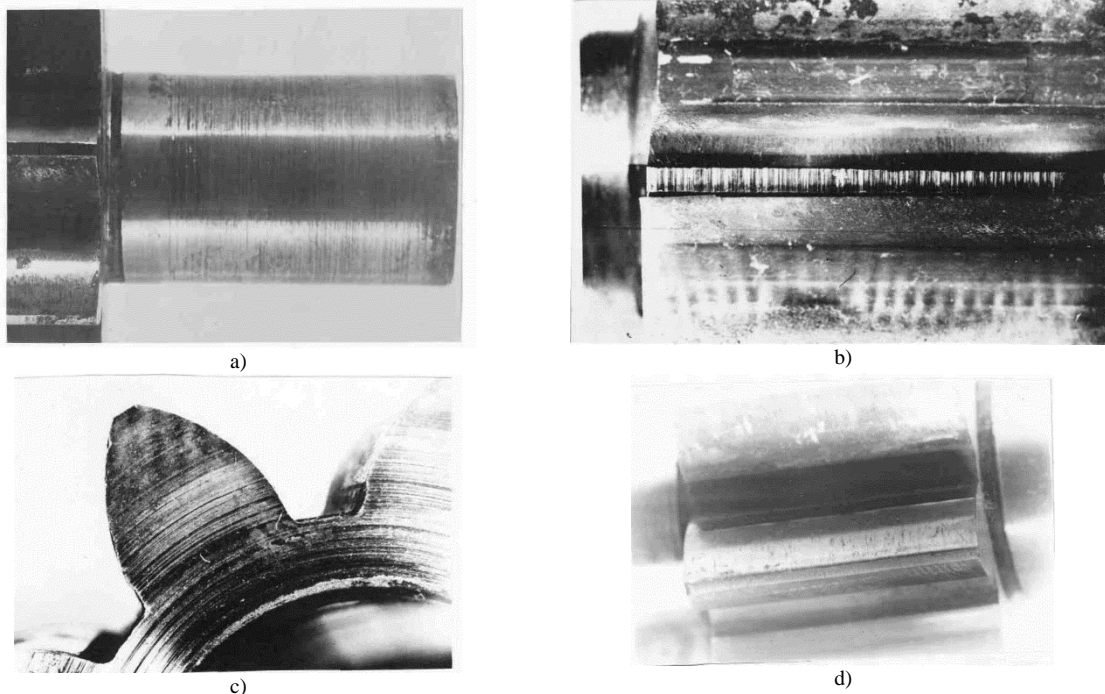

a)

b)

c)

d)

Fig. 4. Traces of abrasive wear on the surfaces of the gear trunnion (a), gear tooth tip (b), gear face (c), and mechanical abrasion of the tooth head (d)

The information on the wear of gear elements was processed in accordance with the methodology [11]. The main characteristics of the wear distributions of GP pump gears are shown in Table 1.

Table 1

Main characteristics of wear distribution on gear working surfaces of pumps GP-46U

Name of the distribution parameters	Pumps that came in for repair for the first time		Pumps that came in for repair for the 2nd and 3rd time	
Wear of gears on the outer diameter, ΔD_i				
Average amount of wear, $\bar{t}$	0.091	0.074	0.348	0.315
Average square deviation, σ	0.088	0.092	0.215	0.196
Asymmetry, A	1.141	2.53	0.369	0.056
Excess, E	1.376	9.45	0.274	-0.769
Coefficient of variation, V	0.967	1.23	0.619	0.624
The law of distribution	Laplace-Charlier	normal	Laplace-Charlier	normal
Probability of acceptance the hypothesis, P	0.85	0.19	0.995	0.975
Wear of the gear trunnions in diameter, Δd_{ui}				
Average amount of wear, $\bar{t}$	0.026	0.018	0,248	0,224
Average square deviation, σ	0.024	0.032	0.116	0.107
Asymmetry, A	1.120	3.59	-0.284	-0.238
Excess, E	1.36	16.13	-0.897	-1.02
Coefficient of variation, V	0.94	1.75	0.467	0.476
The law of distribution	Laplace-Charlier	Uniform	Laplace-Charlier	Laplace-Charlier
Probability of acceptance the hypothesis, P	0.81	0.86	0.927	0.944
Gear wear along the tooth width, Δb_i				
Average amount of wear, $\bar{t}$	0.147	0.106	0.576	0.595
Average square deviation, σ	0.142	0.155	0.273	0.314
Asymmetry, A	1.04	2.7	0.45	0.303
Excess, E	0.532	9.4	0.74	-0.041
Coefficient of variation, V	0.968	1.46	0.474	0.53
The law of distribution	Laplace-Charlier	normal	normal	Laplace-Charlier
Probability of acceptance the hypothesis, P	0.617	0.544	0.997	0.99
Wear of gear teeth along an involute profile, ΔW_i				
Average amount of wear, $\bar{t}$	0.011	0.01	0.028	0.031
Average square deviation, σ	0.033	0.026	0.064	0.065
Asymmetry, A	3.9	3.49	2.84	2.55
Excess, E	16,2	13.23	7.77	7.62
Coefficient of variation, V	2.96	2.65	2.32	1.79
The law of distribution	Uniform	Uniform	Uniform	Uniform
Probability of acceptance the hypothesis, P	0.437	0.37	0.12	0.07
Error in gear tooth direction, F_{β}				
Average amount of wear, $\bar{t}$	-	-	0.077	0.071
Average square deviation, σ	-	-	0.022	0.020
Coefficient of variation, V	-	-	0.285	0.280

Analyzing the results of statistical processing of the working elements of the GP pump drive gear, we come to the following conclusions. The overwhelming majority of gear element wear distributions obey either the normal law or the Laplace-Charlier distribution law (the latter law is obeyed by random variables close to the normal distribution, but having an asymmetry and excess other than zero). And as is known, the wear phenomena are based on a normal distribution law. This indicates the correct approach to solving the problem. The asymmetry and excessiveness of the wear distribution indicators, which determined the discrepancy between the actual distribution and the normal distribution, are usually small and can be attributed to random events.

The results of constructing a statistical model of a worn gear (Table 2) make it possible to establish the relationship between the wear of gear elements.

The obtained dependencies (2) ... (5) are shown graphically in Fig. 5. From the analysis of the obtained regression equations, it follows that there is a linear relationship between the wear of gear elements (see Fig. 5). In all the dependencies, with the growth of the factorial feature – ΔD_{ei}, the effective feature also grows. This suggests that with an increase in wear of one of the surfaces, wear of other working surfaces of the gears also increases.

Table 2

Results of constructing a statistical model of a worn gear

Variable	Average value, $\bar{t}$	Average square deviation, σ	Coefficient of variation, V	Student's t-test, t_{ϕ} at α=0.99	Regression equation $y = ax + b$
Independent variable Wear of gears by outside diameter – ΔD_{ei}	0.47	0.176	-	-	-
Dependent variables Wear of gear trunnions by diameter – Δd_{ui}	0.30	0.27	0.809	t_{ϕ}=6.74 t_{α}=2.79	$\Delta d_{ui} = 0,755\Delta D_{ei} - 0,052$ (2)
Wear of gear teeth by width – Δb_i	0.52	0.23	0.738	t_{ϕ}=5.36 t_{α}=2.79	$\Delta b_i = 0,98\Delta D_{ei} + 0,059$ (3)
Wear of gears on involute profile – ΔW	0.058	0.021	0.751	t_{ϕ}=5.59 t_{α}=2.79	$\Delta W_i = 0,090\Delta D_{ei} + 0,016$ (4)
The gear tooth direction error – F_{β}	0.064	0.035	0.96	t_{ϕ}=18.7 t_{α}=2.79	$F_{\beta} = 0,195\Delta D_{ei} - 0,027$ (5)

As shown by the calculations for the correlation and regression coefficients of all relations (2) ... (5), the following condition $t_{\phi} = r_{xy}\sqrt{n-1} > t_{\alpha}^*$ is fulfilled, which indicates their significance. In addition, condition $F_{po3} > F_{\alpha}^*$ is fulfilled for all regression equations, which indicates the adequacy of the obtained dependencies.
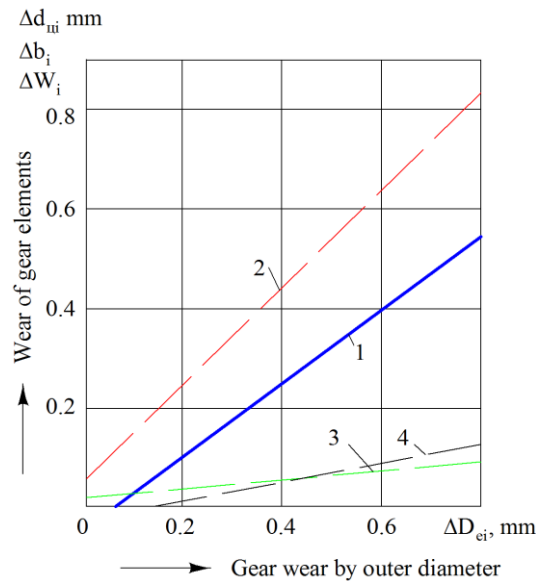
Fig. 5. Graphical display of linear regression equations:
1 – Graph of the regression equation for the wear of the gear width on the wear of the gear by the outer diameter $\Delta b_i = 0,98\Delta D_{ei} + 0,059$ (3); 2 – Graph of the regression equation for the wear of the gear trunnions on the wear of the gear by the outer diameter $\Delta d_{ui} = 0,755\Delta D_{ei} - 0,052$ (2); 3 – Graph of the regression equation for the error of tooth alignment on the wear of the gear by the outer diameter $\Delta W = 0,195\Delta D_{ei} - 0,027$ (4); 4 – Graph of the regression equation for the wear of gears along the involute profile on the wear of the gear by the outer diameter $F_{\beta} = 0,195\Delta D_{ei} - 0,027$ (5)

Thus, the presented results indicate the existence of an unambiguous correlation relationship between gear surface wear.

The obtained equations (2) ... (5) make it possible to determine the wear of each of the working surfaces, knowing the wear of the gears along the outer diameter – ΔD_{ei} with a confidence level $\alpha = 0,99$. In addition, the

equations of the relationship between the wear of gear elements make it possible to create a mathematical image of a worn gear and implement it according to the developed methodology.

Conclusions

Obtained results allowed drawing the following conclusions:

1. The considered part – the drive gear of hydraulic pumps in the form of a system consisting of interconnected parts, its structural parts can be considered as subsystems, and the surfaces, in turn, are elements of the system.

2. It is shown that the predominant type of wear on the working surfaces of gears is abrasive wear. Wear of the involute profile of the gear teeth and splines should be attributed to mechanical abrasion.

3. The distribution laws of wear on the working surfaces of gears and their main numerical characteristics are found. The distribution of gear wear obeys mainly the normal distribution law and also the Laplace-Charlier law.

4. The relationship between the wear of individual surfaces (elements) of the gear was revealed, which became the basis for the presence of system quality (emergence) of the technical system "gear drive of the GP pump", relative to the wear of its elements.

5. The emergence of the technical system "gear drive of the GP pump" made it possible to create a mathematical statistical model, an image of a worn part in the form of linear regression equations system of wear dependence of gear elements on their outer diameter wear. This makes it possible to create a holistic statistical image of the worn part based on a systematic approach to determining one defect, in this case, gear wear along the outer diameter, i.e. to determine the wear of other elements of the part.

6. The resulting mathematical statistical model of a worn part becomes the basis for a systematic approach to justifying the choice of a method for restoring parts and forming routes for the technological process of restoring a part.

References

1. Chernovol M.I., Permyakov O.A., Nemyrovsky Y.B., Shepelenko I.V., Gorbulik V.I. (2023). Methodology of technological design of the process of restoration of parts. Bulletin of the National Technical University "KhPI". Series: Technologies in mechanical engineering: a collection of scientific papers. 2 (8). P.10-16. https://doi.org/10.20998/2079-004X.2023.2(8).02 [Ukrainian]

2. Stetsko A.E. (2013). Technological support of the service life of manufactured and refurbished parts. Lviv, ARS Publishing Company, 240 p. [Ukrainian]

3. Chernovol M.I., Shepelenko I.V. (2023). A systematic approach to the formation of quality indicators of remanufactured parts. Collection of scientific papers. Scientific bulletin. Technical sciences. 7 (38)_I. P.30-36. https://doi.org/10.32515/2664-262X.2023.7(38).1.30-36. [Ukrainian]

4. Ageev M., Chernenko V. (2022). Development and implementation of the concept of ensuring the reliability of repairable parts of vehicles in the process of repair based on system analysis. Bulletin of Priazovsky State Technical University. Series: Technical sciences. (44), P.62-72. https://doi.org/10.32782/2225-6733.44.2022.8. [Ukrainian]

5. Ageev MS, Gritsuk IV, Solovykh EK (2020). Application of combined restoration technologies to increase the service life of vehicle parts. Collection of scientific papers of the Ukrainian State University of Railway Transport. 194. P.81-92. https://doi.org/10.18664/1994-7852.194.2020.230412. [Ukrainian]

6. Frolov E.A., Kravchenko S.I., Popov S.V., Gnitko S.M. (2019). Technological support of the quality of mechanical engineering products. Poltava, 201 p. [Ukrainian]

7. Alexander Permyakov, Yakiv Nemyrovskyi, Eduard Posviatenko and Ihor Shepelenko. (2023). Methodology of technological design in the restoration of parts. *Journal of Physics: Conference Series*, *Mater. Sci. Eng.* 1277 012013, P.1-7. https://doi.org/10.1088/1757-899X/1277/1/012013. [English]

8. Kuleshkov Y.V., Chernovol M.I., Vasylenko F.I. et al. (2002). Statistical methods of processing and analysis of experimental data. Kirovograd., 134 p. [Ukrainian]

9. Chaban G.M. (2020). The use of specialised software for the analysis of economic and mathematical modelling. Effective economy. 9. https://doi.org/10.32702/2307-2105-2020.9.151. [Ukrainian]

10. Chernovol M.I., Kuleshkov Y.V. (2008). The main directions of improvement of gear pumps of agricultural machinery. Bulletin of Agrarian Science. 8. P.52-54. [Ukrainian]

11. Kuleshkov Y.V., Chernovol M.I., Nalyvaiko V.M., Shepelenko I.V. (1999). Methods of statistical processing of experimental data. Bulletin of Ternopil State Technical University. Ternopil. P.71-77. [Ukrainian]

Черновол М.І., Кропівний В.М., Кулєшков Ю.В., Шепеленко І.В., Гуцул В.І. Системний підхід при дослідженні зносів робочих поверхонь деталей автотракторної техніки

Використовуючи принципи системного підходу встановлено взаємозв'язок між зносами окремих поверхонь на прикладі ведучої шестерні насоса типу НШ. Розглянуто ієрархічну структуру деталі, її окремі функціональні частини віднесені до підсистем, а робочі поверхні – до елементів системи. Системний підхід до вивчення зносного стану деталі передбачав, крім виявлення взаємозв'язків між зносами окремих елементів деталі, створення математичної статистичної моделі зношеної деталі як однієї цілої, як системи. Визначені ведучи види зношування робочих поверхонь шестерні. Знайдено закони розподілу зносів робочих поверхонь шестерні та основні числові їх характеристики. Встановлений взаємозв'язок між зносами окремих елементами шестерні став основою наявності системної якості технічної системи «шестерня ведуча насоса НШ» відносно зносів її елементів. Отримана математична статистична модель зношеної деталі у вигляді системи лінійних рівнянь регресії залежності зносів елементів шестерень від зносу їх по зовнішньому діаметру. Це дозволяє використовуючи принципи системного підходу, за даними одного дефекту – зносу шестерень по зовнішньому діаметру, створити цілісний статистичний образ зношеної деталі, тобто визначити зноси інших елементів ведучої шестерні. Отриманні результати дозволяють обґрунтовано підійти до питання вибору способу відновлення деталей та формування маршрутів технологічного процесу відновлення деталі.

Ключові слова: системний підхід, відновлення деталей, знос робочої поверхні, ведуча шестерня, автотракторна техніка, математична статистична модель

Tribotechnical coatings

A.O. Zemlyanoy[1], S.S. Bys[2*], V.V. Shchepetov[1], S.D. Kharchenko[1], O.V. Kharhenko[3]

[1]*General Energy Institute of National Academy of Sciences of Ukraine, Ukraine*
[2]*Khmelnytskyi National University, Ukraine*
[3]*National Aviation University, Ukraine*
E-mail:serhiibys@gmail.com

Abstract

Wear and tear limits the possibilities and shortens the operational life of modern technical systems. Therefore, the importance and necessity of consideration of issues aimed at reducing frictional forces and increasing wear resistance cannot be doubted. The paper summarizes the theoretical and applied results of triboresistance studies of detonation coatings of the Nb-Zr-V-Si-C-MgC2 system under conditions of constant loading in the field of sliding velocities. It has been established that the ratio of the quality of the components that make up the surface modified structures changes. It is noted that at the initial test speeds the presence of lower metal carbides that are part of the coating dominates, with an increase in speed under the current load due to solid-phase and diffusion processes, higher ones are formed in the graphite matrix carbides with enhanced thermodynamic properties.

Key words: detonation coatings, wear intensity, structural-phase composition, graphitization.

Introduction

The problem of durability and reliability of moving joints of machine parts stands out against the background of general technical and industrial achievements. The unshakable existence of the problem is based on the phenomenon of friction, which is associated with one of the most pressing situations in modern technology - wear and tear of machine parts and structures. Wear, as a universal phenomenon of degradation due to friction, limits the capabilities and shortens the service life of modern technical systems. Hence the importance and necessity of considering issues aimed at reducing friction forces and increasing wear resistance.

Objective

The purpose of the work is to generalize the theoretical and applied results of studies of tribological resistance of detonation coatings of the Nb-Zr-V-Si-C-MgC$_2$ system under constant load conditions in a sliding velocity field.

Materials and methods of research

The preparation of the powder mixture was carried out by mechanochemical synthesis using a laboratory attriter of the "IES-1-0.5" type. To prevent sticking of powders to the chamber walls and to optimize the spheroidization process, an anti-adhesive additive in the form of zinc stearite was added to the mixture.

The study of the features of friction surfaces in which activation processes occur, affecting the intensity of mechanochemical reactions, was carried out using a complex method of physical and chemical analysis, including metallography (optical microscope "Neofot-32"), durometric analysis (hardness tester M-400 from LECO), scanning electron microscopy (scanning electron microscope JSM-840), X-ray structural phase analysis (diffractometer DRON-UM1).

The tribological properties of the coatings were assessed by friction of model samples according to the end pattern under conditions of distributed contact. The tests were carried out in continuous sliding mode at a load of 15 MPa, the thickness of the coatings after finishing was 0,750-0,80 mm, roughness Ra = 0,32-0,63.

Tests of detonation coatings were carried out according to a program in which, under similar conditions, coatings of the VK15 type and coatings dusted with alloyed nichrome powder were tested for comparison.

Research results

The main factors determining the course of friction and wear processes are external influences, which determine the degree and gradients of elastoplastic deformation, temperature, level of activation, a number of derivative phenomena and ultimately determine the leading type of wear.

Based on the test results, averaged graphical dependences of wear intensity and friction coefficients in the sliding velocity field are presented at a constant load of 15 MPa (fig. 1). With a monotonous increase in sliding speed under constant load conditions throughout the entire operating test range, the lowest values of wear intensity (curve 1) and friction coefficients (curve 1'), corresponding to normal mechanochemical wear, are found in coatings of the $Nb-Zr-V-Si-C-MgC_2$ system.
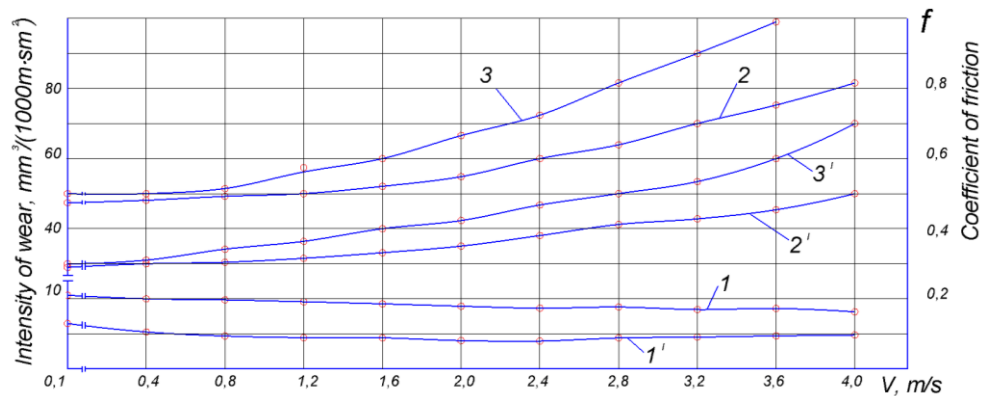

Fig. 1. Dependence of wear intensity (1, 2, 3) and friction coefficient (1', 2', 3') on the sliding speed of coatings: 1, 1' – $Nb-Zr-V-Si-C-MgC_2$ systems; 2, 2' – VK15 (WC-Co); 3, 3' – based on nichrome (Ni-Cr-Al-B). At P = 15 MPa.

Studies of the composition and structure of coatings have made it possible to establish that their structure consists mainly of a finely dispersed mixture, in which strengthening formations are presented in the form of carbide and silicide phases and intermetallic compounds, which are distributed in a solid solution matrix and, thus, represent a structure close to structure of dispersion-strengthened materials. The nature of the interaction of the coating components was determined using the Lanscan program, and it was found that the distribution spectra of Nb, Zr and V along the scan line correlate with the phases of silicon and carbon, which confirms their interaction with the production of the corresponding carbides and silicides, and also determines the possibility of the formation of both solid solutions and ternary compounds.

Analysis of oxygen scanning lines with elements included in the nanocoating showed their phase alignment, which indicates their chemical interaction, causing passivation of the working surface due to the formation of secondary oxide structures. Thus, the obtained research results, supplemented by X-ray diffraction analysis data, allow us to conclude that the initial coatings are an ultradisperse conglomerate of almost uniformly distributed particles of silicides NbSi, $NbSi_2$, ZrSi, Zr_2Si, VSi_2, V_5Si_3 and extensive colonies of carbides NbC, Nb_2C, ZrC, VC, V_2C in a fine-grained matrix of solid solutions of Nb in β-Zr, β-Zr in Nb, V in Nb and Zr.

Under conditions of structural activation under friction loading, the passivating role of secondary structures is played by surface films of oxides and, first of all, SiO_2 and V_2O_5, which are characterized by increased density and adhesive strength, as well as high-quality compact oxides that form Nb and Zr. In addition, the formation of solid solutions of oxygen in niobium and zirconium occurs. Thus, according to X-ray diffraction analysis, a slight increase in the density and lattice period of zirconium has been established, which is, in our opinion, a consequence of the introduction of oxygen atoms into the octahedral pores of the hexagonal lattice and, as a result, the formation of a solid solution. However, the main factor that minimizes molecular adhesion interaction, preventing setting and destruction, is the formation of a surface film of structurally free α-graphite, the formation of which is caused by the thermal decomposition of magnesium carbide [1].

Moreover, the higher the temperature, the greater the amount of carbon converted into graphite and the more graphite is formed. The process is similar to graphitizing annealing. Thus, under friction loading, the running-in of surfaces whose composition includes magnesium carbides, in a certain sense, can be considered as a specific type of heat treatment, accompanied by graphitization.

In figure 2 shows the topography of friction surfaces coated with a graphite film. In fig. 2.b (at V = 1,5 m/s and P = 15 MPa) the graphite film occupies almost the entire working surface, which helps to increase the actual

contact area, reduce the specific load due to filling and smoothing surface microroughnesses, microcracks, and causes the fixation of particles graphite in microcavities of contact interfaces and ensures a reduction and stabilization of the friction coefficient, in addition, it helps to lower the temperature, level out and reduce deformation fields. The contact zone, which directly forms the friction surface, is a thin plastically deformable layer, which, according to micro-X-ray spectral analysis performed on a MAP-3 device (probe diameter 1 μm), is a conglomerate of dispersed phases of complex and simple oxides and compounds of silicides and carbides components included in coating composition.

a   b
Fig. 2. Topography of friction surfaces coated with a graphite film P = 15 MPa:
a - V=0,5 m/s; b - V=1,5 m/s

In figure 3 shows an electron diffraction pattern from the surface of the contact layer. The presence of diffusion halos with textured maxima indicates that the structure corresponds to a directional orientation in the friction field. According to the authors, the pattern of its formation can be represented as a process of amorphization and mechanochemical alloying, including dispersion, grinding of a dispersoid with particles of oxides, silicides and their transformation under the influence of local temperatures and pressures into an oriented ultradisperse structure, which represents a substance with liquid-like properties.

Fig. 3. Electron diffraction pattern from the surface of the contact layer
at V=0,5m/s and P=15 MPa.

In figure 4 shows the qualitative distribution of chemical components over the working surface area. The results of physicochemical phase analysis of secondary structures in the form of surface films based on graphite made it possible, by analyzing the diffraction pattern, to identify carbide, silicide and oxide phases with a significant degree of probability. At the same time, it was possible to establish the patterns of structural changes in the identified phases during their reorganization, which is accompanied under friction conditions by both the transformation of the structural-phase composition of secondary structures, caused by varying external influences (sliding speed, load, temperature), and the stability of the dynamic sequence of the processes of their destruction and formation during friction. Thus, the ratio of the quality of the components that make up the surface structures changes, but their general order (the dynamics of formation and destruction) remains constant.

Thus, in the testing area up to 2,0 m/s, the dominant factor is the presence of low metal carbides included in the coating composition and the presence of their oxide reagents. With an increase in sliding speed under the influence of increased shear strains, temperatures and effective load, as a result of solid-phase tribochemical and diffusion processes in the graphite matrix, a balanced presence of higher carbides is formed, characterized by increased thermodynamic stability, which corresponds to the manifestation of the structural adaptability of materials during friction [2].
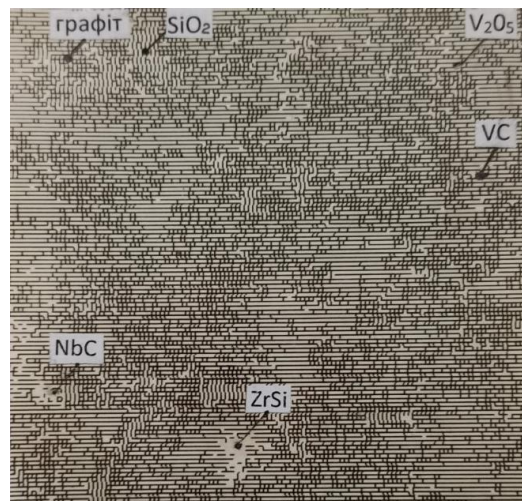
Fig. 4. Qualitative distribution of chemical components over the working surface area.

The nature of the change in the friction coefficient (fig. 1, curve 1') is consistent with the established wear pattern. The decrease in its value and stability with increasing sliding speed confirm the high performance of the studied coatings of the Nb-Zr-V-Si-C-MgC$_2$ system.

In accordance with the presented test results, the developed niobium-based coatings meet high tribological characteristics. The possibility of increasing the operational reliability of coatings through the use of magnesium carbide in their composition, which promotes the formation of carbide graphite under friction loading, has been theoretically substantiated and experimentally confirmed. It should be noted that the presence of magnesium carbide is an effective means of regulating wear and ensuring service life through the formation of modified surface films based on carbide graphite, which, in cooperative mutual consistency with secondary structures, ensure a stable manifestation of minimizing the tribological properties of coatings. Based on this, the amount of magnesium carbide in the coating material may influence the stability of normal mechanochemical wear.

Also tested under similar test conditions were VK15 coatings (fig. 1, curve 2), which are the most widely used tribological material for wear protection of a large range of critical parts of various designs and purposes. However, under the conditions of these tests at sliding speeds of more than 1,7 m/s, the temperature factor begins to influence the tendency to reduce wear resistance.

Coatings based on nichrome (fig. 1, curve 3) alloyed with aluminum and boron, starting from 0,4 m/s, are characterized by a monotonous increase in wear intensity with increasing speed. The structure of the coatings is represented by a nickel-based solid solution and a dispersed mixture of strengthening phases of nickel aluminides, chromium borides, and complex boride compounds. The microhardness was about 10,6 GPa. The protective functions of secondary structures representing heterophase oxide thin-film objects are suppressed by the development of plastic deformation with increasing sliding speed.

Niobium-based coatings containing magnesium carbide and not containing expensive and scarce components meet environmental safety requirements and, due to their operational capabilities, have the prospect of widespread use for the production of competitive tribotechnical equipment.

The most effective use of the studied coatings is to improve the quality of operation of friction units when strengthening and restoring moving joints of control mechanisms, hinges of guide surfaces, cams, sliding supports, lever parts, high-speed and heavily loaded units in which the use of traditional oils and lubricants is undesirable.

It should be noted that the development of coatings containing modified films of carbide graphite, the results of their tests in various friction and wear modes will significantly expand the arsenal of achievements of modern tribological technology.

The studied niobium-based coatings can be used to restore and strengthen worn parts using any technological methods using powder materials.

Conclusions

1. Through theoretical premises and experimental studies, the optimal structural-phase composition of coatings of the Nb-Zr-V-Si-C-MgC$_2$ system was realized. A high level of performance characteristics of coatings was noted, achieved by optimizing the chemical composition and spraying technology.

2. Using modern methods of physicochemical analysis, the structural-phase composition of coatings was studied, the structure of the surface modified layer based on carbide graphite, which prevents molecular adhesion interaction and minimizes friction parameters, was determined.

3. It has been established that the ratio of the quality of the components that make up the surface modified structures changes, it is noted that at the initial test speeds the presence of lower metal carbides that are part of the coating dominates, with an increase in speed under the current load due to solid-phase and diffusion processes, higher ones are formed in the graphite matrix carbides with enhanced thermodynamic properties.

4. The test results form the basis for the development of composite coatings with improved tribological characteristics, which will expand the arsenal of achievements of modern tribological technology. In addition, the developed powders, which do not contain scarce and expensive components, can be used for restoration and strengthening by any technological methods using powder materials.

References

1. Babak V.P., Fialko N.M., Shchepetov V.V., Gladky Ya.M., Bis S.S. Self-strengthening composite nanocrysts // Physico-chemical mechanics of materials. – 2023. – p. 37-43.
2. Kostetsky B.I., Nosovsky I.G., Karaulov A.K. and others. Surface strength of materials during friction // Kiev: Tekhnika, 1976, 296 p.

Зємляной А.О., Бись С.С., Щепетов В.В., Харченко С.Д., Харченко О.В. Триботехнічні покриття

Зношування обмежує можливості та скорочує строки експлуатації сучасних технічних систем. Тому важливість та непохідність розгляду та вирішення питань зниження сил тертя та підвищення опру зношуванню не викликає жодного сумніву. В роботі зроблено узагальнення теоретичних та практичних результатів досліджень трибостійкості детонаційних покрить системи Nb-Zr-V-Si-C-MgC$_2$ в умовах постійного навантаження ковзанням. Встановлено, що змінюється співвідношення якості компонентів, що входять до складу поверхнево модифікованих структур. Відмічено, що на початкових швидкостях випробування домінує наявність нижчих карбідів металів, які входять до складу покриття, при збільшенні швидкості під струмовим навантаженням за рахунок твердофазних і дифузійних процесів вищі утворюються в карбідах графітової матриці. з підвищеними термодинамічними властивостями.

Ключові слова: детонаційні покриття, інтенсивність зношування, структурно-фазовий склад, графітизація

Substantiating the mechanisms of electronic and phonon friction in the conjugation of materials of samples (parts) by the methods of solid state physics

V.V. Aulin*, A.A. Tykhyi, O.V. Kuzyk, A.V. Hrynkiv, S.V. Lysenko, I.V. Zhylova

Central Ukrainian National Technical University, Ukraine
*E-mail: AulinVV@gmail.com

Abstract

The article elucidates the essence of the mechanisms of electronic and phonon friction in the coupling of samples (parts) using the methods of solid state physics.

It is shown that in the triboconjugation of samples made of metallic materials, the flow of fluctuation-electromagnetic and electron-phonon processes should be distinguished. Fluctuation-electromagnetic interactions have long-range effects, and electron-phonon interactions have short-range effects. Based on Lifshitz's fluctuation-electromagnetic theory, the force of friction in moving couplings of metal samples is substantiated, taking into account the frequency ratio in the atomic absorption spectrum and the plasma frequency. A formula for estimating the friction force was obtained, taking into account the dielectric function and the Clausius-Mossotti formula.

The electronic friction force was estimated using the "jelly" model and the generation of electron-hole pairs in the quantum perturbation theory of solid-state physics.

The mechanism of electronic friction was discovered based on the phenomenological theory of braking losses of slow ions in solids. The scheme of the model of the electronic friction mechanism is close to the Persson model, which connects the braking force with the electron scattering process. A refined formula for estimating the electronic friction force is proposed.

The strength of phonon friction is justified on the basis of structural effects that can be induced by the mechanism of breaking adhesive bonds, and perturbation theory. A formula was obtained for estimating the force of phonon friction, taking into account the frequency of phonons, the inverse decay time and the function of the two-dimensional Fourier image of the force of interaction between the atoms of the conjugated surface of the triboelement.

Cases of static and dynamic phonon friction are considered.

Electronic and phonon frictional forces are considered at the nanolevel. The Debye low-temperature approximation and refinement of the expressions for estimating the electronic and phonon friction forces are given, taking into account the type of interatomic potential.

Key words: fluctuation-electromagnetic interaction, electronic friction, phonon friction, perturbation theory, friction force, nanolevel, triboconjugation of samples.

Introduction

The energy of translational movement of tribocouples of samples (parts) is dissipated due to various dynamic mechanisms. Among the most important mechanisms of this type are the processes of fluctuation-electromagnetic interaction and excitation of electrons and phonons [1-3]. Fluctuation-electromagnetic and electron-phonon processes in the friction zone have their own specificity. Effects caused by short-lived excitations of the electron plasma and the formation of a set of electron-hole pairs can be attributed to the latter processes. While the fluctuation-electromagnetic interactions can be considered as long-range effects. This interpretation differs from that used in the work of Tomassoni and Widom [4]. Electronic processes at work in a broader sense are combined with fluctuation-electromagnetic interactions.

It is known from solid state physics [3] that the self-consistent quantum theory takes into account all possible types of excitations in the materials of parts in a single way. At that time, the development of such a theory, the final version of such a theory still needs further development, and possible types of excitations can be considered as subsystems with their own mechanisms. The specification of individual mechanisms is essential for a deeper understanding of the processes occurring in the surface layers of tribocoupled materials of samples (parts).

Literature review

The processes of single-particle excitations are forbidden by the laws of energy-momentum conservation in the absence of damping phonon and plasmon modes [5,6]. In the surface layers of parts materials, in the process of friction and wear, single acoustic phonons are generated by moving atoms, the speed of which is $v > v_s$, where v_s – is the speed of sound. At the same time, phonons are emitted in the cherenkov cone $\cos\theta = v_s / v$. In the presence of finite damping, particles can lose energy for the excitation of quasi-particles at arbitrarily low speeds of their movement [7,8].

Elementary excitations of quasiparticles are always accompanied by the final stages of energy dissipation in the triboconjugation of samples (parts) as a tribosystem in sliding processes. In the mode of contact mode of AFM [9-12], the proportionality of the speed of movement of quasi-particles to the dissipative (viscous) interaction forces of the conjugate surfaces of the samples (parts), which are relatively weak, is observed. In the contact mode, the total work produced by these forces does not exceed the value of $2 \cdot 10^{-22}$ J, while the work of adhesive friction forces is three to four orders of magnitude greater [13-16]. However, this estimate is based on an average velocity of the order of 1 m/s. At the same time, micro-slip occurs in 10^{-12} s, so the work of these forces should be increased by two orders of magnitude. In this case, the viscous force can be comparable to the force of static friction. At that time, dynamic friction plays a significant role in the processes of friction and wear in the tribosystem of parts samples.

A moving fluctuating dipole in the triboconjugates of sample materials (parts) induces electric currents on the friction surface. In this case, Joule damping is the final result of the friction process. In fluctuation-electromagnetic friction forces, accurate ideas about a number of main factors, such as their dependence on speed, distance to the surface, temperature, etc., have not yet been formed. The most general approach to solving the problems of fluctuation-electromagnetic friction is given by the fluctuation-electromagnetic theory of Lifshitz [17, 18].

Purpose

The purpose of the work is to find out the mechanisms of electronic and phonon friction in the coupling of sample materials (parts) based on the fluctuation-electromagnetic theory.

To realize the goal, the following tasks were performed:

1. Justification of the mechanism of fluctuation-electromagnetic friction in the couplings of metal samples (parts).

2. Elucidation of the mechanisms and contribution of electronic and phonon friction in the coupling of metal samples (parts).

Results

If a neutral atom in the material of the sample (part) has a speed v and moves parallel to the surface at a distance z from it, which exceeds the typical atomic dimensions, then a lateral (frictional) force proportional to the speed of movement acts on it. Taking into account the fluctuation-electromagnetic theory in solid-state physics, we can write:

$$F_{fr}^{fet} = \frac{3\hbar v}{8\pi z^5}\int_0^\infty d\omega \left\{ 2\left[x''(\omega)\frac{d\Delta''(\omega)}{d\omega} - \Delta''(\omega)\frac{dx''(\omega)}{d\omega}\right] + \right.$$
$$\left. + \omega\left[x''(\omega)\frac{d^2\Delta''(\omega)}{d\omega^2} - \Delta''(\omega)\frac{d^2 x''(\omega)}{d\omega^2}\right]\right\}\coth\left(\frac{\omega\hbar}{2k_B T}\right),$$

(1)

where ω – is the frequency of the absorption spectrum of the atom of the sample material (details); $x(\omega)$ – atomic polarizability; $\varepsilon(\omega)$ – dielectric function of the part material; $k_B, \hbar, T$ – Boltzmann constant, Planck constant and thermodynamic temperature; $\Delta(\omega)$ – is a complex function depending on the dielectric function, which is equal to:

$$\Delta(\omega) = \frac{\varepsilon(\omega)-1}{\varepsilon(\omega)+1}.$$

(2)

Values with two dashes in formula (1) correspond to the imaginary numbers of the corresponding functions: $x''(\omega)$, $\Delta''(\omega)$. For the normal movement of a neutral particle to the conjugate surfaces of samples (parts), a formula similar to (1) has not yet been obtained.

The analysis of formula (1) shows that at $T = 0$ the force of friction is not equal to zero. This is a physical consequence of the existence of zero fluctuation of the electromagnetic field in materials. If we assume that $T \Rightarrow 0$, then formula (1) takes on a simpler form:

$$F_{fr}^{fet} = \frac{3\hbar v}{4\pi z^5} \int_0^\infty d\omega x''(\omega) \frac{d\Delta''(\omega)}{d\omega}. \tag{3}$$

Based on solid-state physics, the strongest line in the absorption spectrum of an atom is the frequency ω_0. Then, considering the attenuation coefficient equal to zero, for the imaginary part of the part of the polarizability function, we will have the expression:

$$x''(\omega) = \frac{\pi e^2 f_{0tr}}{2 m_e \omega_0} \delta(\omega - \omega_0), \tag{4}$$

where e, m_e, f_{0tr} – are the charge and mass of the electron, as well as the strength of the transition oscillator. Substituting (4) into (3), we use the standard approximation of the Drude-Lorentz model for the dielectric constant of the metal (sample material (parts)), we get:

$$F_{fr}^{fet} = \frac{3\hbar e^2 f_0 \tau^2 v}{4 m_e z^5} \frac{y^2 \left(12 x^4 - 4 x^2 y^2 + 4 x^2 - y^4\right)}{x \left(4 x^4 - 4 x^2 y^2 + 4 x^2 + y^4\right)^2}, \tag{5}$$

where $x = \omega_0 \tau$, $y = \omega_p \tau$, ω_p and τ – plasma frequency and relaxation time of metal electrons. Analyzing formula (5), it can be seen that the sign of the force F_{fr} depends on the ratio of the frequency in the absorption spectrum of the atom and the plasma frequency. When their ratio is $\omega_p \geq \sqrt{2\omega_0}$, the force F_{fr} is a braking force. For the typical metals from which the samples (parts) are made, the specified parameters acquire the following values: $\tau = 10^{-4} - 10^{-5}$ s, $\omega_p = 5\text{-}15$ eV. This condition is almost always fulfilled. At that time, the reverse situation is also possible for the high-frequency absorption lines of the atom: the lateral force F_{fr} can become accelerating . However, it should be noted that the absolute values of the integral of the overlap of the absorption spectra of atoms depend on the values of *x, y* in formula (4). Therefore, for a correct assessment of the total frictional force F_{fr}, a detailed consideration of the absorption spectrum of the atom in a narrow range of frequencies around the value of $\omega_p / \sqrt{2}$.

The lateral force of friction acting in the moving tribosystem of conjugation of samples (parts) in the additive approximation [19] can be obtained from formula (1). To do this, the function $\alpha(\omega)$ is represented by the dielectric function $\varepsilon_1(\omega)$ of the material of the moving sample (parts) using the Clausius-Mossotti formula and integrating it over the volume of the surface layer of the friction zone. As a result, we get the formula:

$$F_{fr}^{fet} = -\frac{3}{64\pi} \frac{\hbar R v}{h^3}, J(\varepsilon_1(\omega), \varepsilon(\omega)), \tag{6}$$

where R – is the radius of curvature of the moving sample surface in the contact zone with the conjugated sample (part); $J(\varepsilon_1(\omega), \varepsilon(\omega))$ – is the frequency integral, which coincides with the similar integral in formula (1) when replacing the expression of the polarizability of the atom with the expression:

$$\Delta''(\omega) = lm\{[\varepsilon_1(\omega) - 1]/[\varepsilon_1(\omega) + 2]\}, \tag{7}$$

It follows from formula (6) that the temperature dependence of the friction force becomes significant under the condition:

$$\omega \hbar \leq 2 k_B T, \text{ when } \coth x \rightarrow x^{-1}, \tag{8}$$

At room temperature we have: $2 k_B T \approx 0,05 eB$. This indicates that the main contribution to the materials of the samples (parts) is given by low-frequency absorption processes. This is similar to dipole relaxations in dielectrics and infrared absorption in ionic and conducting crystals.

Estimates of friction force values according to formula (6) were made for combinations of different types of materials. If $R = 10\text{-}20$ nm, $v = 1$ m/s, $z = 0,2\text{-}0,3$ nm , then at room temperature we obtain the following friction

forces in the range of 0.1-10 nN . Such forces can make a significant contribution to the damping coefficients of lateral oscillations at a Q-factor of the order of 10^4-10^5 .

The value of the factor due to the force of dynamic friction can be estimated by the formula:

$$Q = k_1 v / 2\Omega_1 F, \tag{9}$$

where k_1 – rigidity; Ω_1 – the frequency of the material of the samples (parts), which is an order of magnitude higher than the frequency of normal oscillations. At a stiffness of 100 N/m, a frequency of 10^6-10^7 Hz, a speed of 1 m/s and for a force of 1-10 pN, the Q factor is equal to: $Q = 5 \cdot 10^5 - 5 \cdot 10^7$.

The measurement of the Q-factor shift due to electromagnetic coupling with the surface is a real experimental task.

Electronic friction is a component of fluctuating electromagnetic friction. The mechanism of electronic friction associated with the generation of electron-hole pairs. It was first analyzed by Persson in connection with the problem of damping of lateral vibrations of films adsorbed on a metal substrate [8, 9]. At the same time, the connection between the force of friction, which occurs during the scattering of conduction electrons on the oscillating atoms of the adsorbate , and the change in the resistance of the sample material (parts) was used. If the return time of the damping of the lateral oscillations of the adsorbate atom is denoted by $1/\tau_s$:

$$F_{fr}^e = M_a n_S v / m_e n_e d\tau_s, \tag{10}$$

where M_a and n_S – mass and surface density of film atoms on the surface of the sample (details); m_e , n_e and d – are mass, conduction electron density and film thickness. The coefficient is proportional to the speed and can be considered as the inverse relaxation time $\gamma_s = 1/\varepsilon_s$ associated with an additional electron scattering mechanism. As a result, the specific resistance of the surface layer of the sample material (parts) increases by the amount:

$$\Delta\rho_e = m_e / n_e e^2 \tau_e = M_a n_s / n_e^2 c^2 \tau_s, \tag{11}$$

and the desired decay time τ_s is equal to:

$$\tau_s = \frac{M_a n_s}{n_e^2 e^2 d\Delta\rho_e}, \tag{12}$$

This theory provides acceptable estimates of the damping time of the lateral movement of atoms (molecules) in the surface layers of sample materials (parts) in the case of physical and chemical adsorption. At that time, it was based on a very simplified model that did not take into account the structure of the surface layer and the nature of the distribution of electrons near its surface.

In the quantum theory of perturbations [20], braking losses of material atoms of samples (parts) upon excitation of electrons are considered. A "jelly" model with a sharp potential jump at its spatial boundaries is proposed for conduction electrons. Assuming that the braking force does not change for heavy atoms with a mass of M_a, then the damping time of their lateral motion is equal to:

$$\Delta t_e = \frac{M_a v}{F_{fr}} = \frac{2\pi M_a}{27\hbar r_B^2 k_F^4}, \tag{13}$$

where k_F – is the Fermi vector of electrons (metal) of the sample material (parts); r_B – is the Boriv radius. The estimate according to formula (13) shows that the decay time of atoms of the order $(1,1...1,5) \cdot 10^{-11}$ s. The damping time of the lateral movement of atoms in the sample material (parts) can be reduced with the help of the following factors:

1. Energy losses of atoms with a large nuclear charge should be greater, since the effective charge of heavy atoms is greater than unity.

2. For surface layers of material (films) with a regular N-fold periodic structure, where N – is the number of atoms in the surface layer (film).

The considered theory gives too large values of the electronic friction force and small damping times of the motion of atoms in the surface layers and in adsorbed films.

Another approach to the detection of electronic friction mechanisms is based on the phenomenological theory of braking losses of slow ions in solids: energy losses appear as a result of the hypothetical exchange of electrons belonging to moving atoms. In the triboconjugation of samples (parts), there is an exchange of electrons between their atoms on friction surfaces in the tribosystem. At the same time, each electron of the triboelement that crosses the surface of equal potential of the tribosystem "element 1 - element 2" loses the momentum of relative motion $m_e v$. In fact, this scheme is close to Persson's model, which relates the braking force to the electron scattering process. According to this theory, the energy loss by a neutral atom of triboelement 1 with a nuclear

charge Z_1 and speed v flying at a distance b from an atom of the conjugate surface of triboelement 2 with a nuclear charge Z_2 is equal to:

$$\Delta E = \frac{m_e e^2}{\hbar} \frac{0,35(Z_1 + Z_2)^{5/3}}{\left[1 + 0,16(Z_1 + Z_2)^{1/3} b / r_B\right]^5} v, \qquad (14)$$

Assuming that the material of the sample (parts) has a uniform distribution of atoms with a density n_a, and the moving atom is at a distance z from the surface. After integrating (14) over all possible aiming parameters of atomic motion, we have:

$$F_{fr}^e(z) = \frac{dE(z)}{dz} = -0,7(Z_1 + Z_2)^{5/3} \frac{m_e e^2}{\hbar} n_a v \times \int_z^\infty \frac{b \arccos(z/b) db}{\left[1 + 0,16(Z_1 + Z_2)^{1/3} b / r_B\right]^5}, \qquad (15)$$

The specified theory makes it possible to obtain an expression for the braking force acting on a moving triboelement, using the "jelly" model and the locally flat approximation for the distribution of electrons within the homogeneous contact of the materials of the conjugated surfaces of the samples (parts):

$$F_{fr}^e \approx \frac{3\pi}{10} \left(3\pi^2\right)^{1/3} \hbar v n_e^{4/3} \frac{(R + h/2)^2}{b^2 R^2} (1 + bR) \exp(-b\bar{h}), \qquad (16)$$

where $\bar{h}$ – is the average distance between the conjugate surfaces of triboelements; n_e – is the electron density in the surface layer of the material.

For electrically conductive materials of triboelements in the case of "Al-Al" contact, $b \approx 1,19 \text{нм}^{-1}$, at $R = 20$ nm, $h = 0,2$ nm, $v = 1$ m/s we obtain $F_{fr} \approx 0,67 \text{пH}$ by expression (16). The role of this mechanism in the case of contact of non-conductive materials is insignificant.

Phonon friction is also a component of fluctuating electromagnetic friction. There is still no generally accepted point of view about dynamic phonon friction either. This is partly due to the fact that the corresponding mechanism is manifested on the basis of structural effects that can be induced by the mechanism of breaking adhesive bonds.

Using perturbation theory, it is possible to obtain a formula for estimating the braking force (phonon friction) of a single adsorption atom (film) of the surface layer of the material of the samples (parts):

$$F_{fr}^f = \frac{1}{M} \sum_k \frac{\gamma k_x^2 \left|f(\vec{k})\right|^2 v_a}{\left[\Omega_0(\vec{k})^2 - k_x^2 v_a^2\right]^2 + \gamma k_x^2 v_a^2}, \qquad (17)$$

where $\Omega_0(\vec{k})$ – is the phonon frequency; γ – reverse decay time; k_x – projection of the wave vector $\vec{k}$ on the direction of movement; v_a and M_a – are the speed and mass of the atom in the surface layer (film) of the material of the samples (parts); $f(\vec{k})$ – is a two-dimensional Fourier image of the force of interaction of atoms with the conjugated surface of the triboelement. If the force F_{fr}^f – is periodic, then the function $f(k)$ is proportional $\delta_{\kappa,G}$, where G – is a two-dimensional vector of the inverse lattice. For the case, $\gamma \to 0$ formula (17) takes the form:

$$F_{fr}^f = \frac{\pi}{M} \sum_k k_x \left|f(\vec{k})\right|^2 \delta\left(\Omega_0^2(\vec{k}) - k_x^2 v_a^2\right), \qquad (18)$$

The equality follows from formula (18):

$$\Omega_0(\vec{k}) = k_x v, \qquad (19)$$

which determines the condition of phonon generation in the triboconjugated materials of the samples. At the same time, it is obvious that this equality cannot be fulfilled at speeds lower than the speed of sound. At that time, $\gamma \neq 0$ the more general formula (17) gives the finite force of phonon friction. The value of phonon friction is a small value proportional to the expression $\gamma v_a / \Omega_0^4(G)$, at $v_a \to 0$.

To obtain a realistic estimate of the braking time by a surface layer or an adsorbed film that forms a structure incommensurate with the adsorbate . Triboelement materials must be partially disordered . This breaks the translational symmetry and greatly increases the strength of the phonon friction, or uses an exaggerated phonon decay time (10^{-3} s). In the latter case, it follows from formula (18) that the force of phonon friction is equal to:

$$F_{fr}^f = \frac{\pi^2 N}{GM v_s^2} \left|f(G)\right|^2, \qquad (20)$$

where N – is the number of atoms of the surface layer of the material of the sample (parts) or film; v_s – speed of sound; G – is the minimum vector of the inverted lattice.

In this case, the force of phonon friction does not depend on the speed. Obviously, its value largely depends on the parameters N, v_s, $f(G)$. The results of the study indicate that the assessment of the role of this mechanism of phonon friction requires additional analysis and justification. The speed of phonons in small-sized films is closer to 100 m/s than to 1000 m/s [7,8], and the value of the Fourier factor $f(G)$ should significantly depend on the distance z between the film and the surface, decreasing with increasing z.

Dynamic phonon friction also occurs during the movement of individual atoms, and the corresponding forces of phonon friction can be estimated within the framework of quantum perturbation theory. At the same time, the most significant role is played by the scattering processes of surface phonons in the film or surface layers of the material of the samples (parts). For the high-temperature phonon acoustic spectrum corresponding to the thermodynamic temperature T and the condition $v/v_s < 1$, the force of phonon friction is equal to:

$$F_{fr}^f = \frac{S(k_B T)^2}{(\hbar v_s)^3} |U_G(z)|^2 \frac{v}{v_s}, \tag{21}$$

where $U_G(z)$ – is the two-dimensional Fourier factor of the interaction potential of the atom with the surface of the sample material (details); S – is the area of the unit cell. The dependence on the distance z is determined by a specific type of Fourier factor $U_G(z)$, and the quadratic dependence on the thermodynamic temperature is due to the two-dimensional phonon spectrum of the surface of the sample material (details).

Note that the estimate of the phonon friction force uses the interatomic potential of the form:

$$v(r) = -C_0 r^{-6} \left(1 - 0.5(r_0/r)^6\right), \tag{22}$$

where $C_0 = 3.75 \cdot 10^{-78} J \cdot m^6, r_0 = 3.8 \cdot 10^{-10} m$. Calculations show that the phonon friction mechanism provides the observed retardation time of the order of 1 ns if the atom is actually adsorbed at a distance of 0,3-0,35 nm from the surface.

Phonon friction is considered at the nanolevel . At the same time, the presence of a vacuum gap (of atomic size) between the triboelements does not prevent the passage of phonons, which carry out momentum transfer, and is taken into account due to the change in the speed of sound. In the Debye low-temperature approximation, the force of phonon friction is equal to:

$$F_{fr}^f = \frac{\pi^3}{45} \left(\frac{k_B T}{v_s \hbar}\right)^4 R^2 \hbar v \frac{v_t}{v_s}, \tag{23}$$

where v_t and v_s – are sound speeds through tribocontact and in volumes of material. At $R = 20$ nm, $v = 1$ m/s, $v_s = 6600$ m/s (silicon), $v_t/v_s \approx 0,1$-0,01, $T = 300$ K, the estimate for the friction force gives a value of $F_{fr}^f = 0,5$-5 pN , comparable with those to which other mechanisms of dynamic friction lead.

The tangential stress τ_s applied to the intermediate layer of atoms (molecules) located between the triboelements is a function of the sliding speed $\tau_s = \tau_s(v)$. At the same time, the adsorption film can be in both a solid and a liquid state, alternately " oscillating " between triboelements during the movement of the upper one in the "sticking-sliding" mode, and the thermodynamics of the corresponding phase transition is characterized by a phase diagram in the "temperature-degree of coating" variables.

If the film is in the liquid phase, then the sliding speed of the upper triboelement can be different from zero at arbitrarily small values of the shear stress. If the film has solidified, then $\tau_s \neq 0$ and $v = 0$. The lack of adhesion is therefore associated with the formation of a two-dimensional liquid layer. This is consistent with the results of experimental studies. If the film is in the solid phase and has a structure comparable to the substrate, then this structure is preserved until the tangential stress τ_s reaches a critical level τ_{0s}, at which the film passes into the liquid phase. When the tangential stress is reduced τ_s to values smaller than τ_{0s} This indicates that this model explains the hysteresis of the phonon friction forces in the triboconjugated materials of the samples.

To identify the conditions of the absence of phonon friction in tribosystems, a model of the dynamics of an isolated atomic chain is used. Since the phonon modes of a solid body of finite dimensions are separated from each other by a fairly wide interval, a situation may arise when the distance between the modes exceeds the natural width of the absorption frequency lines. In this case, the transition of translational motion into vibrational modes (and, finally, into thermal energy) is complicated, and the motion can be carried out without losses (absence of phonon friction) for a long period of time. For the acoustic boundary of a three-dimensional cubic sample, the corresponding condition has the form:

$$\frac{(v_s \pi / Na)^2}{\omega} \gg \gamma, \tag{24}$$

where $Na = L$ – is the size of the cubic sample; α – became a cage.

At $v_s = 10^5$ m/s, $L = 1$ cm this condition gives $\gamma\omega < 10^{11}$ c^{-2}, which can be the case for low-frequency acoustic modes.

In the far infrared region (<15 MeV), the attenuation constants were 0,2-1,1 MeV. In this case $\omega\gamma$ =10^{24}-10^{25} s^{-2}. The half-width of the absorption lines was found to be in good agreement with the formula:

$$\gamma = \frac{M_{ad}\omega_0^2}{S_{ad}\rho v_s},\tag{25}$$

where M_{ad} – is the mass of the adsorbate ; ω_0 – frequency of oscillations; S_{ad} – is the surface area occupied by the adsorbate ; ρ and v_s – is the mass density of the substrate and the speed of transverse phonons. Damping of the translational motion of molecules (atoms) in the direction normal to the surface can be satisfactorily explained by the phonon mechanism. This is observed under the condition:

– frequency of oscillations of molecules (atoms) is much less than the frequency of volume phonon modes;

– there are no even weak chemical interactions that can lead to the emergence of a dominant contribution of electronic excitations (electronic friction).

The presented theoretical reasoning is specific to samples (parts) made of metal materials. As for the theory of friction of polymers on a solid surface, a new approach is proposed, according to which the largest contribution to the friction force is related to the contribution of internal friction, due to the fluctuating character of the surface stresses acting on the polymer from the side of the microprotrusions of the solid surface. Another contribution is related to the strength of adhesion. At low sliding speeds, adhesion forces deform the polymer surface in such a way that it fills indentations in the surface relief. At very low relative speeds of movement of triboelements, the first mechanism dominates, since most polymer materials exhibit significant internal friction even at very low frequencies (about 0,1 s^{-1}).

Conclusions

1. It was found that the theoretical understanding of the mechanisms of electron-phonon friction at the nanolevel remains at a rather low level. There is no single quantum theory that self-consistently takes into account all types of elementary processes occurring in the materials of samples (parts) in the contact zone. There is no unified approach regarding the quantitative characteristics and relative role of electronic, electromagnetic, and phonon excitation mechanisms. Today there is no differentiation between them. At that time, there are two types of nanostructure friction: static, independent or weakly dependent on speed, and dynamic, proportional to speed. The microscopic theory of static friction is still phenomenological, and the mechanisms of dynamic friction are more detailed, but require further verification.

2. Macroscopic contact mechanics provides an acceptable interpretation of experimental dependences such as "friction force – load force" and measurements of the area of elastic nanocontacts . At that time, a simple extrapolation of the mechanical properties of the materials of the conjugated samples (parts) to the nanostructural level can lead to significant errors. Parameters such as contact area, shear stress, and work of adhesion at the nano-level can undergo significant changes. It was also found that the existing contact models do not allow describing more complex effects related to the interphase atomic and electronic structure, chemical composition and microscopic mechanisms.

3. The method of molecular (atomic) dynamics when applied to nanoindentation and nanofriction generally gives a satisfactory description of the energy, structure and dynamics of contacts, as well as a number of other tribological effects. In the simulation, ultra- short time intervals, high speeds of nanoprobes and limited statistics of nanoparticles are forced to be used . Increasing the simulation time (or the number of particles) to realistic values is fundamentally impossible due to the huge costs of machine time and the accumulation of errors in the calculation of the kinetic energy of particles.

4. It was determined that all dynamic mechanisms of friction at the nanolevel , despite existing differences, lead to quantitatively close values of friction forces of about 1 pN at probe speeds of 1 m/s. The presence of specific, for different mechanisms, dependences of friction forces on the radius of the probe, temperature and other physical parameters of tribocontacts makes it possible to choose between the available models based on the measurement of damping decrements in the vibration mode. This creates a basis for the development of new methods for diagnosing the parameters of nanostructures by non-destructive methods.

References

1. Aulin V.V. Tribophysical basics of increasing the wear resistance of parts and working bodies agricultural machinery [dys. ... d-ra tekhn. nauk: 05.02.04]. 2014. 447 s. [Ukrainian].

2. Aulin V.V., Lysenko S.V., Velikodnyi D.O., Sponge A.B. A scale-level approach to the analysis of processes in the materials of tribo-junctions of parts of mobile agricultural and motor vehicles. *All-state*

interdepartmental scientific and technical collection. Design, production and operation of agricultural machines, Vol. 47, ch.I. Kropyvnytskyi: National Technical University, 2017. P.52-59 [Ukrainian].

3. Charles Kittel. Quantum Theory of Solids, *2nd Revised Edition*, 1991. 528p [English].

4. Tomassone M.S. and Widom A. Electronic Friction Forces on Molecules Moving near Metals. *Physical Review B*, 1997. 56. 4938-4943 [English].

5. Aulin V., Tykhyi A., Kuzyk O., Lysenko S., Hrynkiv A., Zhylova I., & Livitskyi O. Justification of the effect of the regularities of the flow of nanotribological processes in the materials of joint parts on the increase of wear resistance, reliability and efficiency of the functioning of machines and mechanisms. *Problems of Tribology*, 2023, 28(4/110) [Ukrainian].

6. Tkachuk M.M., Saverska M.S., Kutsenko S.V. Theoretical foundations of contact interaction research and elastic -plastic deformation of machine elements for military and civilian purposes. *Bulletin of the National Technical University "KhPI". Series: Mechanical engineering and CAD*. 2022. No. 1. P. 139-147 [Ukrainian].

7. Tovstyuk K.K. Electron-phonon interaction in the group formalism of perturbation theory. *Bulletin of the National University "Lviv Polytechnic"*, 2004. №513. P. 198–203 [Ukrainian].

8. Tovstyuk K.K., Kuzyk N.I. Effect of acoustic phonons on the electron gas in highly anisotropic and isotropic crystals. *Bulletin of the National University "Lviv Polytechnic"*, 2007. №592. P. 138-142 [Ukrainian].

9. Butt H.-J., Cappella B., Kappl M. Force measurements with the atomic force microscope: Technique, interpretation and applications. *Surface Science Reports*. 2005. Issue 59, No. 1-6. P.1-152 [English].

10. Lanza M. Conductive Atomic Force Microscopy: Applications in Nanomaterials. *John Wiley & Sons*, 2017. 382 p [English].

11. Cappella B., Dietler G. Force-distance curves by atomic force microscopy. *Surface Science Reports*. 1999. Vol. 34, No. 1-3. P. 1-104 [English].

12. Belaidi S., Girard P., Leveque G. Electrostatic forces acting on the tip in atomic force microscopy: Modelization and comparison with analytical expressions. *Journal of applied physics*. 1997. Vol.81, No.3. P.1023-1030 [English].

13. Zavarise G., M. Borri-Brunetto, Paggi M. On the resolution dependence of micromechanical contact models. *Wear*, 2007, vol. 262(1), pp. 42–54 [English].

14. Muller V.M., Yushchenko V.S., Derjaguin B.V. On the Influence of Molecular Forces on the Deformation of an Elastic Sphere and Its Sticking to a Rigid Plane / VM Muller. *J. Coll. Interface Sci*. 1980. V.77. P. 91-101 [English].

15. Pokropivnyi V.V., Skorokhod V.V., Pokropivnyi A.V. Atomistic simulation of adhesion friction and wear of atomic-sharp tungsten surface against iron surface. *Trenie i iznos*, 1996. 17(5), 579-588 [English].

16. Pokropivnyi V.V., Skorokhod V.V., Pokropivnyi A.V. Adhesive phenomena at the interface during nanoindentation, stretch and shock. *Modelling and Simulation in Materials Science and Engineering*. 1997. 5 (6), 579 [English].

17. Landau L.D., Lifshits E.M. The Classical Theory of Fields. *Volume 2. Butterworth-Heinemann*, 1975 - 428p [English].

18. Truesdell C.; Toupin R.A. The Classical Field Theories". In Flügge, Siegfried (ed.). Principles of Classical Mechanics and Field Theory. Prinzipien der Klassischen Mechanik und Feldtheorie. Handbuch der Physik (Encyclopedia of Physics). Vol. III/1. *Berlin–Heidelberg–New York: Springer-Verlag*. 1960. pp. 226-793 [English].

19. Kyasov A.A., Dedkov G.V. Electromagnetic fluctuation interactions of moving particles with cylindrical surfaces. *Surface Science*, 2001. 491, 1-2, 124-130 [English].

20. Yukhnovsky I. R. Fundamentals of quantum mechanics. *Kyiv: Lybid*, 1995. 352 p [Ukrainian].

Аулін В.В., Тихий А.А., Кузик О.В., Гриньків А.В., Лисенко С.В., Жилова І.В. Обґрунтування механізмів електронного та фононного тертя в спряженнях матеріалів зразків (деталей) методами фізики твердого тіла

В статті з'ясовано сутність механізмів електронного та фононного тертя в спряженнях зразків (деталей) методами фізики твердого тіла.

Показано, що в трибоспряженнях зразків з металевих матеріалів слід розрізняти протікання флуктуаційно-електромагнітних і електронно-фононних процесів. Флуктуаційно-електромагнітні взаємодії мають далекодіючі, а електронно-фононні – короткодіючі ефекти. Виходячи з флуктуаційно-електромагнітної теорії Ліфшиця обґрунтовано силу тертя в рухомих спряженнях металевих зразків, враховуючи співвідношення частоти в спектрі поглинання атома і плазмової частоти. Отримано формулу для оцінки сили тертя, враховуючи діелектричну функцію і формулу Клаузіуса-Моссоті.

Оцінку сили електронного тертя проведено, використовуючи модель "желе" та генерацію електрон-діркових пар в квантовій теорії збурень фізики твердого тіла.

Виявлення механізму електронного тертя здійснено, виходячи з феноменологічної теорії гальмівних втрат повільних іонів в твердих тілах. Схема моделі механізму електронного тертя близька до моделі Персона, що зв'язує силу гальмування з процесом розсіювання електронів. Запропоновано уточнену формулу оцінки сили електронного тертя.

Силу фононного тертя обґрунтовано на основі структурних ефектів, які можуть індукуватися механізмом розриву адгезійних зв'язків, та теорії збурень. Отримано формулу для оцінки сили фононного тертя з урахуванням частоти фононів, зворотного часу затухання та функції двомірного Фур'є-образа сили взаємодії атомів спряженої поверхні трибоелемента.

Розглянуто випадки статичного та динамічного фононного тертя.

Електронна та фононна сили тертя розглядаються на нанорівні. Дано дебаєвське низькотемпературне наближення й уточнення виразів для оцінки електронної та фононної сил тертя з урахуванням виду міжатомного потенціалу.

Key words: флуктуаційно-електромагнітна взаємодія, електронне тертя, фононне тертя, теорія збурень, сила тертя, нанорівень, трибоспряження зразків

A comprehensive method of researching the tribological efficiency of couplings of parts of nodes, systems and aggregates of cars

V. Aulin[1*], A. Gypka[2], O. Liashuk[2], P. Stukhlyak[2], A. Hrynkiv[1]

[1]Central Ukrainian National Technical University, Ukraine
[2]Ternopil Ivan Puluj National Technical University , Ukraine
*E- mail : Gypkab@gmail.com

Abstract

In this work, a universal tribometer is proposed to study the tribological efficiency of the couplings of samples and parts. The design of the tribometer made it possible to carry out experimental studies in a wide range of force parameters of the load with their smooth change. A set of characteristics and parameters determined on tribometers during the study of couplings of samples according to the "disk-finger" scheme is given: wear intensity, coefficient of friction, temperature in the contact zone, specific work of destruction, specific energy capacity according to the heat index, electrical criterion for evaluating the structural adaptability of tribo couplings. Modes of friction and wear were determined by the characteristics of changes in the contact electrical resistance parameters: run-in, normal friction and wear, volume destruction. The results of the research of tribological efficiency according to the specified characteristics and parameters are given. For a comparative effect, the samples were strengthened by a complex chemical-thermal method, serial technology and boronization . The results made it possible to identify the characteristic zones of run-in regimes, normal friction and wear, and volumetric destruction. They are confirmed by the received electron microfractographies.

Keywords: tribological efficiency**,** tribo-bonding of samples and parts, tribotechnical parameters, contact electrical resistance, surface strength, operational reliability

Formulation of the problem

The flexibility and mobility of road transport at a relatively low cost of transportation contributes to the development of industrial production, which plays a significant role in the development of the economy of Ukraine. One of the important tasks facing the automotive industry is to improve the operational properties of vehicles by increasing reliability, efficiency and economy. The reliability and efficiency of road transport is largely determined by the phenomena of friction and wear that occur in the tribo couplings of parts of nodes, systems and units of cars. When worn, the tightness of the tribocouplers of parts is broken, the accuracy of their relative placement and relative movements is lost. The processes of jamming, impacts, and vibrations occur, which lead to the breakdown of individual parts, components, systems, and units of cars. The friction process leads to energy losses, overheating of mechanisms, reduced work effort, increased consumption of fuel, lubricants and other operating materials. The positive role of friction is necessary to ensure the operation of braking mechanisms, the clutch mechanism, and wheel movement. The phenomena of friction and wear are mutually conditioned: friction leads to wear, and wear of the surfaces of tribo-coupling parts during operation leads to a change in friction modes. Applied tasks of increasing wear resistance and friction management are the design and implementation in practice of new designs of tribocoupling parts, highly efficient fuel-lubricant and structural materials, optimal measures during car operation. The main directions of significantly increasing the operational reliability and efficiency of cars based on the use of tribology methods are: improving the efficiency of resource-determining structures tribocoupling of parts, reduction of material capacity; increasing the wear resistance and bearing capacity of tribocouplers of parts; increasing the tribological efficiency of conjugations of parts of nodes, systems and aggregates; use of environmentally friendly operating methods; use of new materials with increased anti-friction and friction

characteristics; improvement of seal designs that ensure low friction; ensuring tightness and excluding the ingress of abrasive into the zone of frictional contact and others.

Among the main heavy-duty ones the tribocoupling of car parts is primarily the coupling of parts of fuel and gas distribution equipment of internal combustion engines. The coupling of parts of the cylinder-piston and connecting rod group, crankshaft with main and connecting rod bearings, gearboxes, reducers, belt and chain gears, braking mechanisms and others work in difficult conditions . Technological methods are one of the effective ways of increasing the surface strength, and therefore the wear resistance of the parts' joints. The effectiveness of the application of one or another method depends on the design features of the tribocoupling of parts as a whole and its individual parts and materials, lubrication conditions, power parameters of the load, the nature of the load, and the operating modes of the car.

Analysis of recent research and publications

Solving the problem of increasing operational reliability of heavy-duty vehicles tribocoupling of car parts requires a systematic approach to their tribological efficiency with the development of complex methods of researching tribotechnical characteristics and parameters and kinetic criteria for evaluating processes in the frictional contact zone. The structural-energetic approach [1] allows to systematize ways of searching for optimal solutions in order to increase the surface strength of tribocouplers of parts of nodes, systems and units of cars [2, 3, 4]. The development of the automotive industry shows a constant increase in the specific power of engines [5, 6, 7], an increase in the thermal and mechanical load on the parts of tribo couplings . This leads to a number of negative consequences [8, 9]. Effective ways of researching new methods and technologies, influencing tribotechnical characteristics and parameters of processes in the zone of frictional contact [10, 11, 12] . Along with design and operational tools, this will allow to create a complete set of technical solutions [13, 14], to expand the tribotechnical data bank of nodes, systems and units of cars, to develop practical recommendations for solving issues of applied tribotechnics [15]. This concerns the tribological efficiency of car parts couplings, its connection with technical operation and reliability.

The purpose of the work

The purpose of this work is to develop a comprehensive methodology for researching the tribological efficiency of the couplings of samples and parts according to kinetic criteria for evaluating changes in the main tribotechnical characteristics and indicators: wear intensity, friction coefficient, temperature in the contact zone, specific work of destruction. the energy capacity of the friction system according to the thermal index, the processes of formation, transformation and destruction of dissipative secondary structures in the modes of running-in, normal friction and wear, volumetric destruction by the nature of changes in the contact electrical resistance of tribo-conjugation samples with various methods of strengthening technologies of their working surfaces in wide ranges of smooth changes in the power parameters of the load.

Research results

In order to obtain objective information about the processes in the zone of frictional contact, it is necessary to use modern tribotechnical equipment (tribometers) and a measuring complex to register the main tribotechnical and structural-energy parameters both directly in the process of friction and wear, i.e. in a dynamic and static state . The issue arose of developing a comprehensive methodology for researching the tribological efficiency of part couplings and kinetic criteria for evaluating friction and wear processes in the frictional contact zone. The disadvantages of existing tribometers include: a rather narrow range of force parameters of the load on the sample under study with the gradual nature of their change; lack of reversible nature of movement; imperfect lubrication system of tribocoupler samples; inconvenient shape of the working surface of the sample (friction surfaces) for further metallographic studies; the absence of the possibility of self-installation in the sample attachment mechanism for better practice. The vast majority of tribometers are characterized by varying degrees of accuracy, which leads to the impossibility of comparing the obtained results, creating a single bank of tribotechnical data on the wear resistance of parts, assemblies, systems and units of cars.

In the laboratory of tribological research of the automobile department of the Ternopil National Technical University named after Ivan Pulyuy created a complex of laboratory equipment - a tribometer, which includes: an automatic system for supplying lubricant to the friction zone, a measuring complex for recording the main tribotechnical indicators. Fig. 1 shows the design of the friction assembly and loading mechanism, and Fig. 2 shows the general view of the proposed tribometer.

The study was carried out according to the scheme "end surface of the disc (counterbody) - end surface of the cylinder (sample)". The shape of the contact surface is a plane. The contact scheme of the tribocouples of the samples was chosen to realize the limit mode of lubrication and the impossibility of its exit to the hydrodynamic mode. The flat working surface of the sample is convenient for the process of working in the contacting samples, as well as for their further metallographic studies.
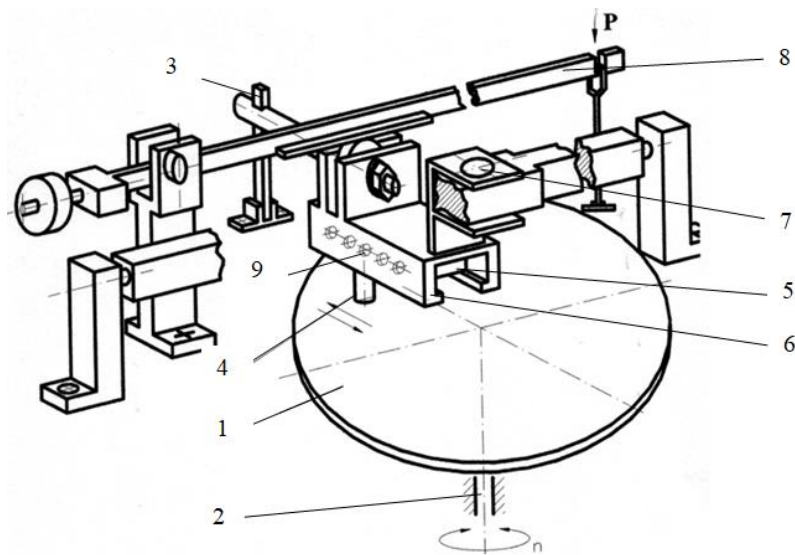
Fig. 1. Schematic representation of the structure of the friction assembly and the tribometer loading mechanism

**Fig. 2. General appearance of the tribometer**

The hydraulic drive of the tribometer, the design of the friction unit and the loading mechanism allow you to smoothly change the power parameters of the load in wide ranges: sliding speed 0.1...12 m/s; specific load on the tested sample 0.2...40 MPa . In addition, the hydraulic drive of the tribometer also ensures the reversible nature of the rotation of the counterbody .

The main units of the tribometer are: a welded frame of increased rigidity, a hydraulic drive, a hydrokinematic scheme shown in Fig. 3, a friction unit and a loading mechanism, a lubricant supply system to the frictional contact zone of tribo-coupling samples.

The designs of the friction unit and the load mechanism are designed to increase the efficiency and reliability of the obtained results by reducing the dynamic loads on the test sample during transient processes and modes of friction and wear, expanding the range of force parameters of the load, the possibility of using the entire working surface of the counterbody . The characteristic features of the tribometer are: simplicity of design, versatility of the drive mechanism, small dimensions, increased rigidity of the friction unit and the load mechanism, openness of the friction unit for visual inspection.

Structurally, the tribometer consists of a welded body (frame), counterbody 1, which, together with its fastening mechanism, is installed on the shaft of the hydraulic motor 2, with the possibility of rotational movement around its own axis. The friction node is equipped with a tension beam 3 to register the moment of friction of the test sample 4, which is placed in the sample receiver 5, with the possibility of its radial movement along the surface of the counterbody. The sample holder is placed in the guide 6, which is hinged at one end to the rotation shaft 7 , and the other end is in contact with the load lever 8 through the bearing. The working position of the sample is relative to the guide, and therefore to the friction surface of the counterbody fixed with the help of screw 9. The longitudinal axis of the guide and the axis of the examined sample are placed in the same plane, which is perpendicular to the working surface of the disc and protects the sample from possible distortions. A significant

increase in the value of the specific load on the test sample is achieved due to shoulders , both on the load lever and on the guide.
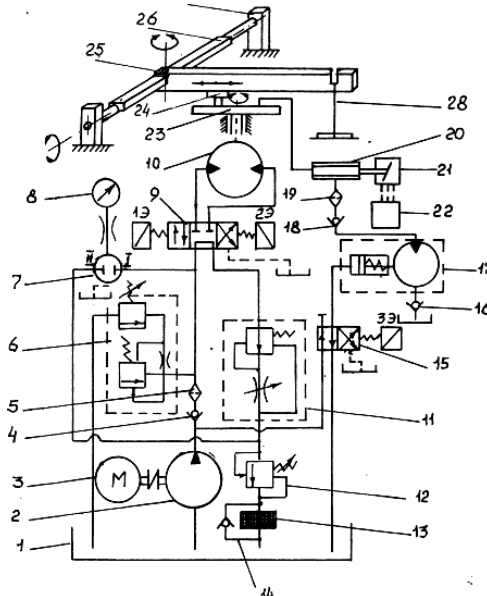
1 – reservoir; 2 – pump BG12-23; 3 – electric motor; 4 - check valve G51-23; 5 – FMS filter; 6 - pressure valve BPG 52-24; 7 - manometer spool ZM2.2- C32O; 8 – manometer MT-160; 9 - hydraulic distributor 64P173-12; 1O - hydraulic motor G15-22; 11 - flow regulator PG55-22; 12 - support valve PG54-24; 13 - oil cooler ; 14 - non-return valve G 51-23; 15 - hydraulic distributor 54BPG73-11; 16 - suction valve; 17 - lubrication station with hydraulic drive ЭС12ОО1; 18 - discharge valve; 19 - filter FLG 18-100; 20 - feeder MI-5 (5E); 200 21 - microswitch MP 2302; 22 - PVE-21-3 control device; 23 – disc; 24 - sample; 25 - lever; 26 - shaft; 27 - rack; 28 – a set of sinkers

Fig. 3. Hydrokinematic diagram of the tribometer

The tribometer is characterized by a simple design, small dimensions, and the convenience of conducting tribological studies. Together with the metallographic analysis of the structural state of tribo-conjugation samples, the tribometer is a complex that possesses a certain degree of perfection. The technical capabilities and reliability of the tribometer are confirmed by the experience of its operation, especially when the tribological efficiency of the couplings of samples and parts is determined. The design of the friction unit and the loading mechanism were designed to increase the efficiency and reliability of the results of tribotechnical studies of the characteristics and parameters of tribo-coupling samples by reducing the dynamic loads on the sample during transient friction and wear processes, as well as to expand the range of force parameters of the load. According to the developed comprehensive methodology for researching the tribological efficiency of heavily loaded couplings of car parts, the following parameters were measured: intensity of mass wear I (weight method), coefficient of friction μ (tensometry), temperature in the contact zone T (thermocouples), the value of contact electrical resistance of the tribocoupling KEO (R), according to electrical measurement circuit (Fig. 4).
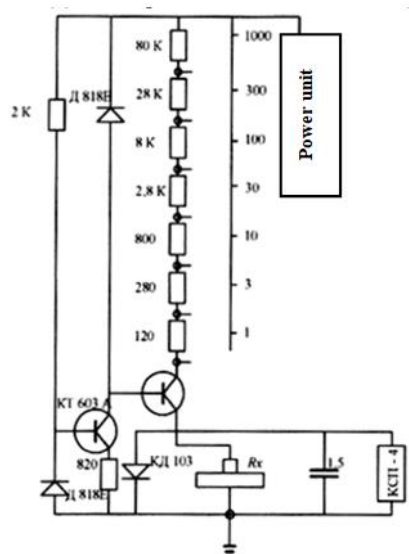

Fig. 4. Electrical circuit for measuring KEO (R) parameters of tribocoupling parts

In addition, the following parameters were calculated: the specific work of destruction of secondary dissipative structures - A_p and the energy intensity of triboconjugation according to the thermal index - ECT $_Q$.

The value of the specific work of destruction A_p characterizes the level of structural adaptability and is determined by the cost of friction work A_{tr} to remove a unit volume of material ΔV from the friction surface:

$$A_p = \frac{A_{тр}}{\Delta V}, \frac{Дж}{мм^3}. \tag{1}$$

The parameter A_p characterizes the processes that take place in the zone of frictional contact of tribocouples and is general for evaluating the processes of surface destruction. The value of this parameter depends on the wear mechanism and can take different values for the same tribocoupler.

The specific energy capacity of the friction system according to the thermal index characterizes the friction work costs for a temperature increase in the contact zone by 1 K. It is an energy criterion for evaluating the range of structural adaptability of tribo-conjugate materials:

$$E_q = \frac{A_{тр}}{\Delta T}, \frac{Дж}{см^2 \cdot с \cdot К}. \tag{2}$$

The criteria A_p and ECT_Q are significant in solving applied problems of tribology: the selection of structural and lubricating materials, determination of optimal force load parameters that ensure structural adaptability, its level and limits.

The control values of the listed parameters were taken as their stable values after each stage of force load (change in sliding speed, normal load. Research was carried out in wide ranges of changes in load parameters with their smooth change, different lubricating media, using different test samples (different processing methods). This made it possible to comprehensively investigate the processes of running-in, normal friction and wear, transitional processes, to fix the critical values of load parameters during the transition to volumetric destruction, and to draw a conclusion about the effectiveness of tribo couplings of samples and parts. The most important for the theory and practice of friction and wear is the range of normal mechano-chemical wear, which is characterized by the dynamic balance of the processes of formation, transformation and destruction of dissipative secondary structures - the range of structural adaptability. Identification by tribotechnical parameters (I, μ, T), KEO (R) and structural parameters (type of dissipative secondary structures) was carried out within the range of structural adaptability. The structure of friction surfaces was studied using a scanning electron microscope of the Cam system Scan 4DV with Link 860 energy dispersive X-ray analysis system.

The proposed electrical criteria for assessing the structural adaptability of tribocoupler materials (KEO (R), ΔT, ΔR, $\Delta R/R_{out}$, R_{out}, R_{st}) made it possible to significantly shorten the research cycle, objectively identify the main tribotechnical parameters with the corresponding structural state of the friction surfaces, and also, to clearly fix the critical points of transition of processes: running-in - normal friction and wear - damage (volumetric destruction). These criteria can be determined with the required accuracy by observing the standardized research conditions: ensuring the conditions of limit friction, equilibrium of the processes of heat generation and heat removal, equilibrium of the processes of formation and destruction of dissipative secondary structures with a wide range of changes in the power parameters of the load with their smooth nature of change, reproduction on an appropriate scale (real operating conditions of the tested tribocouplers of the samples). The specified circumstances led to the development of a fundamentally new tribometer design.

The influence of load modes (p, ν) of tribocouplers of samples and parts on the nature of the change in KEO parameters (R) over time is shown in Fig. 5.

p – specific load; ν – sliding speed; R_{ini} is the initial (preliminary) value of the KEO (R) tribocoupling ; R_{st} – stable (optimal) value of KEO (R) given p, ν data; δR is the magnitude of the drop in R values (strength margin of dissipative secondary structures); $\Delta R = R_{st} - R_{ins}$ - when transitioning to the mode of normal friction and wear; Δt is the time for the tribocoupler to reach a stable KEO value (R); ▨▨▨▨- KEO scattering ranges (R).
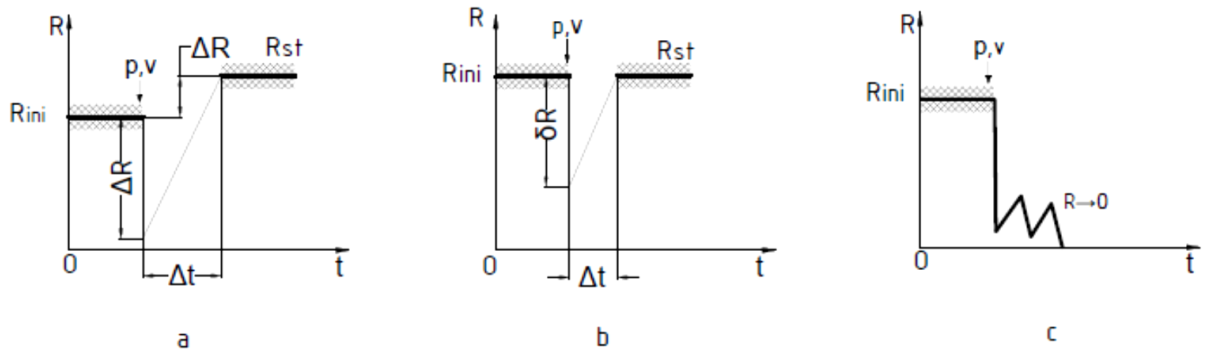

Fig. 5. Schematic representation of the nature of the change in the KEO parameters (R) at the moment of time t from the power load parameters p, ν of the tribocoupler of the samples: a - run-in modes (transient processes); b – modes of normal friction and wear; c - volumetric destruction.

The choice of materials for tribo-coupling parts , methods of their strengthening, lubricating medium, magnitudes and nature of changes in the power parameters of the load was carried out in accordance with the research goal and the possibility of their practical use.

The material of the counterbody - steel SHX15 (HPc=60...63, Ra=0.32μm) was chosen from the point of view of its high wear resistance in comparison with the studied materials of the samples. The material of the studied sample is steel 40X (HPc=48...52, Ra=0.32μm). The working surface of the sample, in order to increase its wear resistance, was subjected to special processing methods. The research was carried out at a constant sliding speed (v= 1.2 m/s) with a smooth change in the value of the specific load R.

An inactive , non-polar, low-viscosity petroleum jelly lubricant was chosen as a lubricating medium with the need to exclude the influence of hydrodynamic and adsorption effects, since technical lubricants have a complex carbon and fractional composition, contain in special additives of active substances, resin-forming products and mechanical impurities.

As an example of studies of the tribological efficiency of sample couplings, Fig. 6.7 shows the results of the main tribotechnical characteristics and parameters for various strengthening technologies: Δ – complex chemical and thermal treatment, o – serial technology, □ – boronizing .
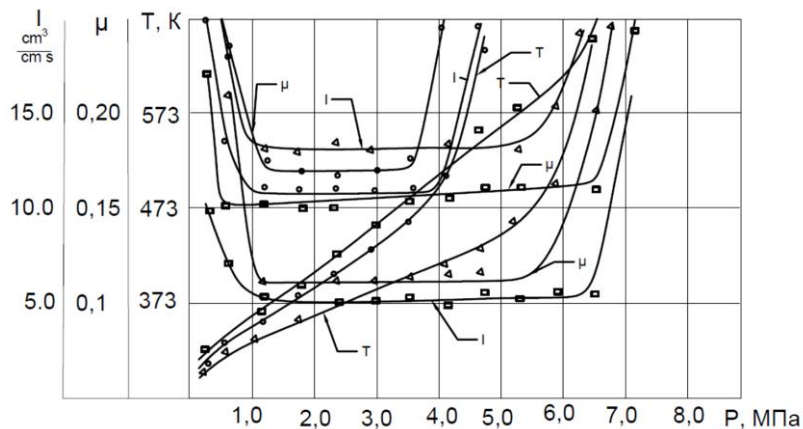
Δ – complex chemical and thermal treatment, o – serial technology, □ – boron treatment .

Fig. 6. Graphical dependence of the intensity of wear J, the coefficient of friction μ, the temperature T in the contact zone on the value of the specific load P.
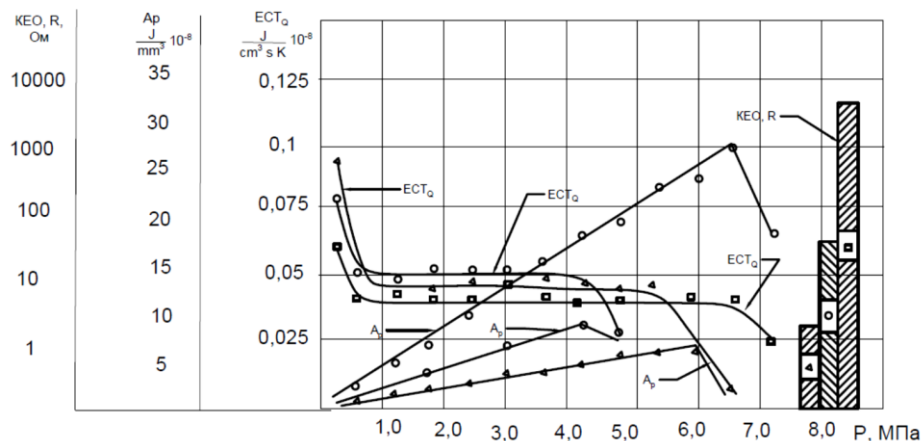
Δ – complex chemical and thermal treatment, o – serial technology, □ – boron treatment

Fig. 7. Graphical dependence of the change in the specific work of destruction Ap , the temperature energy capacity of the friction system on the thermal index ECT $_Q$ and the contact electrical resistance of the KEO tribocoupler (R)

The exit of the tribocoupling to the mode of normal friction and wear after each stage of loading (optimal values of the parameters I, μ, T in the range of structural adaptability), directly during the research process, can be judged by the stabilization of the KEO parameter (R). In addition, according to the kinetics of the change of KEO (R), the processes of completion of tribo conjugation run-in, the ranges of normal friction and wear, the moment of transition to the process of volumetric destruction are recorded

As can be seen from the given graphs, the nature of the change in wear intensity, friction coefficient, and temperature for the studied methods of chemical-thermal strengthening is in accordance with the general pattern of friction and wear. Three characteristic zones are distinguished: 1 – run-in mode (unstable values of these parameters), 2 – range of normal friction and wear (minimum and stable values of these parameters), 3 – transition of tribocoupling to damage mode (volumetric destruction).

The results of studies of the structure of the friction surfaces of the studied samples made of 40X steel strengthened by serial technology are presented in Fig. 8, complex chemical and thermal treatment in Fig. 9 and boronization in Fig. 10.

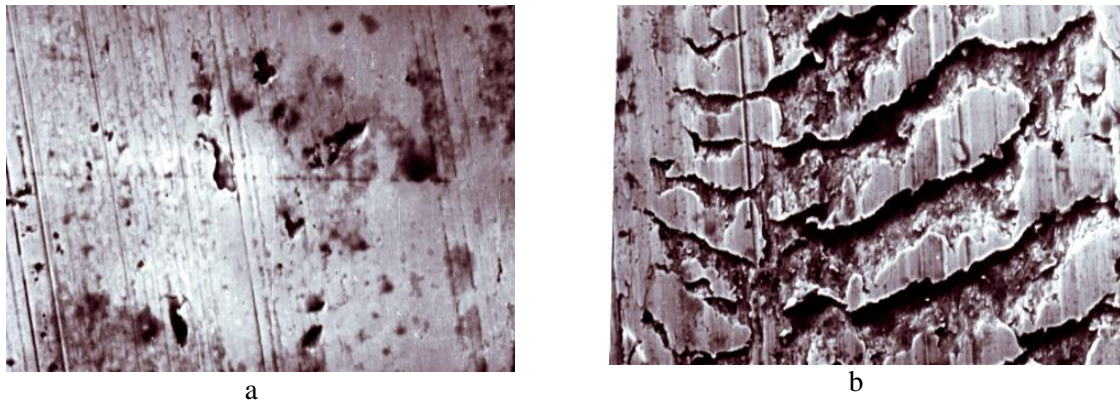a   b

Fig. 8. Electronic microfractograms surface friction sample from steel 40 X strengthened on serial technologies : and - the normal mode friction and wear , b – mode of damage

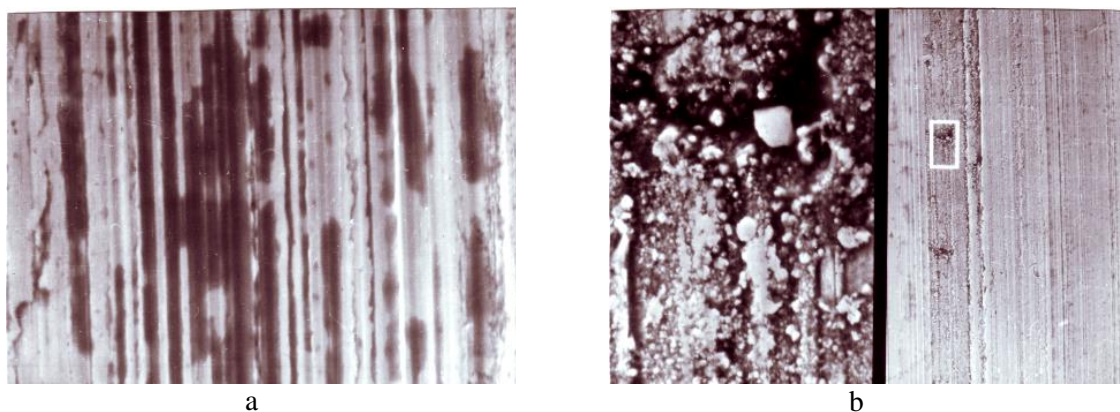a   b

Fig. 9. Electron microfractograms of the friction surface of a sample made of 40 X steel strengthened by complex chemical and thermal treatment: and - the normal mode friction and wear , b – mode of damage

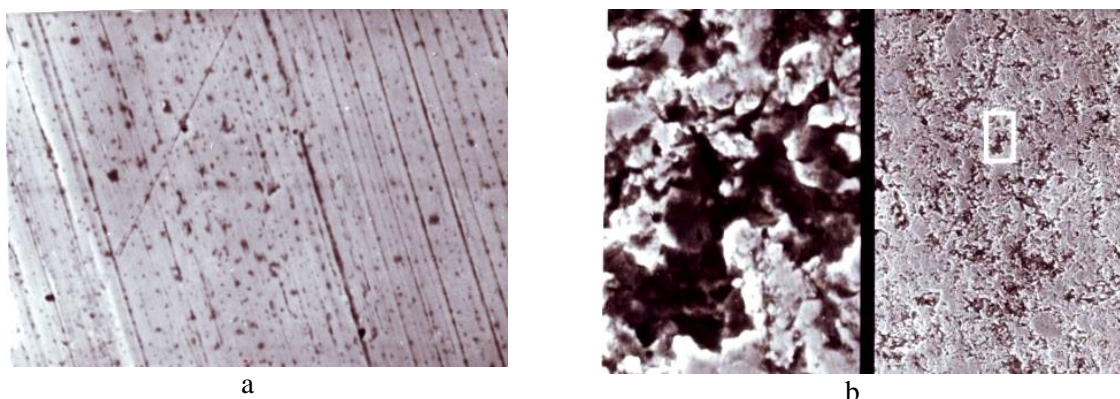a   b

Fig. 10. Electronic microfractograms surface friction sample from steel 40 X strengthened boring : and - the normal mode friction and wear , b – mode of damage

These assumptions are confirmed by electronic microfractograms of the friction surfaces of the studied samples. In the mode of structural adaptability (normal friction and wear), the working surfaces of the samples are covered with appropriate dissipative secondary structures (Fig.s 8a, 9a, 10a); when transitioning to the damage mode, the dynamic balance of the processes of formation and destruction of dissipative secondary structures is disturbed (Fig.s 8b, 9b, 10b) , which leads to volumetric destruction of friction surfaces.

Conclusions

1. A comprehensive methodology for researching the tribological efficiency of the couplings of samples and parts on the proposed design of the tribometer has been developed. The tribometer allows you to study samples according to the "disk - finger" scheme. The flat contact scheme makes it possible to realize different modes of friction, to smoothly change the force parameters of the load in a wide range, and in combination with tribotechnical characteristics and metallographic analysis to more comprehensively characterize the tribological efficiency of tribocouplers of samples and parts.

2. The application of the developed research methodology and kinetic criteria for evaluating operational wear resistance allows identifying the main factors that determine the development of the leading types of wear, studying the mechanisms of their development, and reasonably choosing constructive, technological and operational means of managing the surface strength of tribo-coupling parts , including heavily loaded ones car tribocoupling . In combination with the metallographic study of the structural state of friction surfaces (types of internal combustion engines), the possibility of a comprehensive study of processes in the frictional contact zone with the expansion of the existing bank of tribotechnical data in order to increase the tribological efficiency of couplings of parts of machines for controlling friction and wear processes appeared.

3. A correlational dependence was revealed between the characteristics of changes in tribotechnical parameters: wear intensity, friction coefficient, temperature in the contact zone, structural-energy parameters: specific energy of destruction of dissipative secondary structures according to the thermal index, contact electrical resistance and type of dissipative secondary structures in the range of normal friction and wear. This correlation dependence is universal in nature, as it was discovered during the study of other materials of experimental samples, methods of strengthening friction surfaces, various lubricants and additives, both when the specific load and the sliding speed change.

References

1. Kostetskii , BI; Nosovskii , IG; Karaulov, AK; Iyashko, VA; Surface durability of materials in friction , Technical Publishing , Kiev , 1976, 292 p.

2. Wear Resistance of Eutectic Welding Coatings of Iron-Based Fe–Mn– C–B–Si–Ni–Cr at Increased Temperature Pashechko , M., Dziedzic , K., Stukhliak ,P., Borc , J., Jozwik , J., Journal of Friction and WearJournal of Friction and Wear , 2022, 43(1), pp. 90-94.

3. Gypka A. The tribology of the car: Research methodology and evaluation criteria / O. Lyashuk ,, Y. Pyndus , V. Gupka , M. Sipravska , M. Stashkiv // ICCPT 2019: Current Problems of Transport : Proceedings of the 1st International Scientific Conference , May 28-29, 2019, Ternopil , Ukraine . R. - 231-237. http://dx.doi.org/10.5281/zenodo.3387620

4. Dykha OV (2018). Rozrakhunky trybotekhnichnoi nadiinosti pidshypnykiv kovzannia [Tekhnichnyi service ahropromyslovoho , lisovoho she transport complex No. 13] S. 20-26.

5. Dykha OV (2013). Vuzly tertia mashyn . Rozrakhunky on znosostiikist : navch . possible [Khmelnytskyi : KhNU] 147 p.

6. Voytov VA, Stadnichenko NG (2005). Technologies tribotehnicheskogo vosstanovleniya Overview and analysis perspective [Problemyi tribologii N 2] S. 86 - 93.

7. Priest , M. and CM Taylor , 2000. Automobile engine tribology - approaching the surface . [Wear , 241(2)] 193-203.

8. Sarajevo I.Iu. , Khruliev , OE and Vorobiov , OM (2021). Ekspertna head tekhnichnoho stanu tsylindro-porshnevoi hrupy dvyhuna avtomobilia [Visnyk mashynobuduvannia she transport 13, 1] S.133–139.

9. Zammit , JP., Shayler PJ, Gardiner R., Pegg I. (2012). Investigating the potential that reduce crankshaft main bearing friction during engine warm- up by raising oil feed temperature [SAE Int J Engines 2012; 5(3) paper 2012-01-1216].

10. Stelmakh O., Fu H., Guo Y., Wang X., Zhang H., & Dykha , O. (2022). Adhesion-DeformationHydrodynamic model of friction and wear [Problems of Tribology , 27(3/105)] S.49–54. .

11. Chihos H. (1982). Sistemnyiy analiz v tribonike [Per . with English SA Harlamova . - M.: Mir] 352 p.

12. Aulin , V., Lysenko , S., Hrynkiv , A., Liashuk , O., Gy pka , A., & Livitskyi , O. (2022). Parameters of the lubrication process during operational wear of the crankshaft bearings of automobile engines. Problems of Tribology , 27(4/106), 69–81

13. Dykha OV, Sorokatyi RV, Babak OP (2011). Rozrakhunky she vyprobuvannia on nadiinist mashyn i konstruktsii : navch . possible [Khmelnytskyi : KhNU] 151 p.

14. Kim , S.; Ahn , YJ; Jang , YH Frictional Energy Dissipation for Coupled Systems Subjected that Harmonically Varying Loadsv Tribology International , 2019, 134, 205-210. DOI: 10.1016/j.triboint.2019.01.021.

15. Lyasuk , OL; Gypka , AB; Tesla , VO Operational methods of increasing the wear resistance of friction pairs of a car . Innovative technologies of development and efficiency of motor transport operation : International scientific and practical Internet conference , Central Ukrainian National Technical University Kropivnitsky , Collection of scientific materials (November , 14-15), Ukraine : Kropivnitsky , 2018, pp . 212-217.

Аулін В.В., Гупка А.Б., Ляшук О.Л., Стухляк П.Д., Гриньків А.В. Комплексна методика дослідження трибологічної ефективності спряжень деталей вузлів, систем та агрегатів автомобілів

В даній роботі для дослідження трибологічної ефективності спряжень зразків і деталей запропоновано універсальний трибометр. Конструкція трибометра дозволила проводити експериментальні дослідження в широкому діапазоні силових параметрів навантаження при їх плавній зміні. Наведено комплекс характеристик і параметрів, які визначаються на трибометрів при дослідженні спряжень зразків за схемою «диск-палець»: інтенсивність зносу, коефіцієнт тертя, температура в зоні контакту, питома робота руйнування, питома енергоємність по тепловому показнику, електричний критерій оцінки структурної пристосовуваності трибоспряжень. За характерами зміни параметрів контактного електроопору визначали режими тертя і зношування: припрацювання, нормальне тертя і зношування, об'ємна деструкція. Наведені результати дослідження трибологічної ефективності за зазначеними характеристиками та параметрами. Для порівняльного ефекту зразки зміцнювали комплексним хіміко-термічним способом, серійною технологією та боруванням. Результати дали можливість виділити характерні зони режимів припрацювання, нормального тертя та зношування, об'ємної деструкції. Вони підтверджені отриманими електронними мікрофрактографіями.

Ключові слова: трибологічна ефективність, трибоспряження зразків і деталей, триботехнічні параметри, контактний електроопір, поверхнева міцність, експлуатаційна надійність